DR 876

DSE-5221-T1

PASSIVE SOLAR CALCULATION METHODS

Final Report

MASTER

By
Zulfikar O. Cumali
A. Osman Sezgen
Robert Sullivan

June 15, 1979

Work Performed Under Contract No. EM-78-C-01-5221

CCB/Cumali Associates
Oakland, California

U.S. Department of Energy

DISTRIBUTION OF THIS DOCUMENT IS UNLIMITED

Solar Energy

NOTICE

This report was prepared as an account of work sponsored by the United States Government. Neither the United States nor the United States Department of Energy, nor any of their employees, nor any of their contractors, subcontractors, or their employees, makes any warranty, express or implied, or assumes any legal liability or responsibility for the accuracy, completeness or usefulness of any information, apparatus, product or process disclosed, or represents that its use would not infringe privately owned rights.

This report has been reproduced directly from the best available copy.

Available from the National Technical Information Service, U. S. Department of Commerce, Springfield, Virginia 22161.

Price: Paper Copy $6.50
Microfiche $3.00

DISCLAIMER

This report was prepared as an account of work sponsored by an agency of the United States Government. Neither the United States Government nor any agency Thereof, nor any of their employees, makes any warranty, express or implied, or assumes any legal liability or responsibility for the accuracy, completeness, or usefulness of any information, apparatus, product, or process disclosed, or represents that its use would not infringe privately owned rights. Reference herein to any specific commercial product, process, or service by trade name, trademark, manufacturer, or otherwise does not necessarily constitute or imply its endorsement, recommendation, or favoring by the United States Government or any agency thereof. The views and opinions of authors expressed herein do not necessarily state or reflect those of the United States Government or any agency thereof.

DISCLAIMER

Portions of this document may be illegible in electronic image products. Images are produced from the best available original document.

DSE-5221-T1
Distribution Category UC-59

FINAL REPORT

PASSIVE SOLAR CALCULATION METHODS

CONTRACT NUMBER: EM-78-C-01-5221

Zulfikar O. Cumali
A. Osman Sezgen
Robert Sullivan

DISCLAIMER

This book was prepared as an account of work sponsored by an agency of the United States Government. Neither the United States Government nor any agency thereof, nor any of their employees, makes any warranty, express or implied, or assumes any legal liability or responsibility for the accuracy, completeness, or usefulness of any information, apparatus, product, or process disclosed, or represents that its use would not infringe privately owned rights. Reference herein to any specific commercial product, process, or service by trade name, trademark, manufacturer, or otherwise, does not necessarily constitute or imply its endorsement, recommendation, or favoring by the United States Government or any agency thereof. The views and opinions of authors expressed herein do not necessarily state or reflect those of the United States Government or any agency thereof.

CCB/CUMALI ASSOCIATES
2930 LAKESHORE AVENUE, OAKLAND, CALIFORNIA 94610 (415) 465-0511

JUNE 15, 1979

This document is
PUBLICLY RELEASABLE
Barry Steele
Authorizing Official
Date: 7-19-07

DISTRIBUTION OF THIS DOCUMENT IS UNLIMITED

PROJECT IDENTIFICATION

This report documents a portion of the work accomplished under DOE contract number EM-78-C-01-5221, Development of Passive Solar Calculation Methods. It is the final report and encompasses the period from October 15, 1978 through June 15, 1979. Results within each of the following tasks are discussed (see Statement of Work - Appendix H.2):

1. TASK 1 - Evaluation of Existing Analysis Techniques
2. TASK 2 - BLAST/DOE-1 Program Interface and Comparison with BR-202
3. TASK 3 - Development of Analytic Relationships Between the Thermal Balance and Weighting Factor Techniques
4. TASK 4 - Development and Evaluation of Alternative Analysis Techniques
5. TASK 5 - Multiple Thermal Zone Analysis

TABLE OF CONTENTS

A. INTRODUCTION 1

B. ANALYTICAL DEVELOPMENT OF SPACE SPECIFIC WEIGHTING FACTORS 3

C. FREQUENCY RESPONSE METHODS 12

D. SENSITIVITY STUDY 24

E. WEIGHTING FACTOR/THERMAL BALANCE DISCUSSION 76

F. SUMMARY 84

G. REFERENCES 85

H. APPENDICES

1. Sensitivity Study Tabulated Data 86
2. Statement of Work 101

A. INTRODUCTION

Within the immediate future, Passive Solar design techniques will become an important part of the architectural community's resources. The critical nature of fossil fuel supplies and the uncertain effects of present day nuclear technology make it imperative that alternative energy sources be explored. However, prior to Passive Solar design methods becoming commonplace, as with any new development certain initial steps must be taken to isolate those factors which directly influence the feasibility of such methods. This report documents a portion of the current work being done in Passive research and development under Department of Energy Contract number EM-78-01-5221, Development of Passive Solar Calculation Methods.

The Statement of Work for this contract is listed in the Appendix. Five specific tasks were identified as part of the study as follows:

1. Evaluation of Existing Analysis Techniques
2. BLAST/DOE-1 Program Interface and Comparison with BR-202
3. Development of Analytic Relationships Between the Thermal Balance and Weighting Factor Techniques
4. Development and Evaluation of Alternative Analysis Techniques
5. Multiple Thermal Zone Analysis

This report documents a continuation of the effort detailed in reference 1 and represents the final report of the aforementioned DOE contract. Specific discussions relating to each of the tasks above are contained herein; however, the results reported are primarily concerned with Tasks 1, 4 and 5. The results of Tasks 2 and 3 are fully documented in Reference (1).

Section B presents an analytical treatment related to the generation of space specific weighting factors using a recursion relationship which employs a heat balance of both the outside and inside surface. After which the multizone problem is discussed, the analysis of which is facilitated through the use of the calculated weighting factors.

To simplify the treatment of a parametric study contained in Section D, Section C details the use of frequency domain methods such that the amplitude ratio and phase shift characteristics for a sinusoidal excitation are derived for the thermal load resulting from radiation heat gain/loss and space air temperature fluctuations.

As stated above, Section D, presents the results of a parametric study related to variable floor properties, radiation distributions and space sizes. The weighting factors generated for each perturbation, which are listed within the Appendix, were used to define the expected differences in space response characteristics.

Reference 1 describes various methods available for use in calculating thermal loads and a specific comparison was made of two techniques: weighting factor and thermal balance. Section E of this report describes additional studies made using these methods without the program peculiar aspects inherent in the first comparison.

The Appendix, in addition to containing the tabulated results of the parametric study, also includes a specific discussion for each of the tasks outlined within the statement of work.

B. ANALYTICAL DEVELOPMENT OF SPACE SPECIFIC WEIGHTING FACTORS FOR MULTIPLE ZONES

Reference 1 presented an analytical treatment describing the derivation of space specific weighting factors using a recursion technique. The method employed used the load response to a unit radiation and/or space air temperature pulse to define the weighting factors through a convolution scheme which was also developed in Reference 1. The outside surface temperature was assumed to be zero thus eliminating the need for a heat balance solution at the external surface. While this procedure is valid for internally generated excitation pulses, its use is limited in that responses to excitations arising from outside sources can not be ascertained.

This section of the report documents an extension to the basic method which allows for temperature variations on both inside and outside surfaces. A recursion relationship similar to what was previously developed is shown to be valid for this more general case.

The internal surface heat balance equation can be written as follows:

$$A_i \left[X_i(0) + h_i^I + \sum_{m=1}^{NS} G_{i,m} \right] T_i^I(t) - A_i \sum_{m=1}^{NS} G_{i,m} T_m^I(t)$$

$$- A_i Y_i(0) T_i^O(t) = A_i h_i^I T_R(t) + q_{R_i}^I(t) \qquad \text{(B.1)}$$

$$- A_i \left[\sum_{j=1}^{t} \left(X_i(j) T_i^I(t-j) - Y_i(j) T_i^O(t-j) \right) \right]$$

It is noted that the radiation coupling between the surfaces has been linearized and the radiation related physical constants have been absorbed into the shape factors between surfaces i and m, $G_{i,m}$. In this equation, the superscripts, I and O, refer to the inside and outside surfaces; the arguments of the various terms refer to time; and:

A_i = area of surface i

h_i^I = inside surface convection coefficient of surface i

h_i^O = outside surface film coefficient of surface i

NS = number of surfaces determining the space

$q_{R_i}^I$ = radiant flux impinging on surface i

T_i^I, T_i^O = inside and outside surface temperatures at surface i

T_R = space air temperature

X_i, Y_i, Z_i = response factors of surface i

In order to obtain a solution, the inside surface heat balance equation must be coupled with the outside surface balance equation. This can be written as:

$$A_i \left[Z_i(0) + h_i^O \right] T_i^O(t) - A_i Y_i(0) T_i^I(t) = A_i h_i^O T_i^A(t) + q_{R_i}^O(t) - A_i \left[\sum_{j=1}^{t} \left(Z_i(j) T_i^O(t-j) - Y_i(j) T_i^I(t-j) \right) \right] \quad \text{(B.2)}$$

where

$q_{R_i}^O$ = incident solar and thermal radiation fluxes absorbed by the outside surface on surface i

T_i^A = outside air temperature to which the external surface is exposed

Defining the heat flux coupling, $\phi_i(t)$, (conduction) between the inside and outside surfaces in terms of response factors:

$$\phi_i(t) = A_i \left[\sum_{j=1}^{t} \left(X_i(j) T_i^I(t-j) - Y_i(j) T_i^O(t-j) \right) \right] \quad \text{(B.3)}$$

for $0 \leq i \leq NS$. This represents the heat flux out of the inside of surface, i; also

$$\phi_i(t) = A_i \left[\sum_{j=1}^{t} (Z_i(j)T_i^O(t-j) - Y_i(j)T_i^I(t-j)) \right] \qquad (B.4)$$

for $NS+1 \leq i \leq 2NS$. This represents the heat flux into the outside of the surface.

Equations (B.1) and (B.2) represent 2NS equations in 2NS unknowns - the inside and outside surface temperatures. These equations can be put in the following matrix form:

$$\begin{bmatrix} C_{1,1} \cdots C_{1,NS} & C_{1,NS+1} \cdots C_{1,2NS} \\ C_{2,1} & \\ \vdots & \\ C_{2NS,1} \cdots & C_{2NS,2NS} \end{bmatrix} \bullet \begin{bmatrix} T_1^I(t) \\ \vdots \\ T_{NS}^I(t) \\ T_1^O(t) \\ \vdots \\ T_{NS}^O(t) \end{bmatrix} = \begin{bmatrix} B_1^I \\ \vdots \\ B_{NS}^I \\ B_1^O \\ \vdots \\ B_{NS}^O \end{bmatrix} \qquad (B.5)$$

where for $i = \leq NS$

$$C_{i,i} = A_i \left[X_i(0) + h_i^I + \sum_{m=1}^{NS} G_{i,m} \right]$$

$$C_{i,m} = -A_i G_{i,m} = C_{m,i} = -A_m G_{m,i} \qquad (B.6)$$

$$B_i = A_i h_i^I T_R(t) + q_{R_i}^I(t) - \phi_i(t)$$

and for NS + i $\leq$ i $\leq$ 2NS

$$C_{i,i} = A_i \left[Z_i(0) + h_i^0 \right]$$

$$C_{i,m} = -A_i Y_i(0) = C_{m,i} = - A_m Y_m(0) \qquad (B.7)$$

$$B_i = A_i h_i^0 T_i^A(t) + q_{R_i}^0(t) - \phi_i(t)$$

This matrix includes the thermal balance on both the internal and external surfaces together with the conductive couplings between the inside and outside surfaces and the radiative couplings of both sets of surfaces to the environment.

Equation (B.5) can be solved for a radiation pulse and/or space air temperature pulse, as indicated in Reference 1. For the radiation pulse:

$$\sum_{i=1}^{NS} q_{R_i}^I(0) = 1 \text{ and } q_{R_i}^I(t) = 0 \text{ at } t \geq 1$$

and for the air temperature pulse:

$$T_R = 1 \text{ at } t = 0$$

$$T_R = 0 \text{ at } t \geq 1.$$

Unlike the methodology developed in Reference 1, this equation can also be solved for a unit excitation pulse in either heat gain or outside temperature as follows:

$$q_{R_i}^0(t) \text{ or } T_i^A(t) = 1 \quad \text{at } t = 0 \text{ for some construction i}$$

$$q_{R_i}^0(t) = T_i^A(t) = 0 \quad \text{at } t = 0 \text{ for all other constructions}$$

$$q_{R_i}^0(t) = T_i^A(t) = 0 \quad \text{at } t \geq 1 \text{ for all i}$$

The solution temperatures in equation (B.5) are obtained by inverting the [C] matrix:

$$[T] = [C]^{-1} \cdot [B] = [K] \cdot [B] \tag{B.8}$$

For j = t, with $\phi_n(0) = 0$, these can be written as:

$$T_i(t-j) = T_i(0) = \sum_{n=1}^{2NS} K_{i,n} B_n(0) \tag{B.9}$$

where

$$B_n(0) = A_n h_n^I T_R(0) + q_{R_n}^I(0) \quad \text{for } 1 \leq n \leq NS$$

and

$$B_n(0) = A_{n-NS} h_{n-NS}^0 T_{n-NS}^A(0) + q_{R_{n-NS}}^0 \quad \text{for } NS + 1 \leq n \leq 2NS$$

For j < t

$$T_i(t-j) = - \sum_{n=1}^{2NS} K_{i,n} \phi_n(t-j) \tag{B.10}$$

since for all times other than t = 0 both external and internal excitation quantities are zero. Substitution of equations (B.9) and (B.10) into equations (B.3) and (B.4) yields:

For $1 \leq m \leq NS$

$$\phi_m(t) = - \sum_{j=1}^{t-1} A_m X_m(j) \sum_{n=1}^{2NS} K_{m,n} \phi_n(t-j) + A_m X_m(t) \sum_{n=1}^{2NS} K_{m,n} B_n(0)$$

$$+ \sum_{j=1}^{t-1} A_m Y_m(j) \sum_{n=1}^{2NS} K_{m+NS,n} \phi_n(t-j) + A_m X_m(t) \sum_{n=1}^{2NS} K_{m+NS,n} B_n(0) \tag{B.11}$$

and for $NS + 1 \leq m \leq 2NS$

$$\phi_m(t) = - \sum_{j=1}^{t-1} A_{m-NS} Z_{m-NS}(j) \sum_{n=1}^{2NS} K_{m,n} \phi_n(t-j) + A_{m-NS} Z_{m-NS}(t) \sum_{n=1}^{2NS} K_{m,n} B_n(0)$$

$$+ \sum_{j=1}^{t-1} A_{m-NS} Y_{m-NS}(j) \sum_{n=1}^{2NS} K_{m-NS,n} \phi_n(t-j) - A_{m-NS} Y_{m-NS}(t) \sum_{n=1}^{2NS} K_{m-NS,n} B_n(0)$$

(B.12)

The weighting factors are determined by obtaining the load response to the previously mentioned pulse input quantities, i.e., by summing the convection gain of the air due to each of the zone defining surfaces.

$$Q(t) = \sum_{m=1}^{NS} A_m h_m^I [T_R - T_m^I(t)] \tag{B.13}$$

A recursion relationship can be developed by considering the load contribution from each surface, both internal and external, thus for $t \geq 1$:

$$Q_m(t) = A_m h_m \sum_{i=1}^{2NS} K_{m,i} \phi_i(t)$$

$$= A_m h_m^I \sum_{i=1}^{NS} K_{m,i} \phi_i(t) + A_m h_m^O \sum_{i=NS+1}^{2NS} K_{m,i} \phi_i(t) \tag{B.14}$$

with $h_m^O = h_{m+NS}^I = h_m$ for $m \geq NS+1$ being used to preserve the subscript nomenclature, substitution of equations (B.11) and (B.12) into (B.14) yields after further reduction:

$$Q_m(t) = A_m h_m \sum_{i=1}^{NS} K_{m,i} \left[\sum_{j=1}^{t-1} \left(\frac{Y_i(j)}{h_{i+NS}} Q_{i+NS}(t-j) \right.\right.$$

$$\left. - \frac{X_i(j)}{h_i} Q_i(t-j) \right) + A_i X_i(t) \sum_{n=1}^{2NS} K_{i,n} B_n(0)$$

$$\left. - A_i Y_i(t) \sum_{n=1}^{2NS} K_{i+NS,n} B_n(0) \right]$$

$$+ A_m h_m \sum_{i=NS+1}^{2NS} K_{m,i} \left[\sum_{j=1}^{t-1} \left(\frac{Y_{i-NS}(j)}{h_{i-NS}} Q_{i-NS}(t-j) \right.\right.$$

$$\left. - \frac{Z_{i-NS}(j)}{h_i} Q_i(t-j) \right) + A_{i-NS}(t) \sum_{n=1}^{2NS} K_{i,n} B_n(0)$$

$$\left. - A_{i-NS} Y_{i-NS}(t) \sum_{n=1}^{2NS} K_{i-NS,n} B_n(0) \right] \qquad \text{(B.15)}$$

The total load is simply the summation of all the component loads:

$$Q(t) = \sum_{m=1}^{NS} Q_m(t) \qquad \text{(B.16)}$$

Therefore, for all times after t = 0, the resultant load can be determined by past values. This development which includes outside surface temperature fluxuations can thus be used for determining the coupling effect between zones and is also a more accurate method of generating the radiation/space air temperature weighting factors for a particular zone.

The following paragraphs deal specifically with the solution of the multizone heat transfer problem.

1. Multiple Thermal Zone Analysis

Thermal load analysis procedures related to inter-zone heat transfer have been somewhat unwieldy in the past because of the invariably large heat balance matrix required for solution. The general approach to such a problem involves the simultaneous solution of up to 2·n·NS equations, where n is the number of spaces,and NS, the number of surfaces within each space. Reference 16 presents a discussion of such a technique which is strictly related to a thermal balance matrix solution.

It appears that an alternative technique might be possible using methods developed by CCB/Cumali Associates during the course of work conducted within this contract. The following approach, however, needs first to be coded and actually tested for efficiency and accuracy prior to specific recommendations being made.

The concept employs the same basic structure currently in DOE-1, in that a constant space temperature load profile is initially generated for each space afterwhich the variable space temperature is determined. Several procedures can be used to isolate the constant temperature load; however, in this discussion, only the modified thermal balance method is treated. The modified thermal balance is based on an assumed initial surface temperature for each surface within a space, which is determined by averaging the temperatures from the previous hour for each of the other surfaces. An iterative approach is then used to calculate the actual surface temperatures based on the difference between assumed and calculated values being below some minimum value. This procedure would be used for all surfaces for all spaces defined. At this point, these temperatures are translated into space loads for subsequent use by the variable temperature algorithm.

The recursion relationship discussed in the previous section is used in the next step to isolate the varying space temperature effect. An outside temperature pulse would be applied to each surface from which external temperature weighting factors are generated to be used to define

a set of simultaneous equations for solution of an incremental space temperature and load quantity due to the other space temperature changes. These increments would be added to the temperatures and loads calculated for each room independently which is accomplished in the Systems portion of DOE-1.

C. FREQUENCY RESPONSE METHODS

Weighting factors are generated by application of a distributed unit flux or temperature pulse from which a time response in space load is produced. To enable a more efficient interpretation of the influence of individual parameters on the resulting weighting factors and also to obtain an indication of the resultant load response arising from the use of specific weighting factors, an investigation was undertaken to determine the applicability of frequency response methods of analysis. Rather than generating a load or temperature time history response for a set of factors, it was envisioned that with a frequency domain analysis, an immediate observation could be made of the damping inherent in the weighting factors themselves.

The discussion that follows relates to an analysis of the radiation and conduction type weighting factors as presently defined in the literature. Following this presentation a technique is proposed for use with the space air temperature weighting factors.

1. Radiation/Conduction

The space load response to an arbitrary flux input excitation can be expressed in Z-transform format as follows:

$$Q(Z) = \frac{V_0 + V_1 Z^{-1}}{1 + W_1 Z^{-1}}\, q(Z) \qquad (C.1)$$

where

$q(Z)$ = input excitation Z-transform

$Q(Z)$ = output Z-transform

V_0, V_1, W_1 = weighting factors from a previously computed load response to a unit pulse input, (with $V_1 = (1+W_1)-V_0$).

The Z-transform is defined for discrete time series analysis through application of the equation $Z = e^{s\Delta t}$ which enables the s-plane or Laplace transform of a continuous function to be analyzed in a discrete manner. The application of this equation maps the complex s-plane

into a series of concentric circles in the Z-plane. For example:

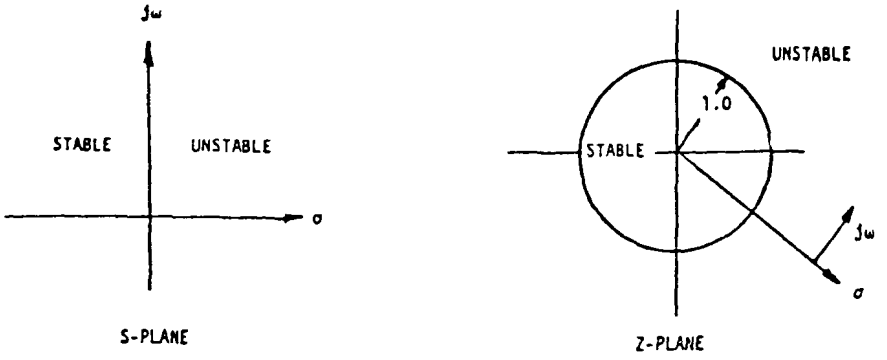

Because of the periodicity of $e^{s\Delta t}$, with $s = j\omega$, one must apply a bilinear transformation to the Z-plane to enable the use of all the continuous time system frequency domain methods of analysis. These tools for analyzing systems, such as Bode Diagrams, Nichols Charts and root locus procedures, are well known and have proven very useful for indicating system stability and isolating parameter influence on system characteristics. By introducing this new bilinear transform, R, such that:

$$Z = \frac{1 + R}{1 - R} \quad \text{with } R = j\upsilon \tag{C.2}$$

the Z-transform of a function can be conveniently analyzed in the υ complex plane. With $Z = e^{j\upsilon\Delta t}$, υ is related to ω as follows:

$$\omega = \frac{2}{\Delta t} \tan^{-1}(\upsilon) \tag{C.3}$$

Rearranging equation (C.1) such that:

$$Q(Z) = K \frac{(Z+a')}{(Z+b')} q(Z)$$

where

$$K = V_0$$

$$a' = V_1/V_0$$

$$b' = W_1$$

and substituting equation (C.2) for Z yields:

$$Q(R) = K_R \frac{(R+a)}{(R+b)} q(R) \tag{C.4}$$

where

$$K_R = K \frac{(1-a')}{(1-b')} = V_0 \frac{(1-V_1/V_0)}{(1-W_1)}$$

$$a = \frac{(1+a')}{(1-a')} = \frac{(1+V_1/V_0)}{(1-V_1/V_0)} \tag{C.5}$$

$$b = \frac{(1+b')}{(1-b')} = \frac{(1+W_1)}{(1-W_1)}$$

The frequency response to a sinusoidal input, $q(t) = \text{Sin } \upsilon t$ can be obtained by the standard procedures using the R-transform, equation (C.4). Thus a frequency/amplitude plot can be generated by letting $R = j\upsilon$.

In general, if a system transfer function is:

$$G(j\upsilon) = C\frac{(j\nu + Ze)}{(j\nu + Po)} \tag{C.6}$$

where Ze represents a zero position and Po is the pole position, the corresponding amplitude ratio for a unit magnitude sinusoidal input would be:

$$M = C \left(\frac{\nu^2 + Ze^2}{\upsilon^2 + Po^2}\right)^{1/2} \tag{C.7}$$

A Bode diagram approach can be used to relate the frequency to the amplitude ratio. Simplification of the analysis results when one employs the well known asymptotic relationships, for example, with:

$$\upsilon = 0 \qquad M = C \frac{Ze}{Po} \tag{C.8}$$

$$\upsilon = \infty \qquad M = C$$

From equations (C.4) and (C.5) and realizing that $V_1 = (1+W_1)-V_0$, this implies:

$$\upsilon = 0 \qquad M = 1.0 \tag{C.9}$$

$$\upsilon = \infty \qquad M = \frac{2V_0 - (1 + W_1)}{(1 - W_1)}$$

Using these asymtotes and realizing that the break frequency positions would be at $\upsilon = b$ and $\upsilon = a$ (see equations C.5), a generalized Bode diagram can be constructed from which the real frequency response can easily be obtained by application of a 3 db correction at each breakpoint. Figure C.1 presents such a composite amplitude ratio plot relating values of V_0 and W_1 to the frequency and amplitude ratio. The common ratio or W_1 weighting factor can be directly related to the frequency since the pole position or (b) root in equation (C.4) is strictly dependent on W_1. The second breakpoint or (a) root is obtained from expression (C.9) for $\upsilon = \infty$. Figure C.2 shows the corresponding composite asymtotic phase diagram in which:

$$\phi = \text{Tan}^{-1}\left(\frac{\upsilon}{a}\right) - \tan^{-1}\left(\frac{\upsilon}{b}\right) \tag{C.10}$$

To realize the application of these curves, consider figure (C.3) which presents the load time responses of a room of both lightweight and heavyweight construction to a unit sinusoidal radiation input with a period of 24 hours. The weighting factors used to generate the responses are also listed on the figure. To preclude the need for generating such a sinusoidal response, one can use the procedure shown on figures (C.4) and (C.5) to obtain essentially the same information without resorting to a time response generating program. Figure (C.4) presents the amplitude ratio for varying input excitation frequencies resulting from application of the techniques discussed herein. The low frequency asymptotic value is 1.0 (see equation (C.9) and figure (C.1)). The intermediate frequency approximation is the 20 db/decade slope between the two breakpoint positions; and the high frequency

asymptotic value is defined at the intersection of the V_0 and W_1 values (see figure C.1). Applying a 3 db correction at each breakpoint yields the real frequency response. The resultant amplitude ratio values for an input period of 24 hours agrees with the time response value. Figure C.5 presents the corresponding phase shift diagram, although in this case only the asymptotic approximation curve is shown. The development of the resultant curve follows from application of the techniques stated on figure C.2. By application of these methods, a direct comparison can be made of the relative amplitude and phase shift differences one can expect from varying sets of weighting factors. This information is very useful from the standpoint that for a space specific set of weighting factors, the expected damping and time displacement of, for example, solar radiation can be somewhat quantified and parametric studies run on the space properties.

2. Space Air Temperature

As presented in References [1] and [3] a transfer function relating load changes to space air temperature fluxuations can be written as follows:

$$\Delta Q(Z) = \frac{G_0 + G_1 Z^{-1} + G_2 Z^{-2}}{1 + P_1 Z^{-1}} \Delta T(Z) \qquad (C.11)$$

where

$\Delta T(Z)$ = air temperature excitation input Z-transform

$\Delta Q(Z)$ = load output Z-transform

G_0', G_1', G_2', P_1 = weighting factors from a previously computed load response to a limit air temperature input at zero conductance such that:

$$\sum_{j=1}^{3} G_j' = 0.0$$

By application of a conductance correction to account for temperature fluxuations from a reference state, the transfer function, K(Z), in equation (C.11) can be written as:

$$K(Z) = \frac{G_0' (1-Z^{-2})}{1 + P_1 Z^{-1}} + \frac{G_1' Z^{-1}(1-Z^{-1})}{1 + P_1 Z^{-1}} + K_t \qquad (C.12)$$

where K_t is the conductance in units of BTU/HR-°F and

$$G_0 = G_0' + K_t$$

$$G_1 = G_1' + P_1 \cdot K_t$$

$$G_2 = G_2'$$

Using the same precedure as presented in the previous section, i.e., transforming to the R-domain results in:

$$K(R) = K_R \frac{R^2 + (\frac{C+dC+b+a}{C-b})R + (\frac{Cd}{C-b})}{(R+1)(R+d)} \qquad (C.13)$$

where

$$a = \frac{4G_0'}{1-P_1} \qquad b = \frac{2G_1}{1-P_1} \qquad C = K_t \qquad (C.14)$$

$$d = \frac{1+P_1}{1-P_1}$$

$$K_R = C-b$$

As in the radiation weighting factor case, a Bode diagram can be constructed for this transfer function using asymtotic approximation methods. The second order zero expression in (C.14) can be written as:

$$R^2 + 2\xi\omega_n R + \omega_n^2 \qquad (C.15)$$

thus

$$\omega_n = \sqrt{\frac{Cd}{C-b}}$$

$$2\xi\omega_n = \frac{C + dC + b + a}{C - b} \qquad (C.16)$$

The amplitude ratios corresponding to υ near zero and infinity would be:

$$\upsilon = 0 \qquad M = \frac{K_R \omega_N^2}{d} \qquad (C.17)$$

$$\upsilon = \infty \qquad M = K_R$$

From equations (C.14) this implies:

$$\upsilon = 0 \qquad M = K_t \qquad (C.18)$$

$$\upsilon = \infty \qquad M = K_t - \frac{2G_1'}{1-P_1}$$

Results from the parametric study discussed in Section D herein indicate that a simplification of equation (C.13) is possible. Because of the nature of the room response to a unit excitation as used in the generation of the space air temperature weighting factors, the damping associated with the second order expression ($2\xi\omega_n$) in equation (C.15) was in all cases much larger than the corresponding frequency term (ω_n^2) and its value was of the order of 1.0. Thus equation (C.15) can be approximated by the two first order roots:

$$(R+1)\ (R+\omega_n^2) \qquad (C.19)$$

and the corresponding transfer function, equation (C.13) can be written as:

$$K(R) = K_R \frac{(R + \frac{Cd}{C-b})}{R + d} \qquad (C.20)$$

The breakpoint positions for the frequency response would occur at:

$$\nu = \frac{Cd}{C-b} \qquad \text{and} \qquad \nu = d$$

FIGURE C.1 - COMPOSITE AMPLITUDE RATIO vs FREQUENCY FOR A UNIT RADIATION SINUSOID INPUT

Low Frequency Asymtote is 1.0 at intersection of W_1 and $A_o/A_i = 1.0$

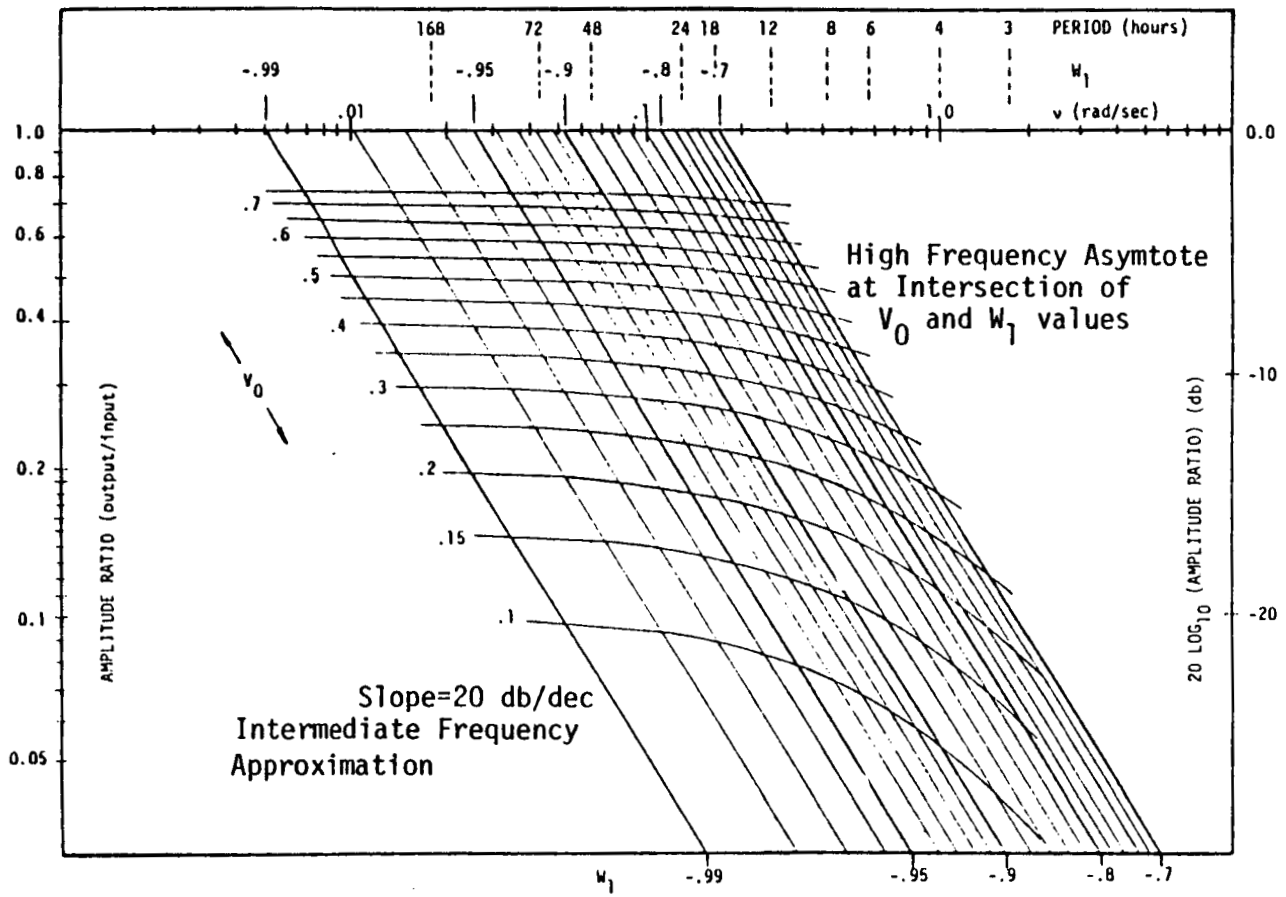

FIGURE C.2 - COMPOSITE PHASE ANGLE vs FREQUENCY FOR A UNIT RADIATION SINUSOID INPUT

Low Frequency Asymtote is 0.0 at Intersection of W_1 and Phase Angle = 0.0

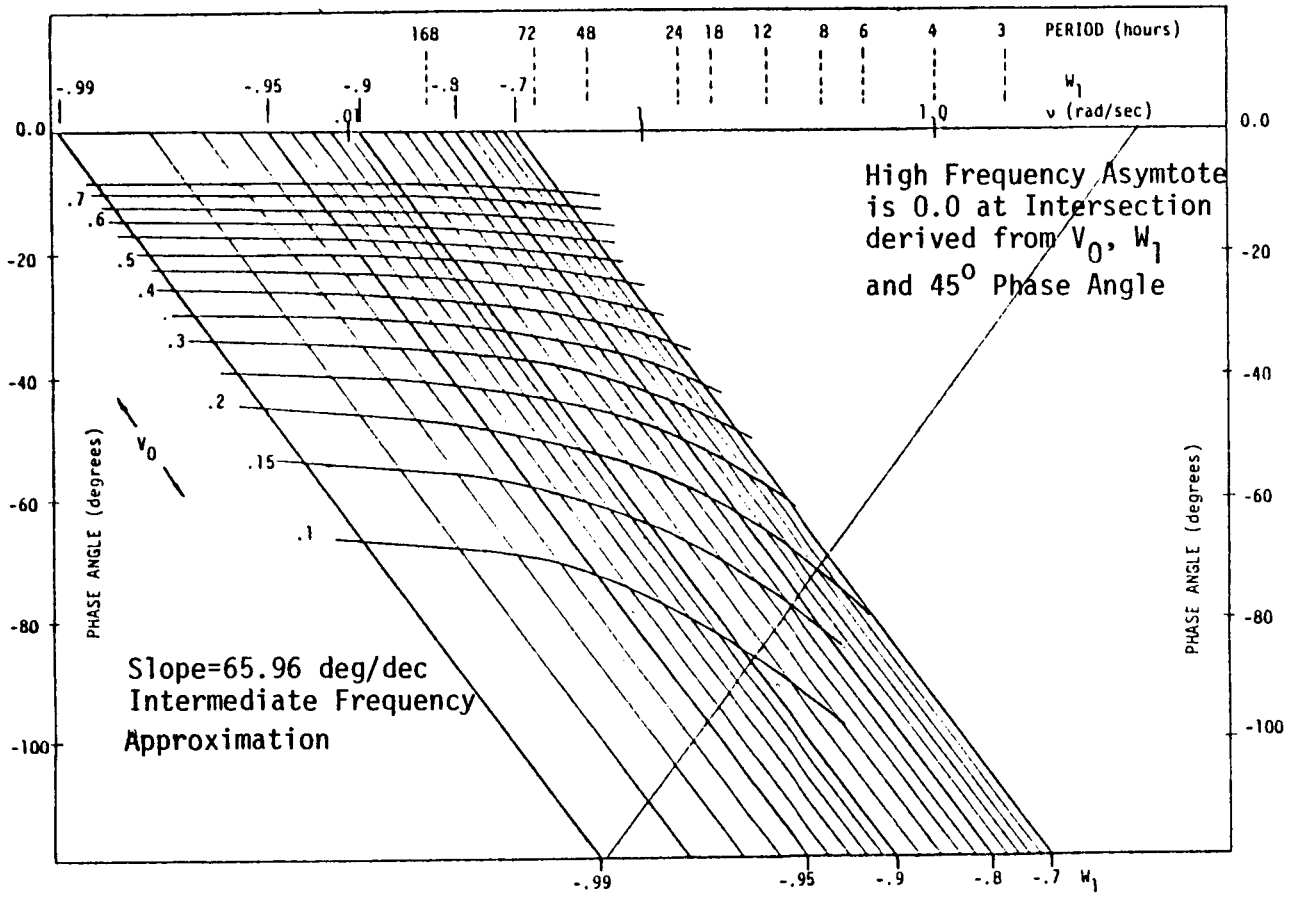

FIGURE C.3 - TIME RESPONSE FOR A UNIT SINUSOIDAL RADIATION INPUT

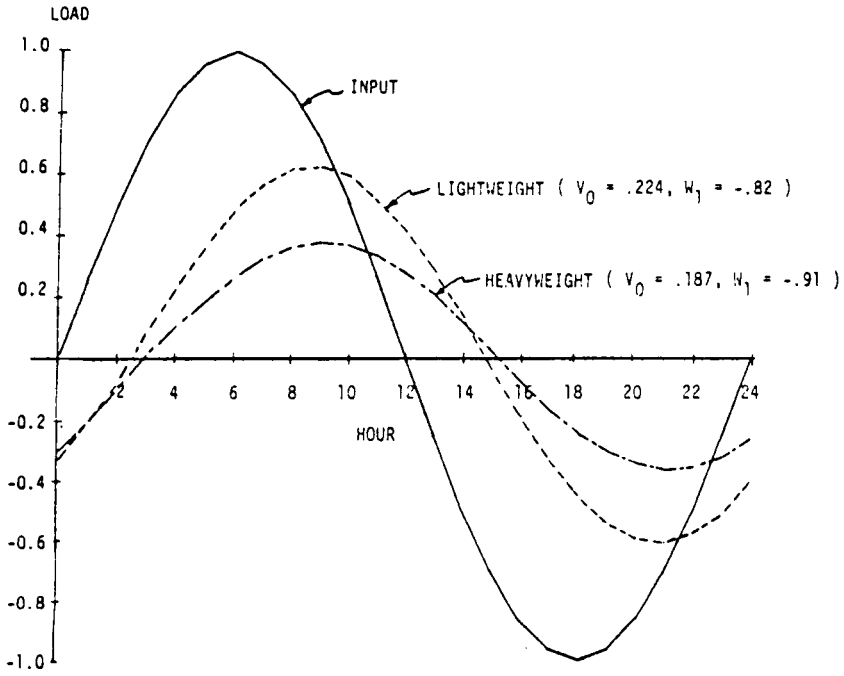

FIGURE C.4 - RESPONSE AMPLITUDE RATIO vs FREQUENCY FOR A UNIT RADIATION SINUSOID INPUT

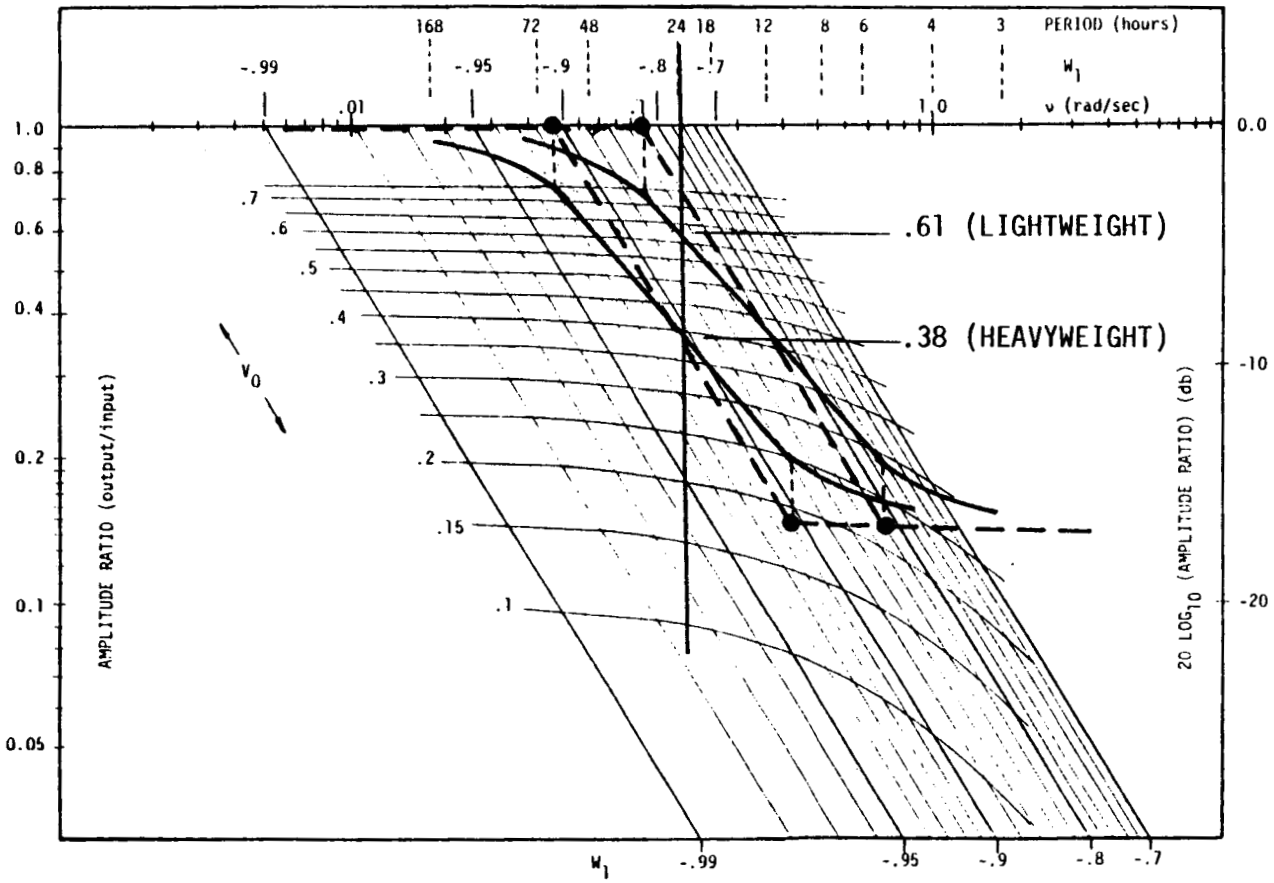

FIGURE C.5 - RESPONSE PHASE ANGLE vs FREQUENCY FOR A UNIT RADIATION SINUSOID INPUT

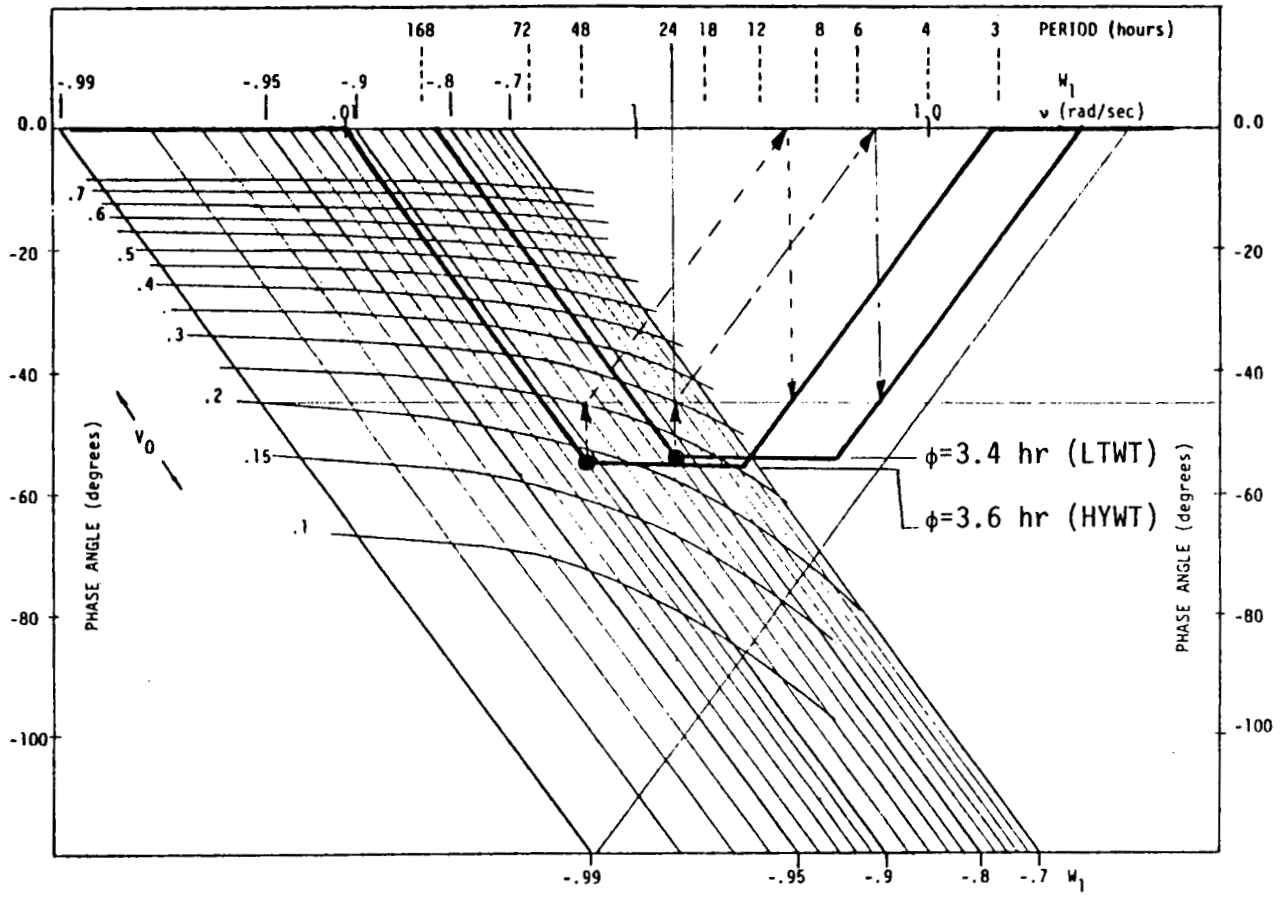

D. SENSITIVITY STUDY

This section discusses the results of a sensitivity study made to provide insight into the effects of various parameters which influence the magnitude of room response characteristics. A structure similar to the BR202 space defined in Reference 1 was used as a baseline from which room dimensions and specific wall characteristics were perturbed. Figure D.1 presents a description of the space which consisted of a south facing wall composed of concrete and insulation with a window covering approximately 41% of the wall area; a north facing wall constructed of brick and plaster; east and west facing partition walls; and a floor and ceiling constructed of concrete and tile. The room was assumed to be surrounded on all sides by similar spaces with the exception of the south facing wall.

The recursion relationship used for generating space specific weighting factors (see Reference 1) was used to obtain the room response and weighting factors for both radiation and air temperature pulses. Figure D.2 presents a description of the flow used for the analysis. For the radiation pulse study, the distrubution of the radiation was designated as the outermost element. Within this loop were contained two distinct sets of parametrics: a variation on room size for various floor thickness, conductivity and density values; and a parametric on both floor and ceiling inside convection coefficient quantities for a designated base case. The air temperature pulse study included each of the above, also, with the exception that the distribution function was of course unnecessary.

The discussion to follow relates the results of the radiation pulse and room air pulse analysis separately, although certain conclusions concerning the effect of a particular parameter are the same for both cases. Appendix H.1 contains tabulated data reflecting the specific values of the weighting factors generated for each parameter varied.

1. Radiation Pulse Analysis

The space heating/cooling load at any time, t, due to a radiative heat gain can be obtained by convolution with a set of previously tabulated weighting factors which relate the load response due to a unit input heat gain/loss (see Reference 1). An equation such as:

$$Q(t) = \sum_{j=0}^{k} V(j)q(t-j) + \sum_{j=1}^{k-1} W(j)Q(t-j) \qquad (D.1)$$

represents such a convolution, where the V(j) and W(j) are the weighting factors, q(t) represents the heat gain/loss and Q(t) the resultant load. Much of the past work in the development of weighting factors (see References 4 and 7) has concentrated on the V_0 and W_1 terms in the above expression. V_0 is, in fact, the response value at t=0 (i.e. Q(0)) for a unit pulse input (q(0)=1); W_1 the common ratio which is the ratio of succeeding response values when that ratio reaches a constant value. Because of the large number of perturbations made to the parameters studied herein, this analysis will also utilize these two variables to give an indication of expectant radiative load response. It should be noted that k in expression (D.1) should be of the order of 2 or possibly 3. This is particularly important for highly delayed surfaces in which the response factor common ratio isn't established until t > 10. Additional information regarding this fact is given in Section E of this report.

For a unit pulse heat gain input, the load response itself should equal unity. However, because of the conductance associated with the particular construction utilized, losses are experienced such that the instantaneous load, integrated over time is less than one. However, when generating weighting factors the losses are accounted for by defining the V_1 term to be:

$$V_1 = 1 - V_0 + W_1 \qquad (D.2)$$

This procedure ensures system stability and thus as discussed in Section C of this report, Figures C.1 and C.2 can be used to ascertain

approximate values of expected amplitude ratio and phase shift due to a sinusoidal input function. Intuitively, one would expect the loss function to increase with time such that at t=0 there are no losses and therefore the V_0 term in conjunction with the common ratio would adequately approximate the expected response.

The distribution of radiative type heat gains is directly related to the source of the radiation. Typically, for a south facing window, for example, one would expect the floor surface of a space to be affected by solar radiation more than the other surfaces within a space. Likewise for radiation arising from equipment and occupants within a space, a more evenly distributed situation would occur. In both instances, however, the floor characteristics exert a major influence on space load response. Thus, the discussion below details the sensitivity study results due to perturbations in the floor thickness, conductivity and density; after which, the variable inside convection coefficient results are analyzed. Lastly, the distribution of radiation and room size characteristics are presented. The specific radiation distribution used for the variable properties presentation was one in which eighty percent of the total was input to the floor and the remaining twenty percent distributed uniformly by surface area. This situation would represent a response to a direct solar radiation input heat gain. The resultant trend in load response, however, would also be valid for an evenly distributed pulse. The baseline space is as defined in Figure D.1.

(a) Floor Properties

Figures D.3, D.4, and D.5 present the time response for a unit pulse input for varying thickness, conductivity and density of the floor surface. The corresponding composite amplitude ratio and phase shift diagrams are shown on Figures D.6 and D.7. As one would expect with increasing thickness and decreasing conductivity the amplitude ratio decreases and phase shift increases.

This is easily seen by application of the techniques discussed in Section C, which for illustrative purposes, Figures D.8 and D.9 are presented for the two endpoints in the thickness variation. One of the most interesting trends as seen on Figure D.6 and tabulated in Appendix H.1 is the insensitivity of the V_0 coefficient for varying thickness. In each case studied, for thickness greater than .333', the V_0 value is constant. The variation of thickness with common ratio for the baseline configuration is presented on Figure D.10. A linear relationship exists between these two variables for the situation where V_0 is varying (low value of thickness and common ratio). As the thickness increases and the response becomes more delayed (see Figure D.3) an asymtotic relationship becomes apparent. Thus, for very large subsequent changes in thickness, the common ratio change is minimal. Since the common ratio appears to be related to the delay in response, i.e., high common ratios ($W_1 > .9$) imply more delay, this limit in common ratio also implies a limit in the expected amount of delay. This is somewhat important for passive solar structures because the delay is proportional to the phase shift characteristics of the response.

The conductivity variation in the floor surface affects both the V_0 and W_1 coefficients as seen on Figure D.6. The corresponding amplitude ratio and phase shift change for the two endpoints are not as large as those values associated with varying thickness (see Figures D.11 and D.12); however, some measure of control is prevalent. Since the conductivity is directly related to the first value of tne internal response factor of the surface which in turn is inversely related to the initial response through the $[C]^{-1}$ matrix (see Reference 1), low conductivities imply large initial responses; therefore the increase in delay that results from a reduced conductivity is counterbalanced by an increased initial response. The actual variation in V_0 and W_1 with conductivity is presented on Figure D.13. The aforementioned inverse relationship with V_0 is easily apparent.

Perhaps the most confusing parameter analyzed was the density of the floor surface. As seen on Figure D.6 and D.14, the density is also inversely related to the initial response value, V_0. However, the common ratio trend is not as straightforward. Both above and below a certain minimum density any change in density subsequently increases the resultant W_1 value and thus reduces the amplitude ratio. This is to be expected for increasing density and at the present time no explanation can be given for the same occurrence for low density values. The amplitude ratio and phase shift characteristics are shown on Figures D.15 and D.16 for the endpoints.

The conclusions to be drawn from the floor properties study are as follows:

(1) The thickness of the surface appears to exercise the most control over the resultant load response, particularly the delay in response associated with the common ratio term, W_1.

(2) The conductivity influences both the initial response V_0, and common ratio value. Since decreasing conductivity is associated with increasing V_0 and W_1, explicit control of the resultant response is not as clear cut as the thickness capability.

(3) The density likewise affects both V_0 and W_1. However, above a certain minimum density, the common ratio increases with decreasing initial response; thus a more positive passive solar load response can be obtained as expected for high densities.

(b) Floor/Ceiling Inside Convection Coefficients

The sensitivity of the space response due to variations in the floor/ceiling convection coefficients were analyzed in this portion of the study. As stated in Reference 7 the direction of

heat flow within a space in combination with the horizontal orientation of the floor/ceiling surfaces results in significant variations in the convection coefficient values. In this analysis, the floor coefficients were varied from h_{i_f} = .2 to h_{i_f} = 1.0 and the ceiling values from h_{i_c} = .162 to h_{i_c} = .7. Table H.1.7 contains the tabulated results of the weighting factors generated and Figure D.17 presents the responses for a unit radiation pulse input for the endpoints of the h_i envelope which is contained on Figure D.18. Also presented on this figure are the four possible heat flow characteristics. The amplitude and phase shift characteristics of the endpoints are shown on Figures D.19 and D.20.

Since the radiation distribution was primarily input to the floor surface (80%), the ceiling coefficient does not have much influence. However, as will be discussed later, for a more evenly distributed pulse, the ceiling value increases in importance. The maximum differences in amplitude ratio and phase shift for a sinusoidal input with a 24 hour period for the endooints are of the order of .2 and 2.1 hr respectively.

These results indicate that the inside convection coefficient values exercise a strong influence on resultant weighting factor values. Generation of space specific weighting factors should therefore be based on the expected air flow direction. Of primary importance is the effect the floor coefficient has on the resultant response.

(c) Space Size

One of the major uncertainties at the start of this analysis was the effect of space size changes on resultant load response values. Figure D.2 lists the perturbations applied to the space size values. The length and width variations ranged from 10' to 40' for square and rectangular shaped structures. The height was held constant at 10' and the ratio of window area to south wall area was maintained at 41%. As seen in Appendix H.1 the V_0 and W_1

variation for all cases tested was negligible, of the order of 5%. Figure D.21 presents a graphical display of the coefficient variations for changing floor properties and room sizes. A more significant effect was realized on the room air temperature factors which is discussed below.

(d) Radiation Distribution

As stated in Section D.1 of this report, the distribution of radiative heat gains is directly related to the source of radiation. The previous results have discussed a distribution in which 80% of the input was on the floor surface. To ensure as complete an analysis as possible, a distribution of radiation by surface area was also made for each of the previously discussed parameters.

The primary effect resulting from changing the distribution from the floor to the other surfaces was an increase in the initial response value, V_0, which for the same common ratio yields a higher amplitude ratio. Figure D.22 shows the variation of V_0 and W_1 for the two distributions studied to include the variation in thickness, conductivity and density of the floor surface for the base room size (20 x 20 x 10).

The actual response to a unit pulse input for the base case properties is presented on Figure D.23 and the resultant surface component contributions to the totals are shown on Figures D.24 and D.25. In both instances, the floor characteristics dominate the total response. However, for the evenly distributed case the other surfaces combine to generate a larger initial response. The resultant amplitude ratio and phase shift characteristics for the base case are as shown on Figures D.26 and D.27. The aforementioned increase in amplitude ratio for the evenly distributed case is approximately proportional to the ΔV_0 value while the phase angle difference is roughly 5° for the frequency

range of interest.

A much more significant effect due to the distribution of radiationis seen by considering Table H.1.7 in Appendix H.1 and Figure D.28 which includes the inside convection coefficient parametric variation for the floor and ceiling surfaces. For the evenly distributed pulse, the ceiling h_i value has a more pronounced effect on the initial response value, V_0. Therefore, the suggestion made in Section D.1.(b) regarding the calculation of specific weighting factors for each flow direction is additionally substantiated by these results.

This portion of the study indicates that:

(1) The distribution of radiation is important and that a well defined procedure should be used to determine the form of the distribution.

(2) The inside convection coefficients of the floor and ceiling and the calculated space specific weighting factors should be made variable to account for possible reversals in heat flow direction.

2. Space Air Temperature Pulse Analysis

The weighting factor technique of determining zone loads and temperatures is composed of two distinct phases: initially a constant space temperature thermal load profile is generated by convolution of the heat gain components with a set of radiation/conduction/convection weighting factors. The thermal load so generated is used in the second phase in which space temperature weighting factors are applied to determine the space temperature profile. This section discusses the results of the parametric study related to the generation of the space temperature weighting factors.

As stated in Reference 1, the space air temperature variation with heat extraction rate, in its simplest form, is represented by an expression such as:

$$\sum_{j=0}^{\infty} P_j \, \Delta Q(t-j) = \sum_{j=0}^{\infty} G_j \, \Delta T(t-j) \qquad (D.3)$$

Where the P_j and G_j are weighting factors, $\Delta T(t)$ is the temperature difference between a reference condition and the actual room temperature, and $\Delta Q(t)$ the thermal load variation. The G coefficients in expression (D.3) are determined by application of a conductance correction to a set of G' coefficients resulting from application of a unit air temperature pulse at zero conductance. This conductance correction accounts for temperature fluctuations from the reference value. A frequency domain analysis similar to that discussed for the radiation weighting factors was used to relate an input sinusoidal ΔT to the corresponding output ΔQ. The appropriate relationships for transforming from the Z plane to a continuous plane are given in Section C of this report.

Appendix H.1 contains the tabulated results of the parametric study. The same floor property perturbations discussed previously were applied in addition to the convection coefficient values of the floor and ceiling surfaces and the room size variations.

(a) Floor Properties

Figures D.29, D.30 and D.31 present the time response for a unit air temperature pulse input for varying thickness, conductivity and density of the floor surface. The response trends in each case are similar to those due to the radiation pulse previously analyzed. Application of the frequency response techniques discussed in Section C resulted in a transfer function (see equation (C.13)) consisting of a second order numerator expression and two first order denominator terms. However, the damping and low

frequency associated with the second order system resulted in a much more simplified transfer function consisting of a first order zero and pole, the values of which were a function of the response common ratio, conductance, and second response term (see Section C). In fact, the amplitude ratio asymptotic limits for $\nu = 0$ was the conductance of the space itself. For $\nu = \infty$ the value was a function of the three items mentioned above (see equation C.18)). In most cases tested, for the same room size, the limit variation was of the order of 7%. Thus the perturbations applied to thickness, conductivity, and density resulted in primarily frequency shifts with minimal impact on amplitude ratio and phase shift magnitudes. Figures D.32 through D.37 show the amplitude ratio and phase angle response characteristics for each of the end points in the parameter variations. As in the radiation pulse analysis, the thickness exercises the most influence. For frequencies with periods less than 12 hours and more than one month, varying thickness has no effect on the response. However, between these extremes, the thinner the floor surface, the less ΔQ resulting from a sinusoidal temperature input. For an input frequency of 48 hours, the ΔQ would be approximately 130 BTU/°F. This implies of course that the thicker walls tend to require more heat extraction/ventilation because of their increased absorption capability. The same is true for low conductive floors and high density floors although the effect is not as pronounced. The implication of these results indicate the following situation: thick, low conductive, high density floors tend to smooth out over time loads due to radiative heat gains which is a positive passive solar attribute; however, these same floors require more heat extraction/ventilation energy to maintain a constant room temperature.

(b) Floor/Ceiling Inside Convection Coefficients

Figure D.38 contains the amplitude ratio limit envelope due to the floor/ceiling convection coefficient perturbations. The

influence of the convection coefficient values is somewhat the same as the previously discussed radiation case. The ΔQ required per unit space air temperature input varies from approximately 30 BTU/°F for low frequencies to 350 BTU/°F at high frequencies for the baseline space definition. The amplitude ratio and phase shift for the two endpoints are shown on Figures D.39 and D.40. Calculation of the space air weighting factors as a function of airflow is recommended.

(c) Space Size

As in the radiation pulse analysis, the effect of space size on resultant room air temperature weighting factors was unknown. However, whereas the radiation factors indicated a minimal effect, the space air weighting factors were definitely influenced by size characteristics. As an example, consider Figure D.41 which presents the amplitude ratio asymtotic limit values for $\upsilon = 0$ and $\upsilon = \infty$ at varying room sizes using the baseline floor properties. The effect of the high conductance associated with the south facing window and thus the space width is immediately apparent, i.e., larger changes in limit values are prevalent with space width increments than with space length changes. This is particularly true for the low frequency situation. At high frequencies, changes in the length/width dimensions result in approximately the same amplitude ratio limit value. Thus, space sizing could be accomplished using the conductance quantity associated with the space.

FIGURE D.1 - BASELINE SPACE DESCRIPTION - PARAMETRIC STUDY

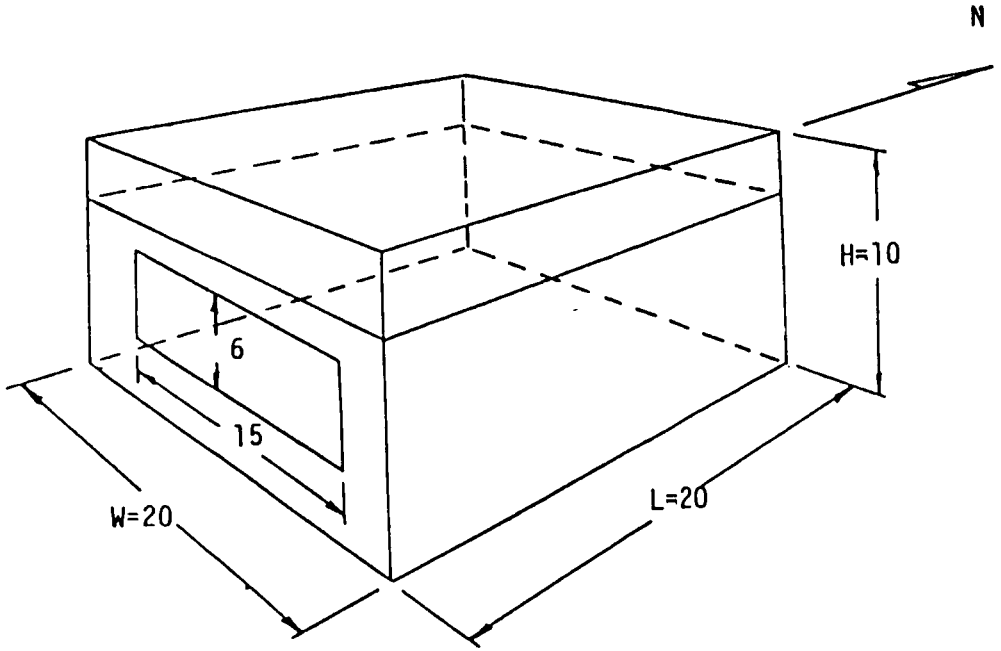

SURFACE	MATERIAL	THICKNESS (ft)	CONDUCTIVITY (Btu/hr-ft-°F)	DENSITY (lbs/ft³)	SPECIFIC HEAT (Btu/lb-°F)
South Wall	Out Film Resistance = .25				
	Concrete	.5	.75	140	.156
	Insulation	.0833	.35	20	.25
North Wall	Out Film Resistance = .715				
	Plaster	.0417	.42	100	.2
	Brick	.3333	.44	70	.156
	Plaster	.0417	.42	100	.2
East/West Wall	Partition	.1666	.167	90	.2
Ceiling	Acoustic Tile	.0625	.035	30	.2
Floor	Concrete	.3333	.75	140	.156
	Tile	Resistance = .08			
Window	Glass	Resistance = .514			

FIGURE D.2 - PARAMETRIC STUDY FLOW DIAGRAM

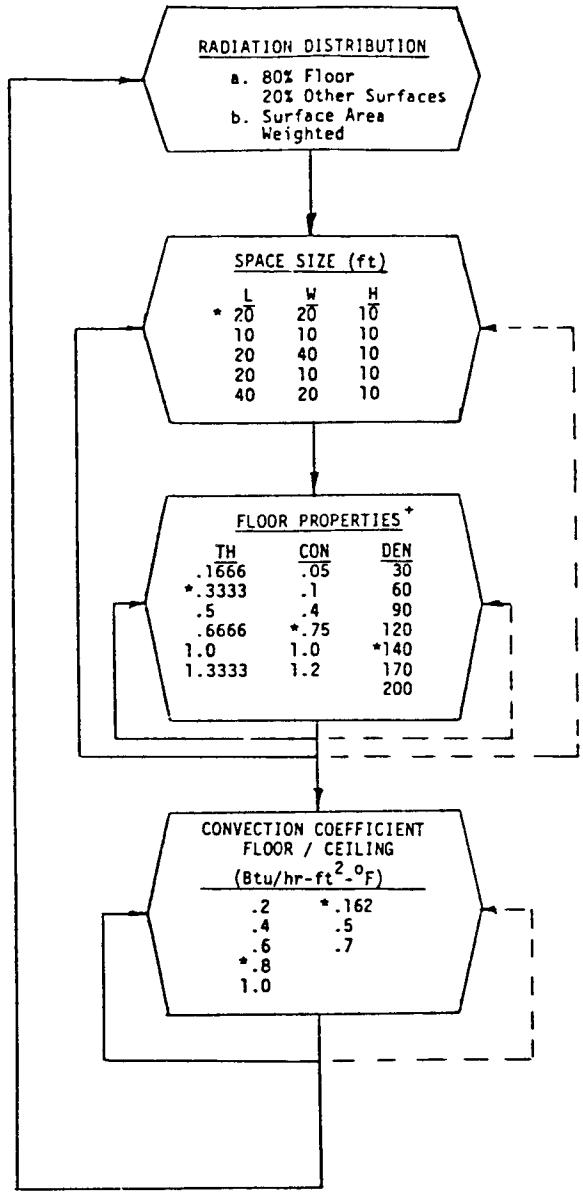

——— RADIATION PULSE PERTURBATIONS

– – – – – SPACE AIR TEMPERATURE PULSE PERTURBATIONS

• BASELINE SPACE VALUES

\+ UNITS: TH - ft
CON - Btu/hr-ft-°F
DEN - lb/ft^3

FIGURE D.3 - RESPONSE TO A UNIT RADIATION PULSE FOR VARYING FLOOR THICKNESS

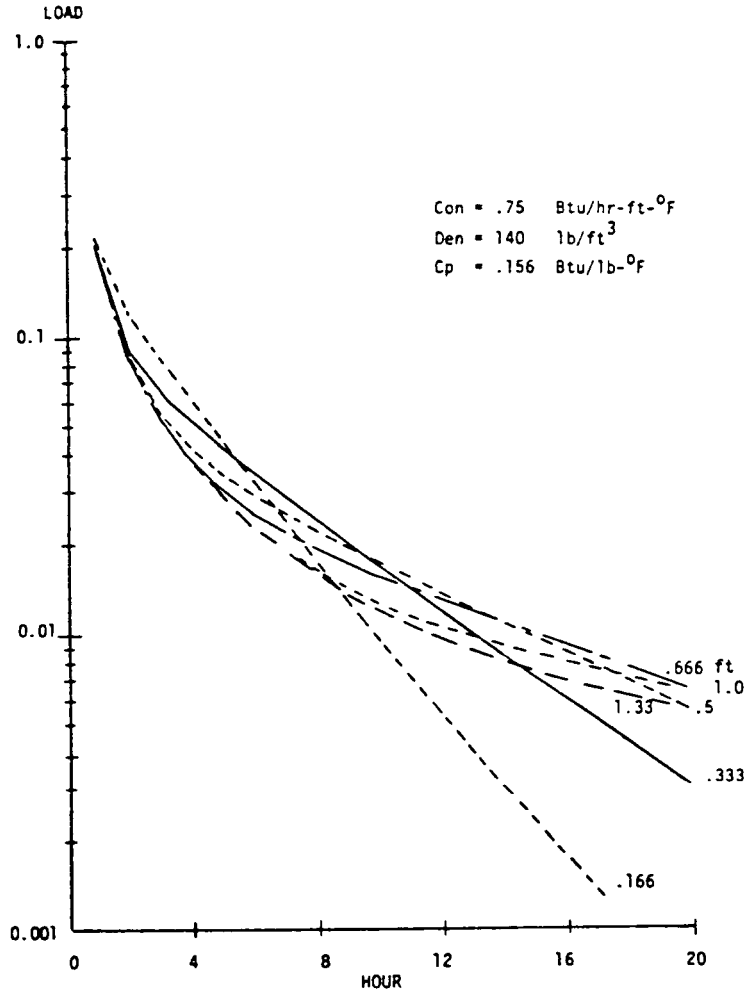

FIGURE D.4 - RESPONSE TO A UNIT RADIATION PULSE FOR VARYING FLOOR CONDUCTIVITY

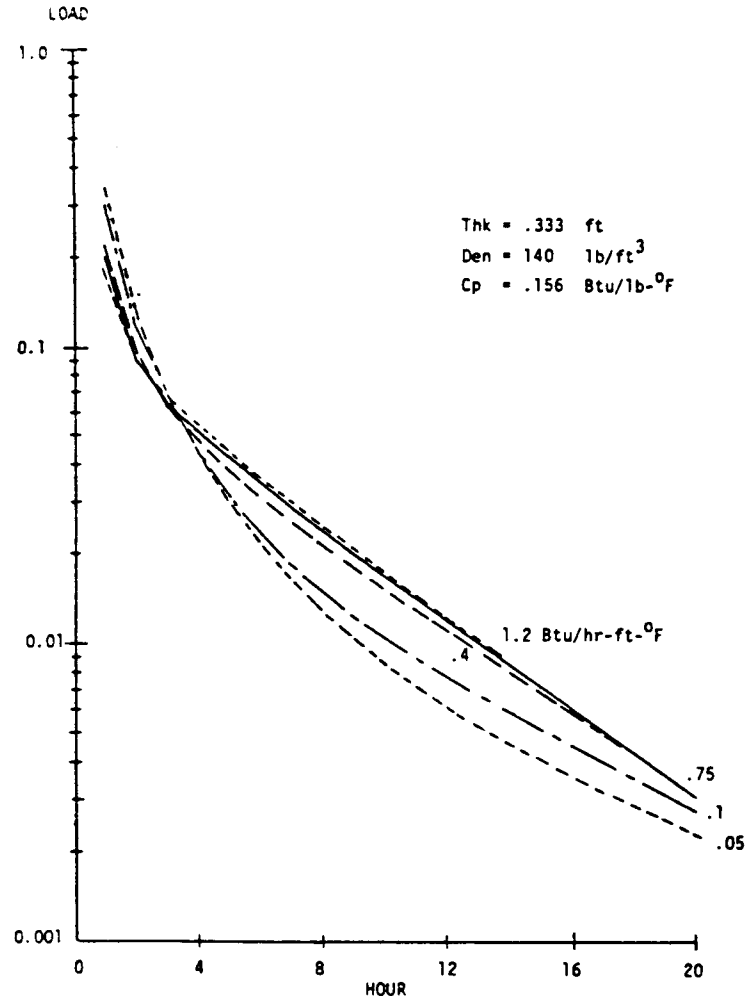

FIGURE D.5 - RESPONSE TO A UNIT RADIATION PULSE FOR VARYING FLOOR DENSITY

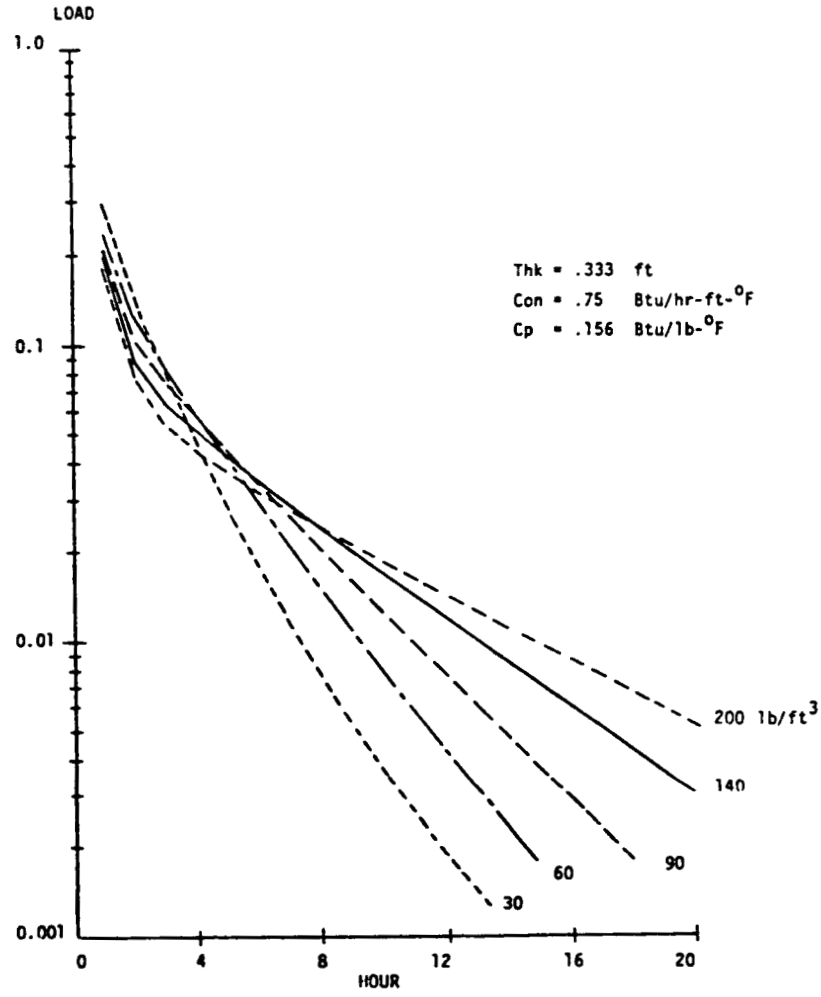

FIGURE D.6 - COMPOSITE RESPONSE AMPLITUDE RATIO vs FREQUENCY FOR A UNIT RADIATION INPUT FOR VARYING FLOOR THICKNESS, CONDUCTIVITY AND DENSITY

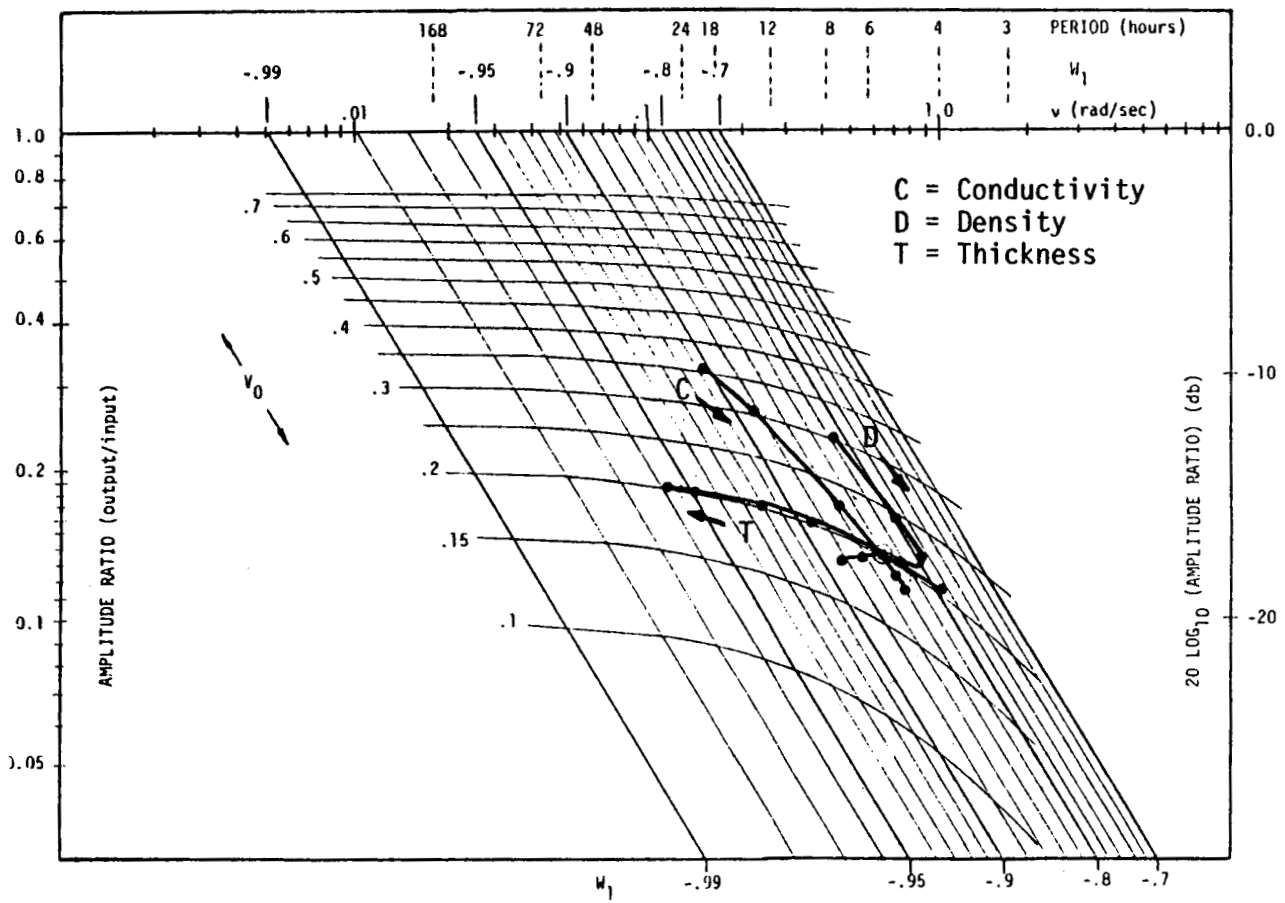

FIGURE D.7 - COMPOSITE RESPONSE PHASE ANGLE vs FREQUENCY FOR A UNIT RADIATION INPUT FOR VARYING FLOOR THICKNESS, CONDUCTIVITY AND DENSITY

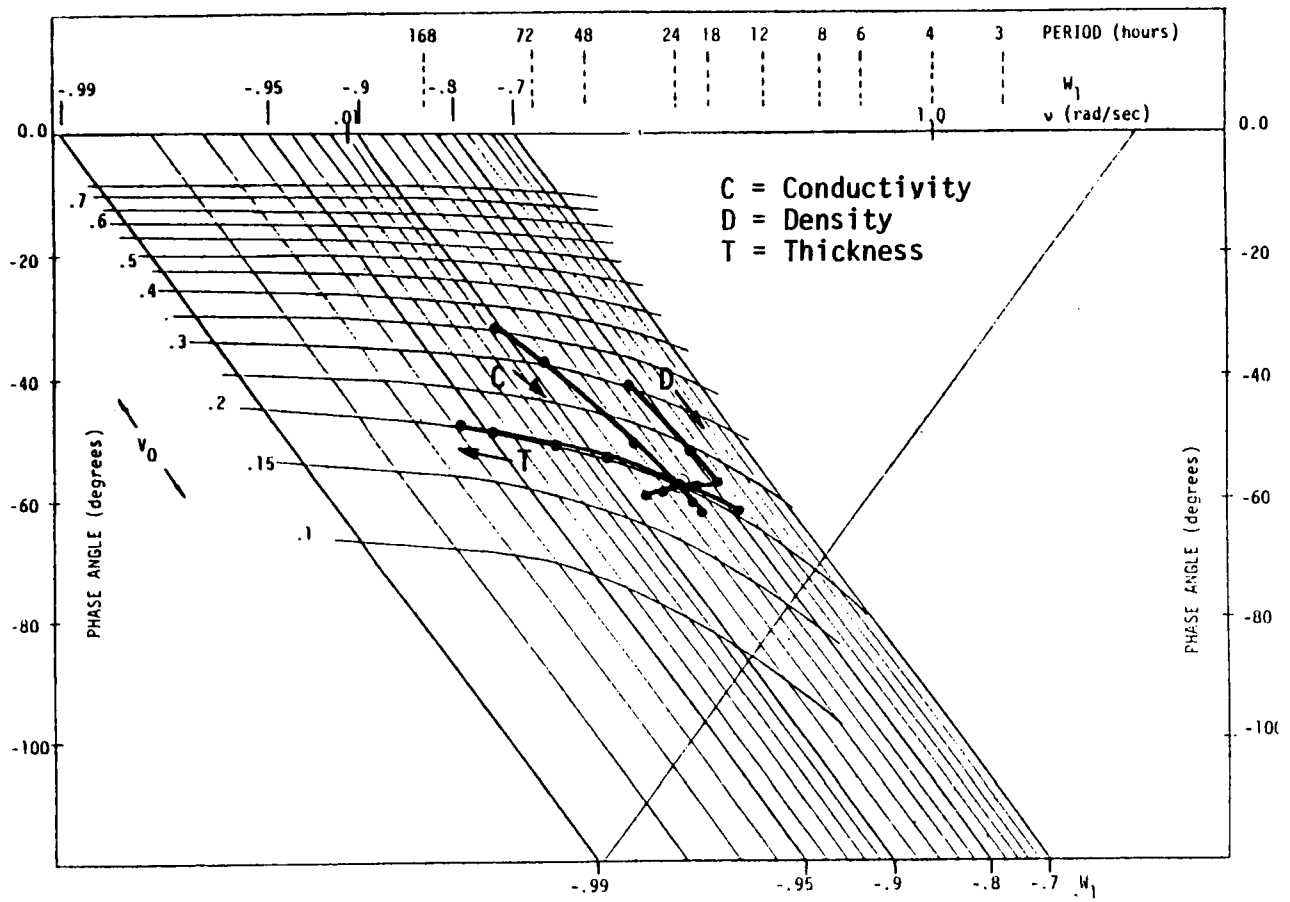

FIGURE D.8 - RESPONSE AMPLITUDE RATIO vs FREQUENCY FOR A UNIT RADIATION INPUT FOR VARYING FLOOR THICKNESS

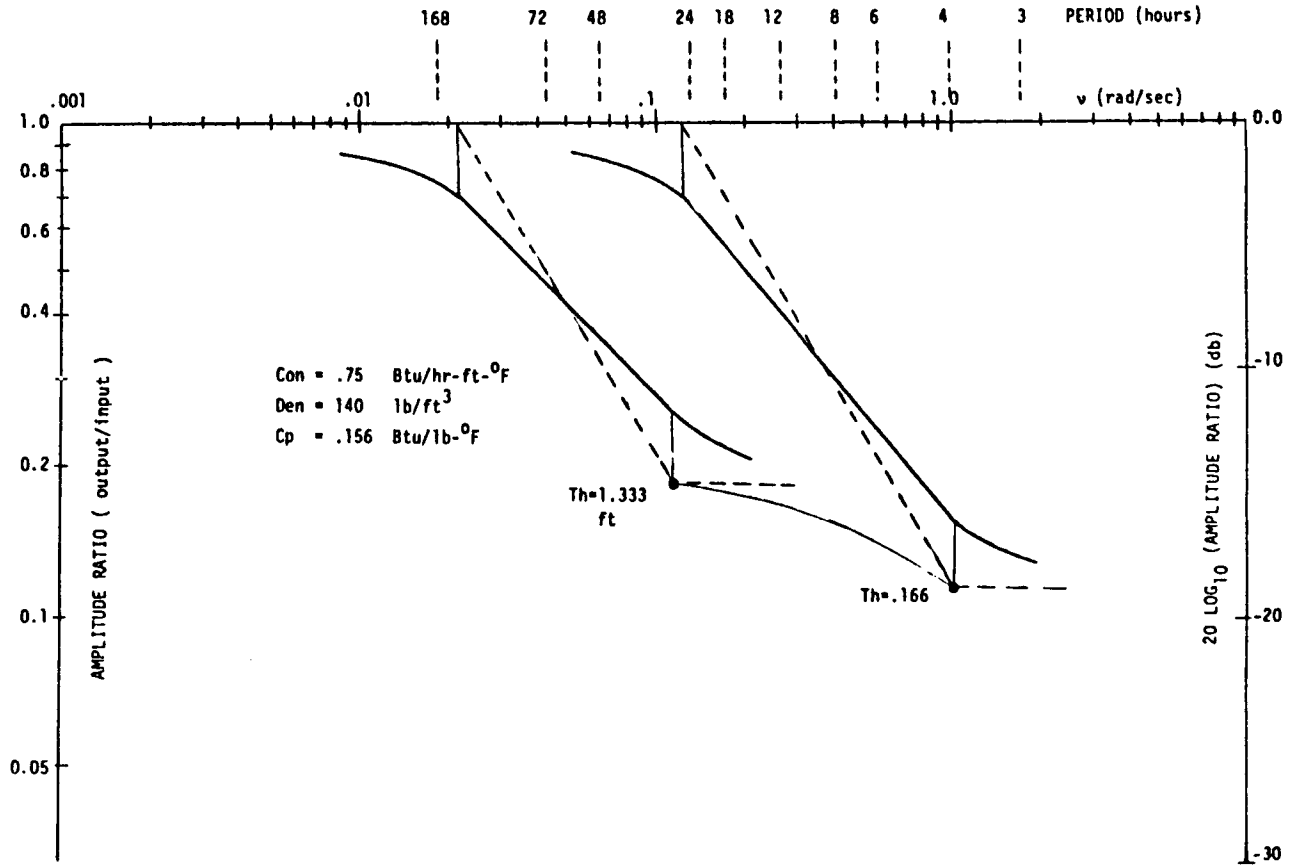

FIGURE D.9 - RESPONSE PHASE ANGLE vs FREQUENCY FOR A UNIT RADIATION INPUT FOR VARYING FLOOR THICKNESS

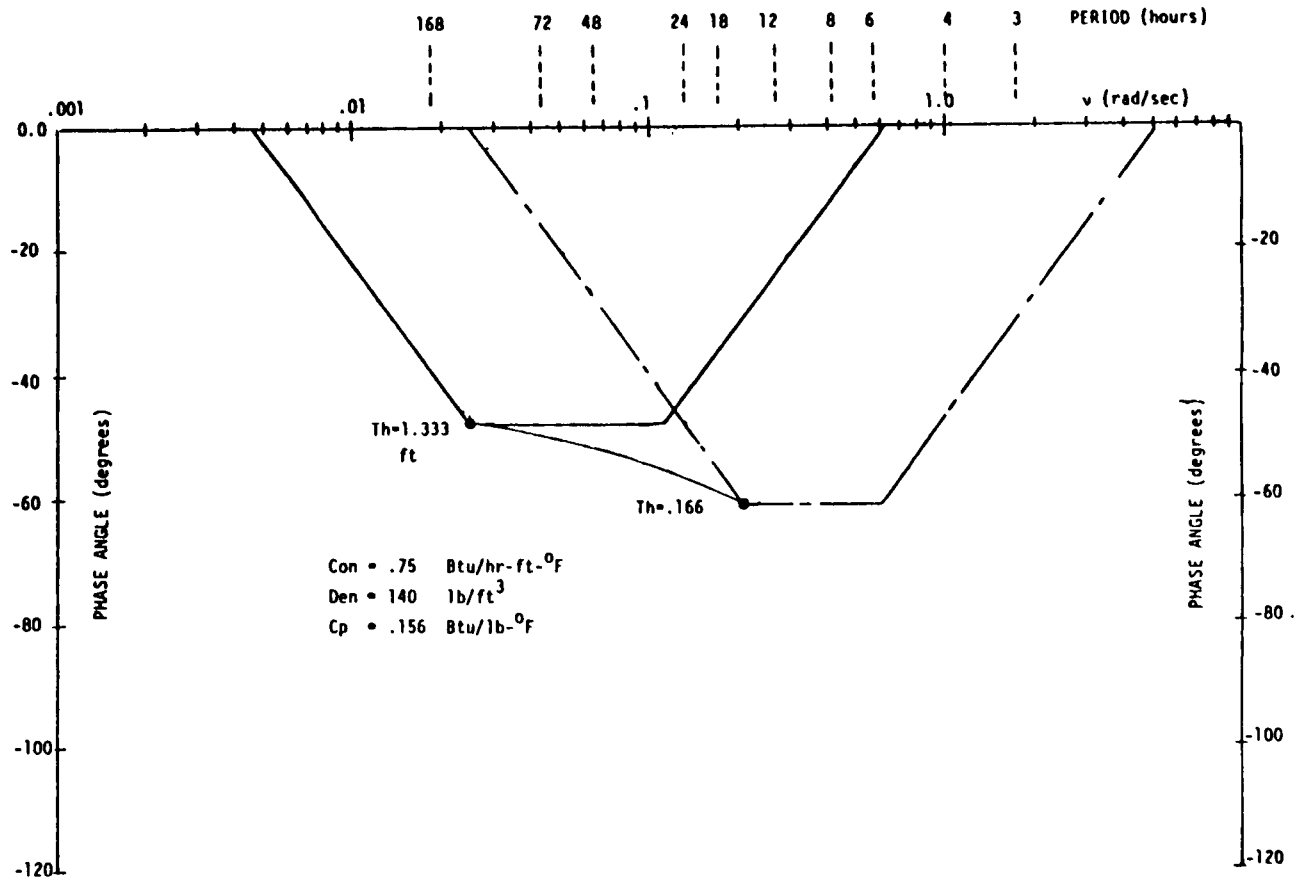

FIGURE D.10 - RESPONSE COMMON RATIO VARIATION WITH FLOOR THICKNESS FOR A UNIT RADIATION PULSE

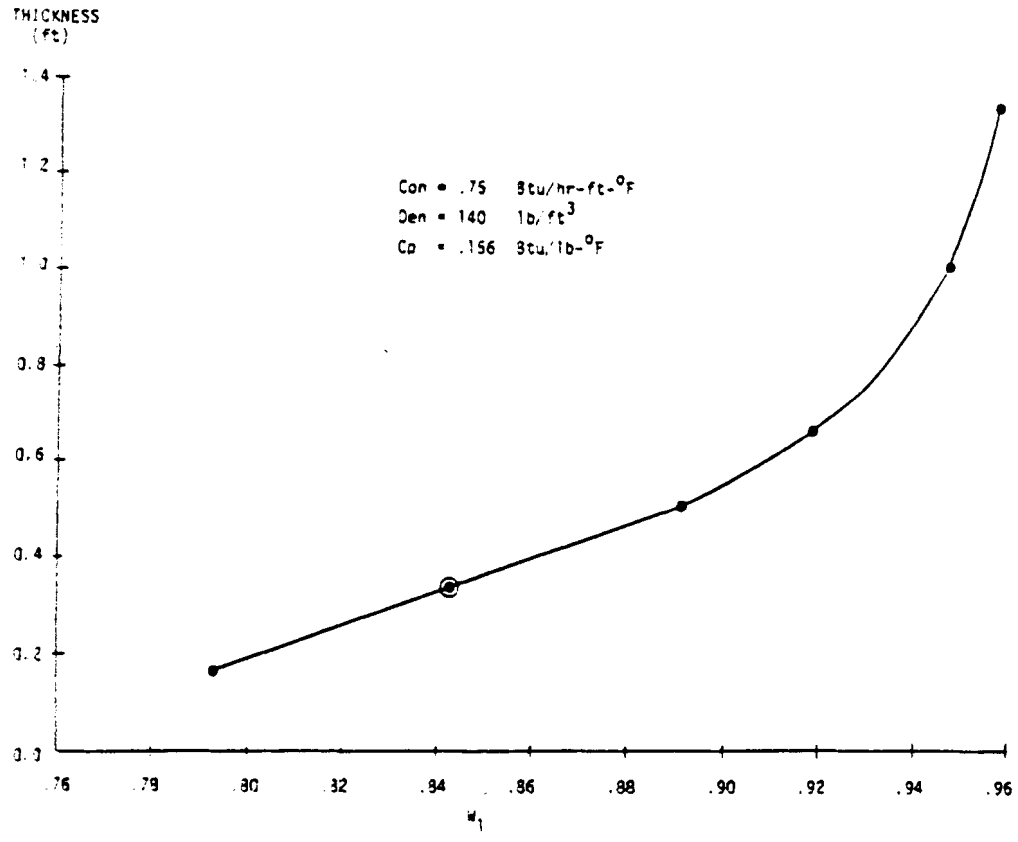

FIGURE D.11 - RESPONSE AMPLITUDE RATIO vs FREQUENCY FOR A UNIT RADIATION INPUT FOR VARYING FLOOR CONDUCTIVITY

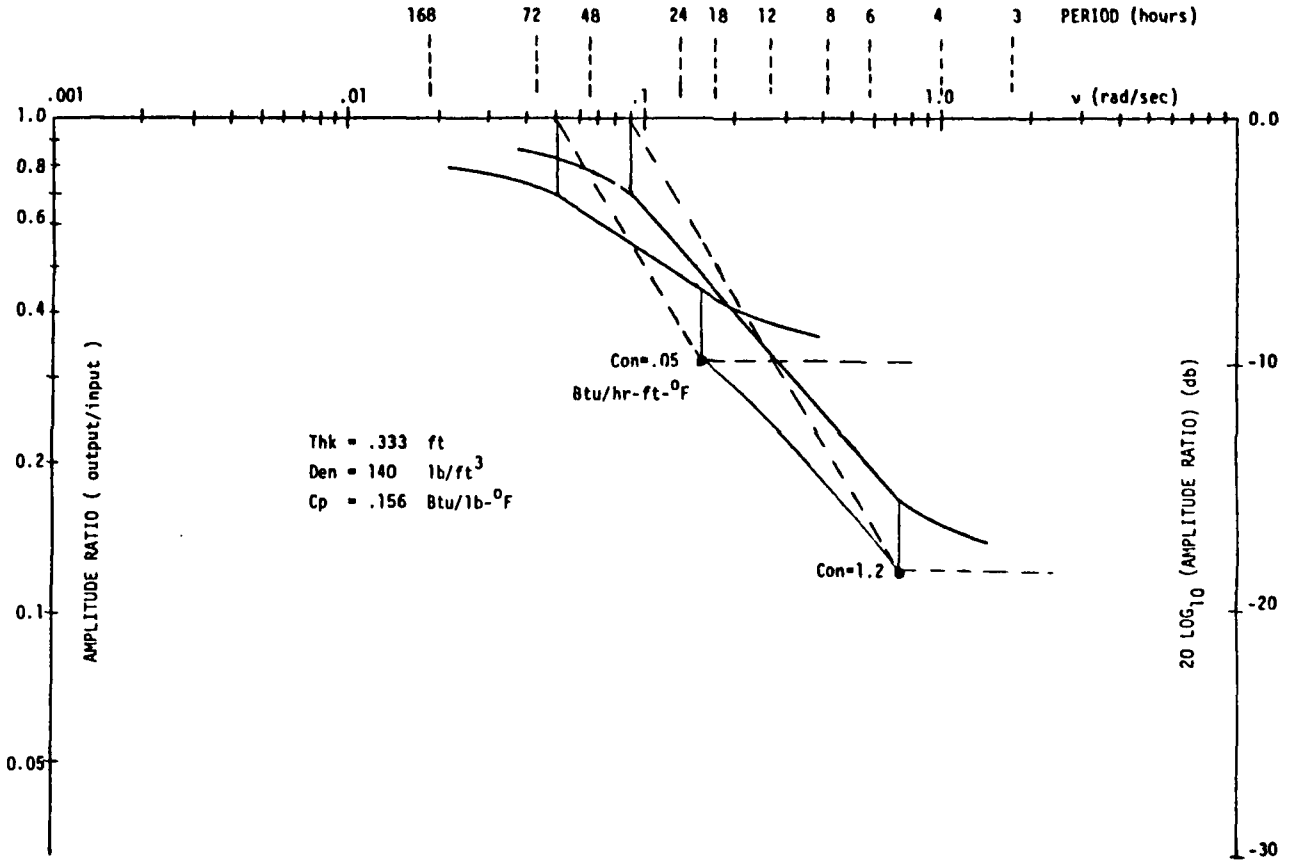

FIGURE D.12 - RESPONSE PHASE ANGLE vs FREQUENCY FOR A UNIT RADIATION INPUT FOR VARYING FLOOR CONDUCTIVITY

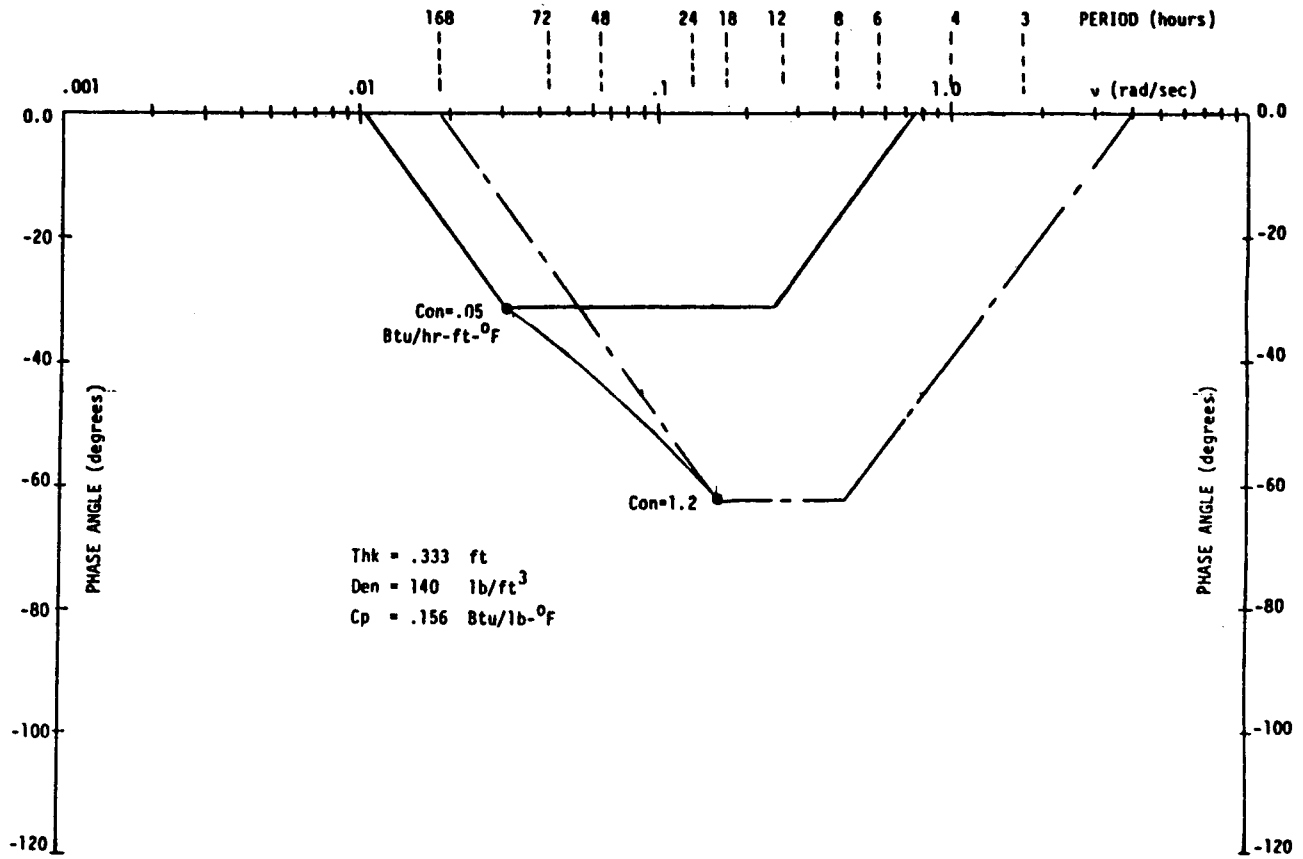

FIGURE D.13 - INITIAL RESPONSE AND COMMON RATIO VARIATION WITH FLOOR CONDUCTIVITY FOR A UNIT RADIATION PULSE

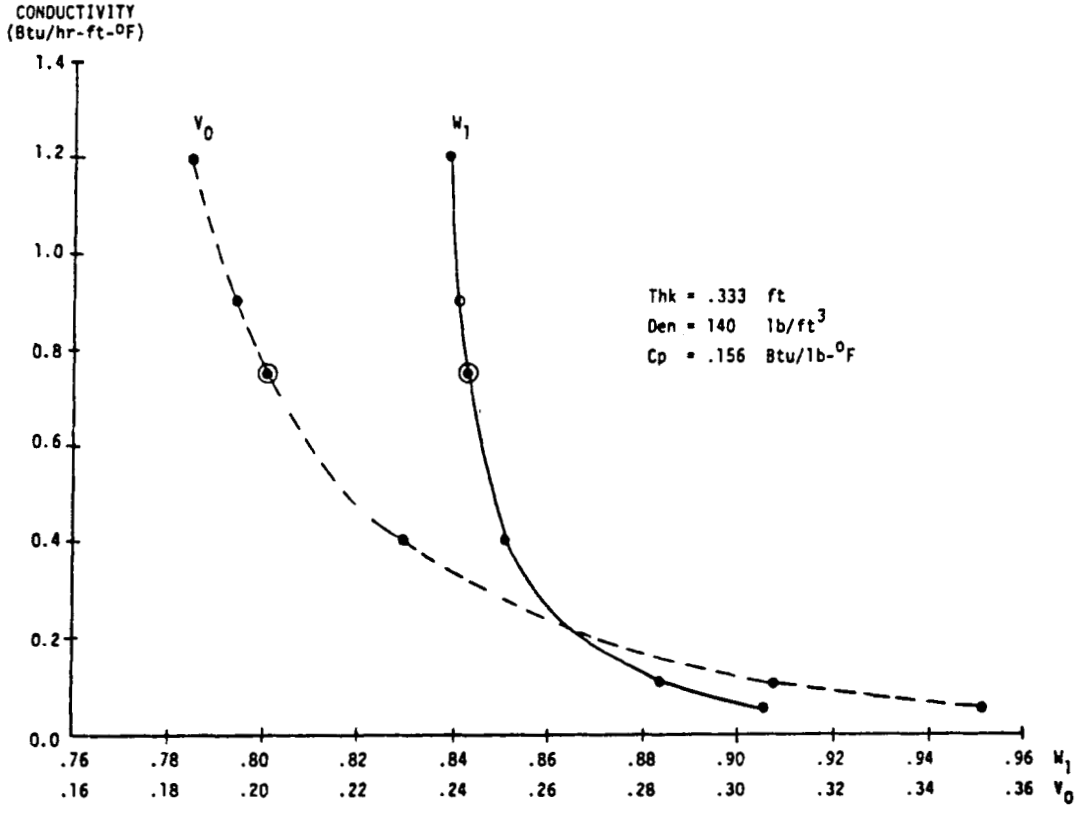

FIGURE D.14 - INITIAL RESPONSE AND COMMON RATIO VARIATION WITH FLOOR DENSITY FOR A UNIT RADIATION PULSE

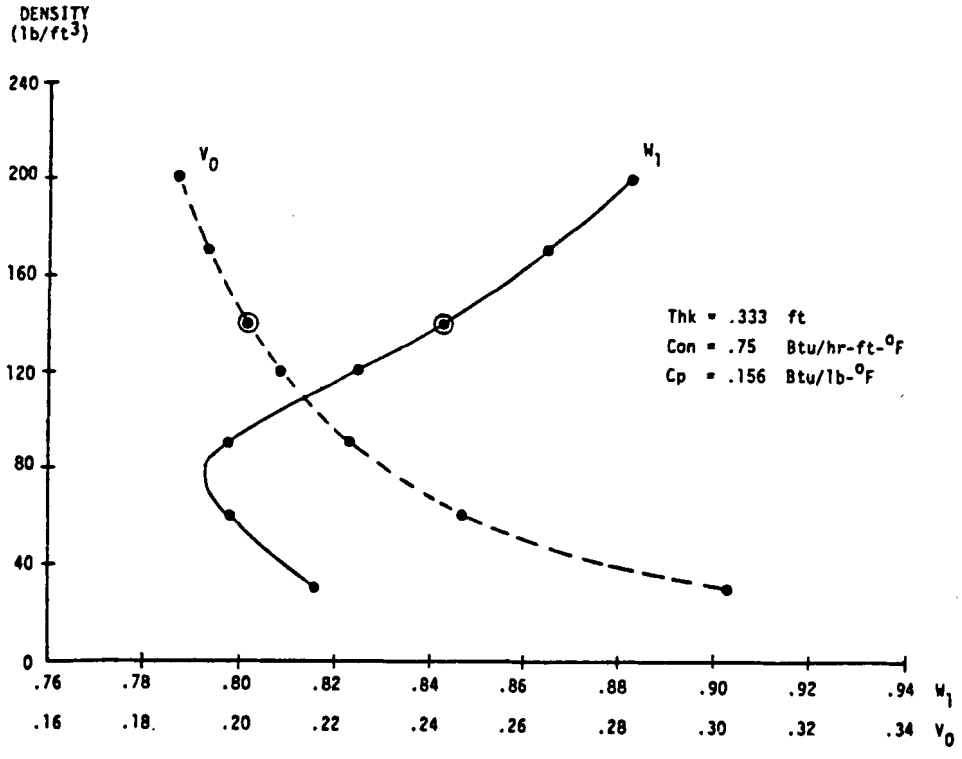

FIGURE D.15 - RESPONSE AMPLITUDE RATIO vs FREQUENCY FOR A UNIT RADIATION INPUT FOR VARYING FLOOR DENSITY

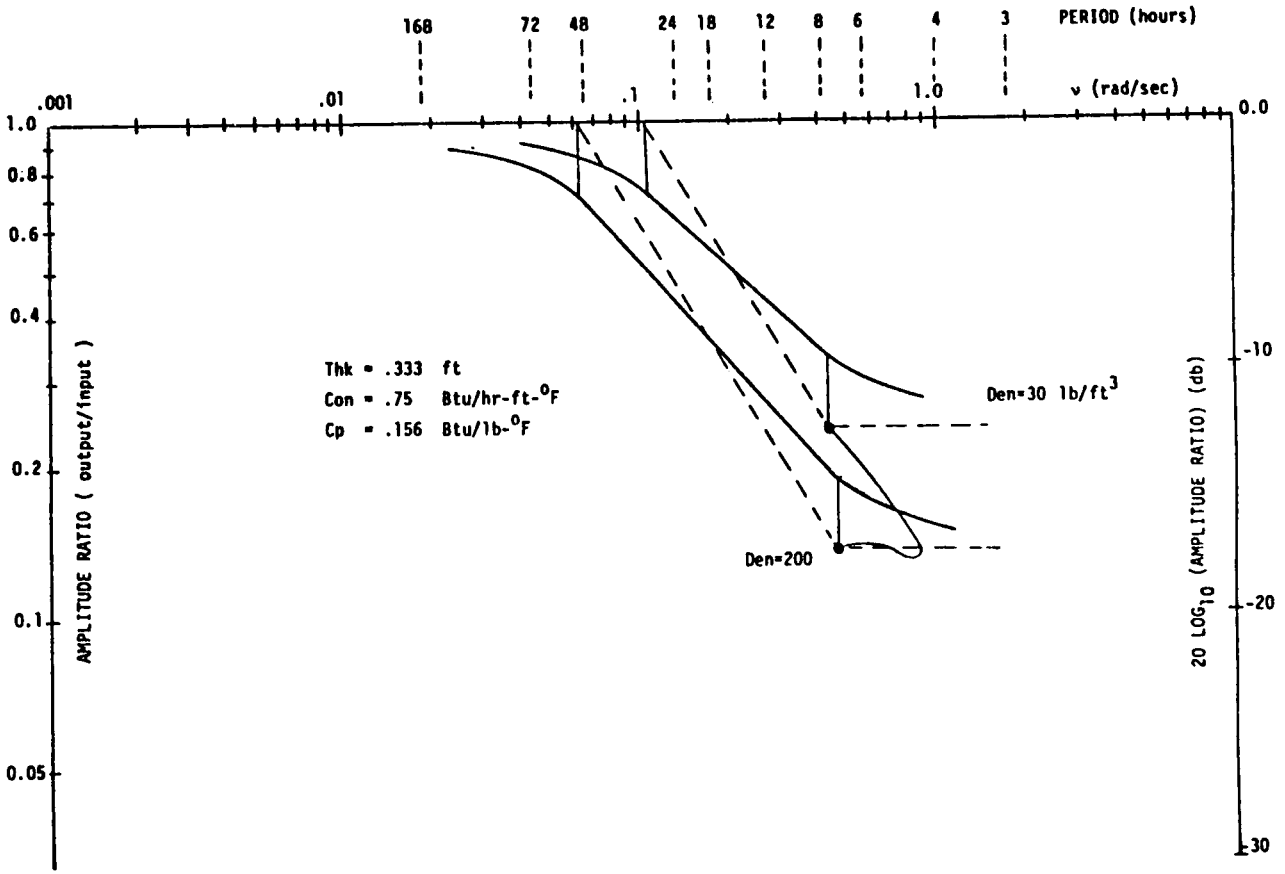

FIGURE D.16 - RESPONSE PHASE ANGLE vs FREQUENCY FOR A UNIT RADIATION INPUT FOR VARYING FLOOR DENSITY

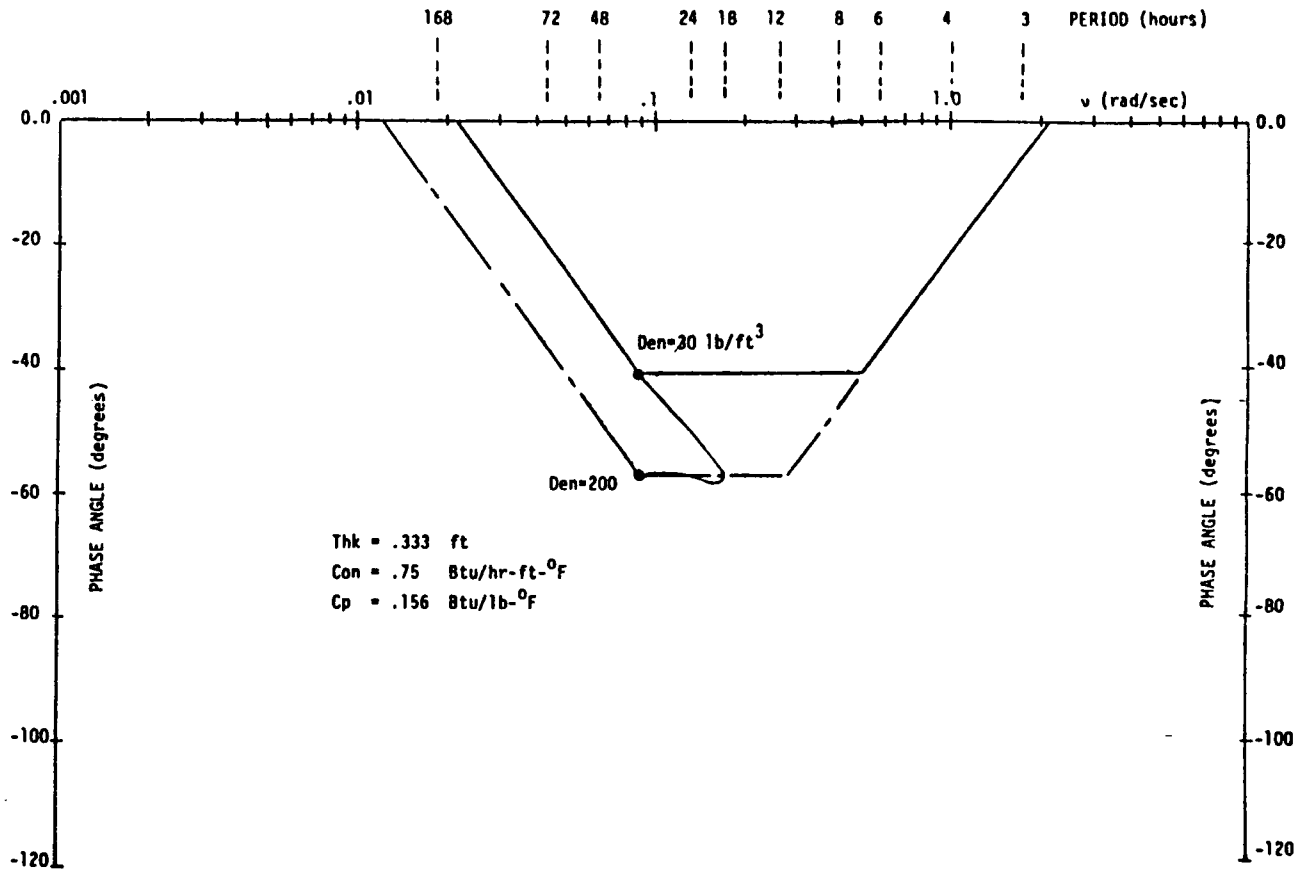

FIGURE D.17 - RESPONSE TO A UNIT RADIATION PULSE FOR VARYING FLOOR/CEILING CONVECTION COEFFICIENTS

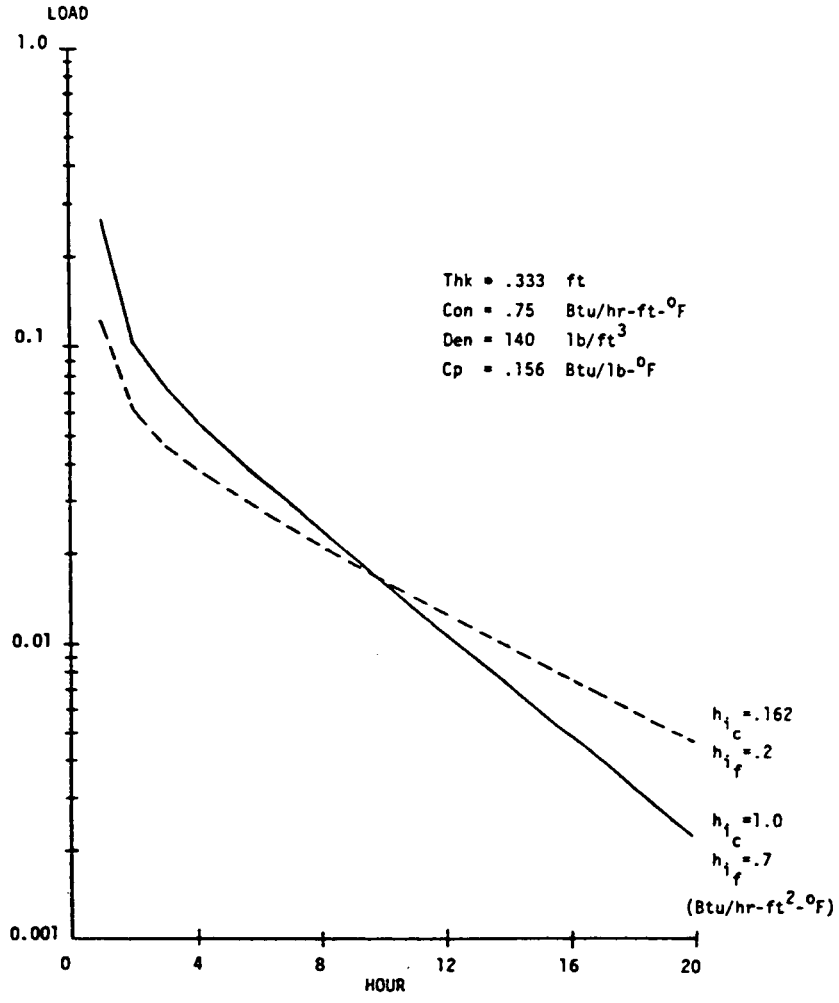

FIGURE D.18 - INITIAL RESPONSE AND COMMON RATIO VARIATION WITH FLOOR/CEILING CONVECTION COEFFICIENTS FOR A UNIT RADIATION PULSE

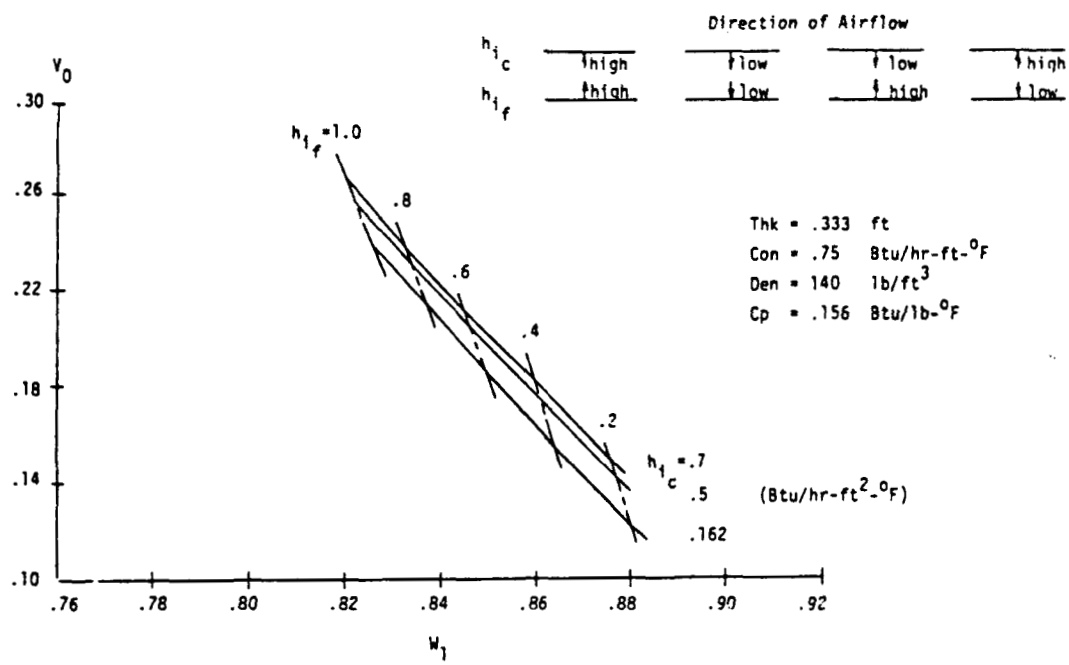

FIGURE D.19 - RESPONSE AMPLITUDE RATIO vs FREQUENCY FOR A UNIT RADIATION INPUT FOR VARYING FLOOR/CEILING CONVECTION COEFFICIENTS

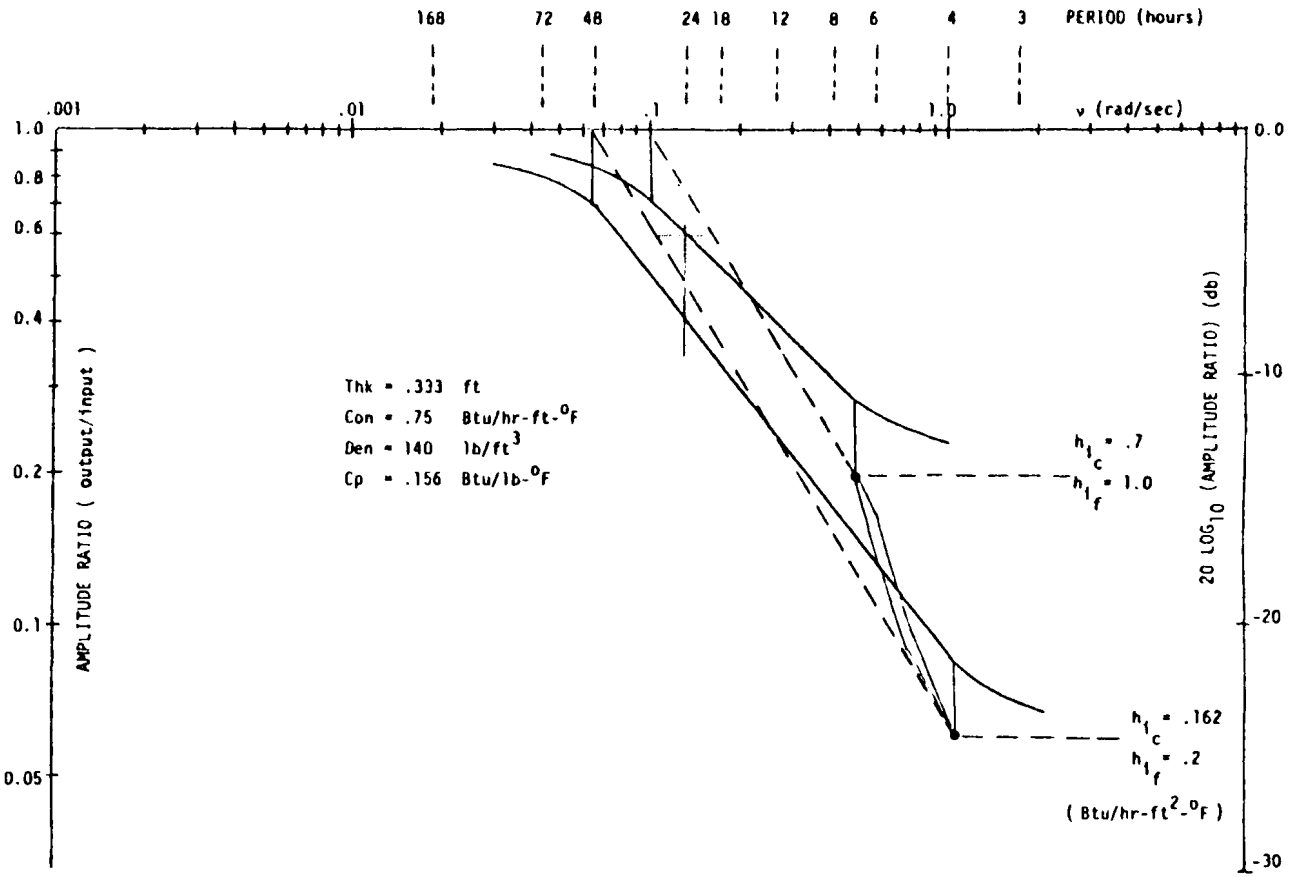

FIGURE D.20 - RESPONSE PHASE ANGLE vs FREQUENCY FOR A UNIT RADIATION INPUT FOR VARYING FLOOR/CEILING CONVECTION COEFFICIENTS

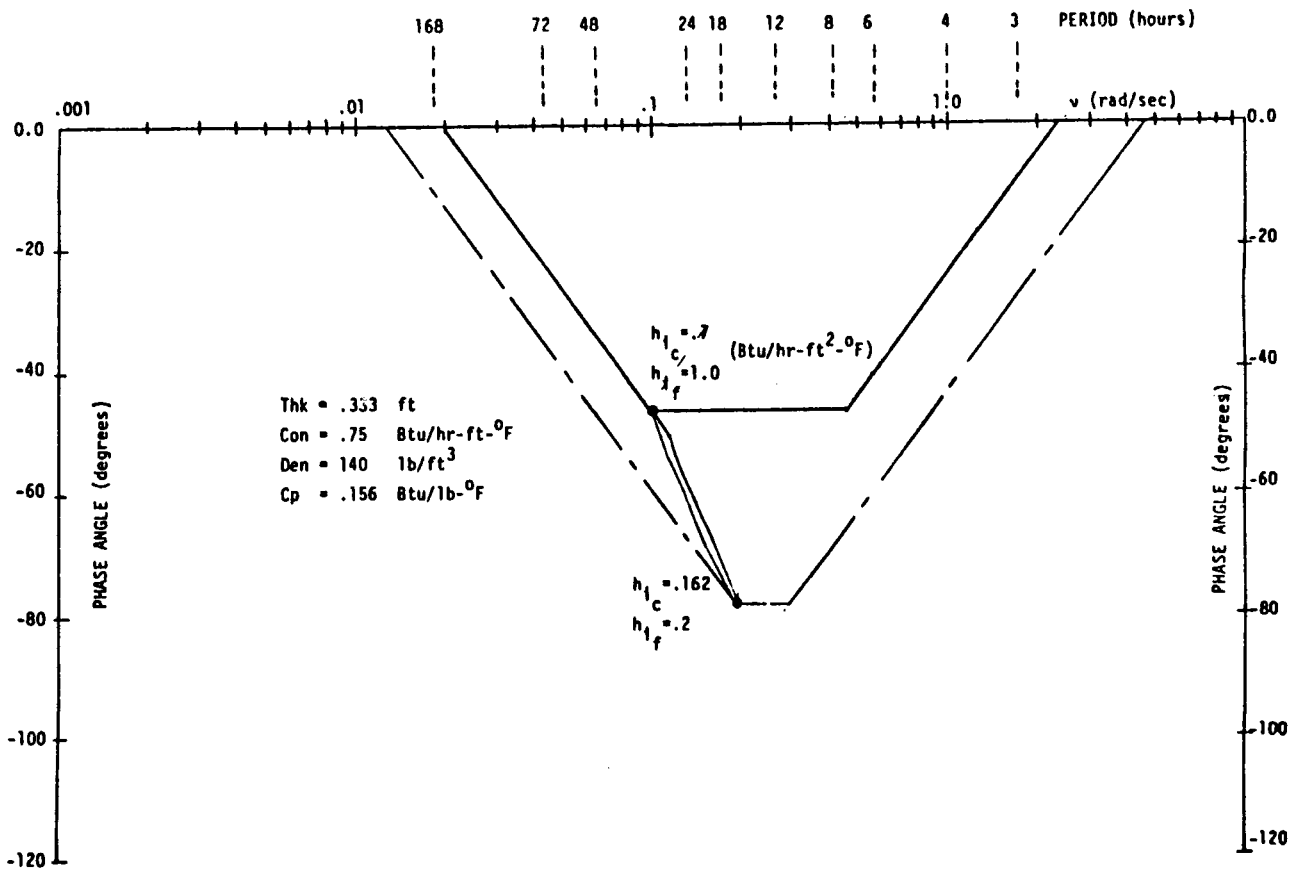

FIGURE D.21 - INITIAL RESPONSE AND COMMON RATIO VARIATION WITH SPACE SIZE FOR A UNIT RADIATION PULSE

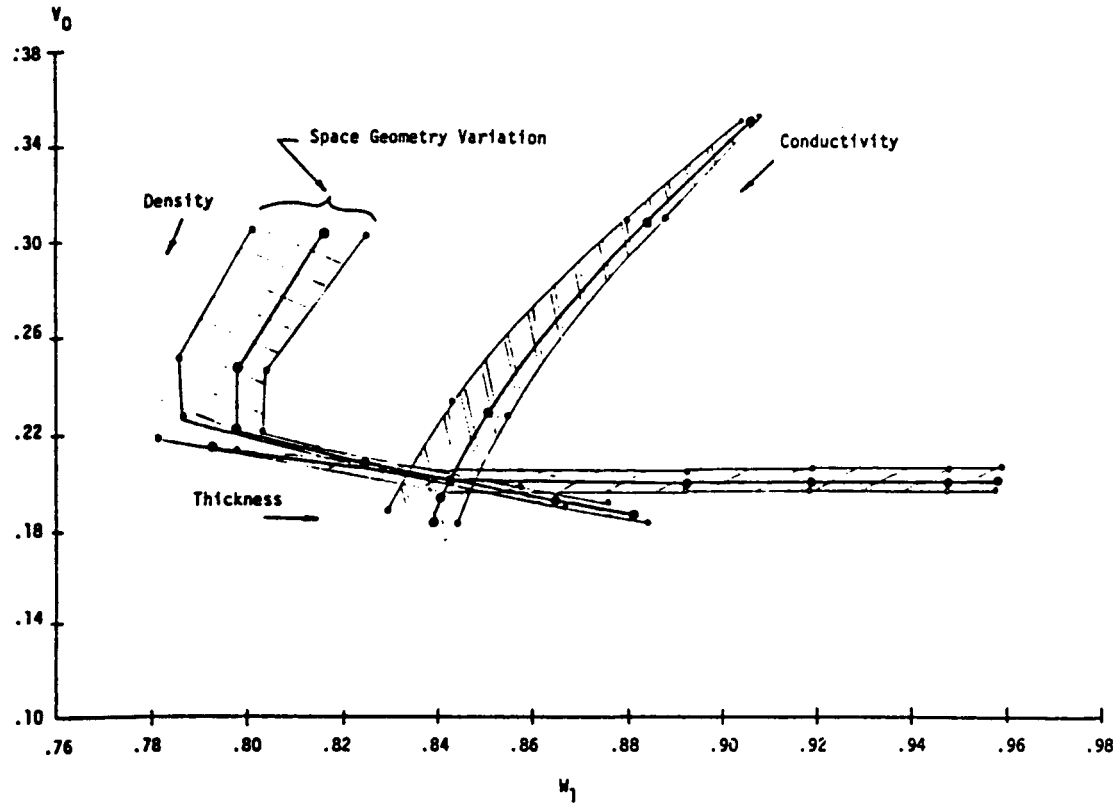

FIGURE D.22 - INITIAL RESPONSE AND COMMON RATIO VARIATION WITH RADIATION DISTRIBUTION FOR A UNIT RADIATION PULSE

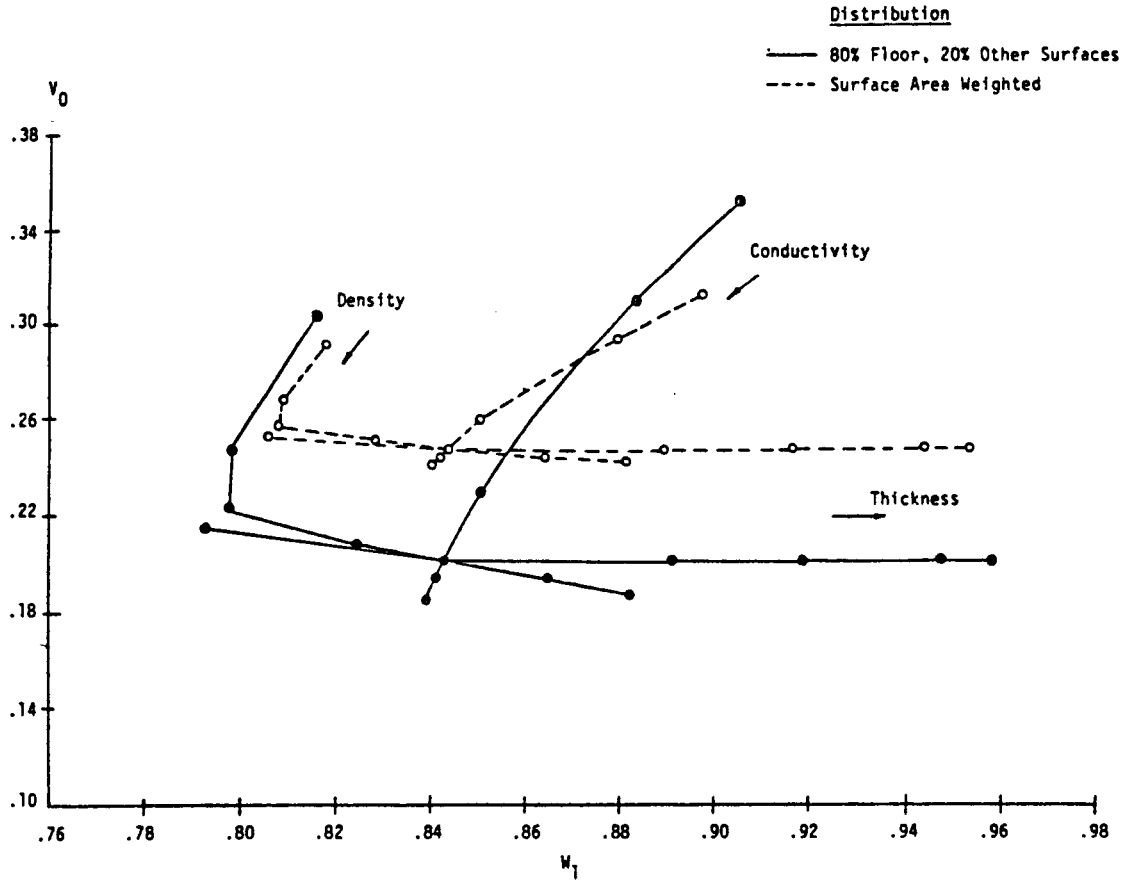

FIGURE D.23 - RESPONSE TO A UNIT RADIATION PULSE FOR VARYING RADIATION DISTRIBUTION

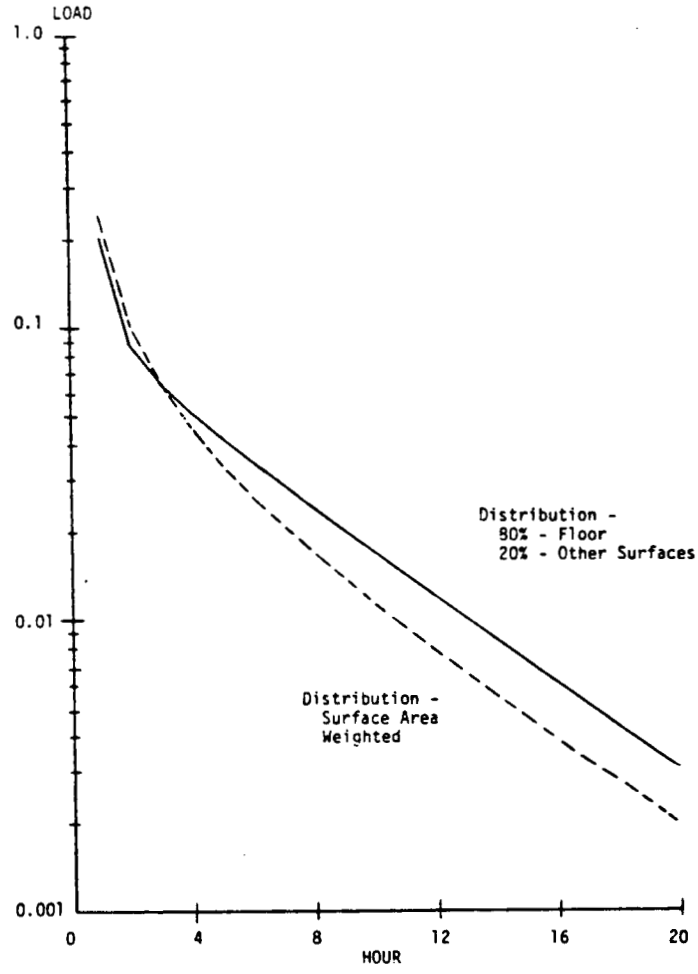

FIGURE D.24 - SURFACE COMPONENT RESPONSE TO A UNIT RADIATION PULSE
(DISTRIBUTION: 80% FLOOR, 20% OTHER SURFACES)

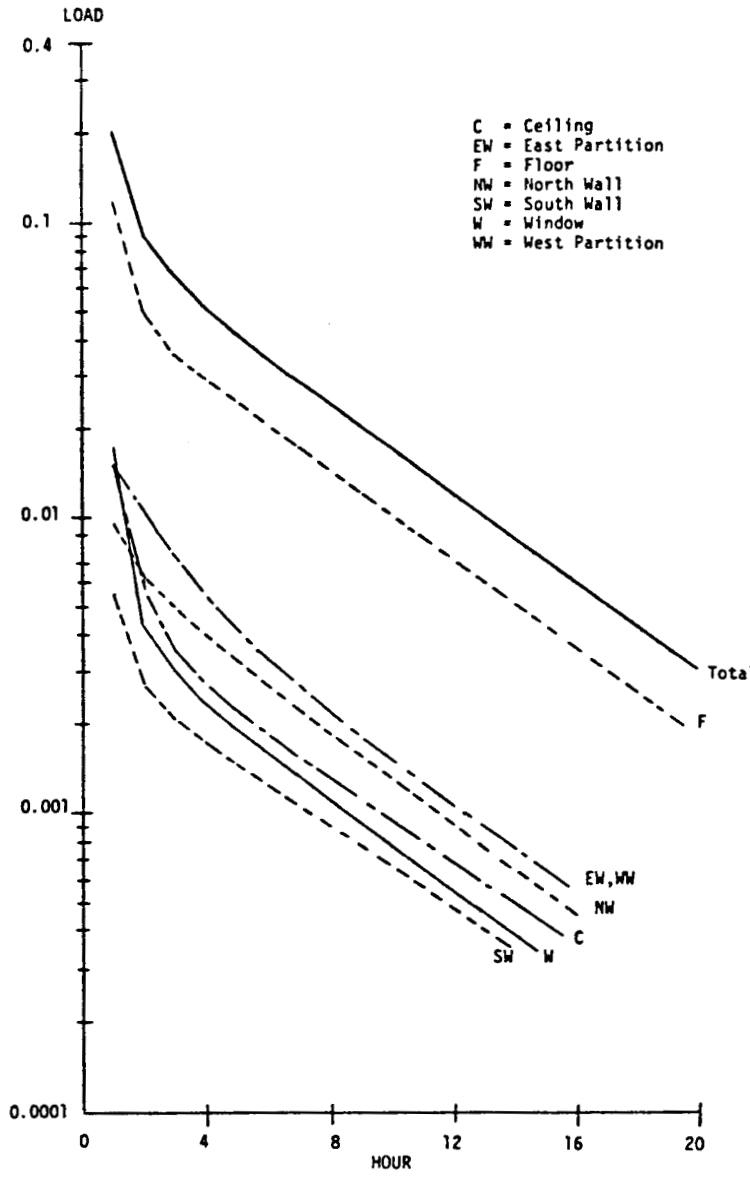

FIGURE D.25 - SURFACE COMPONENT RESPONSE TO A UNIT RADIATION PULSE
(DISTRIBUTION: SURFACE AREA WEIGHTED)

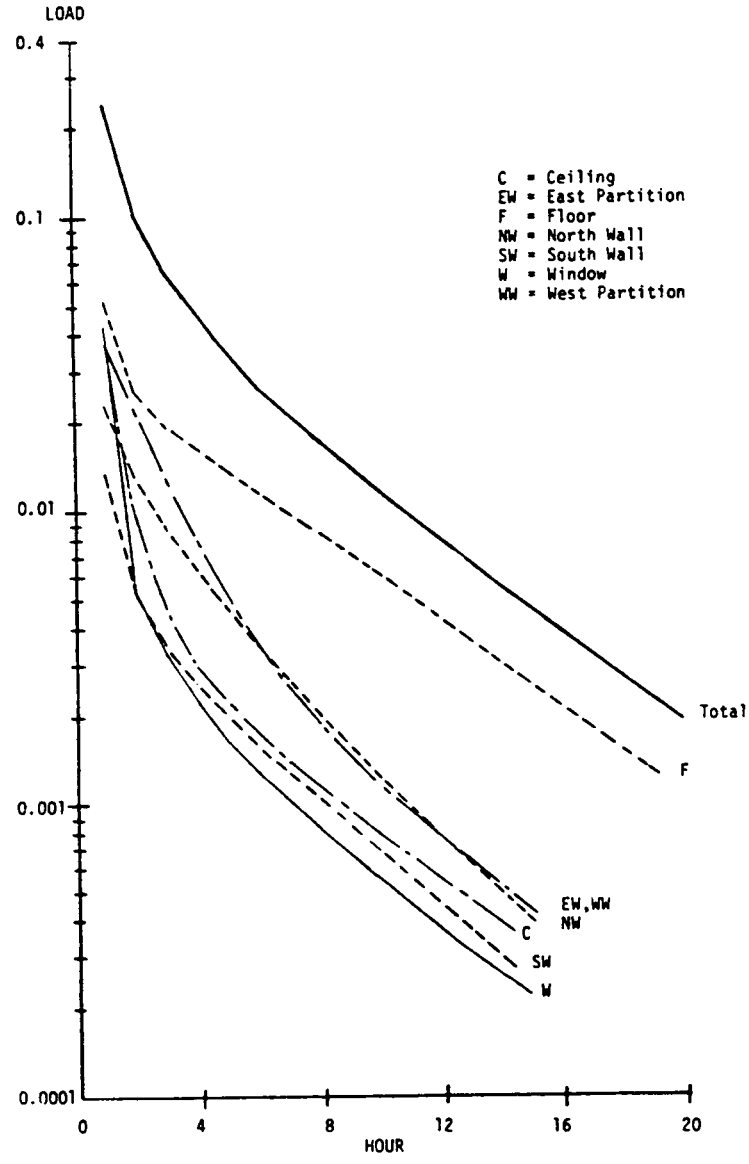

FIGURE D.26 - RESPONSE AMPLITUDE RATIO vs FREQUENCY FOR A UNIT RADIATION INPUT FOR VARYING RADIATION DISTRIBUTION

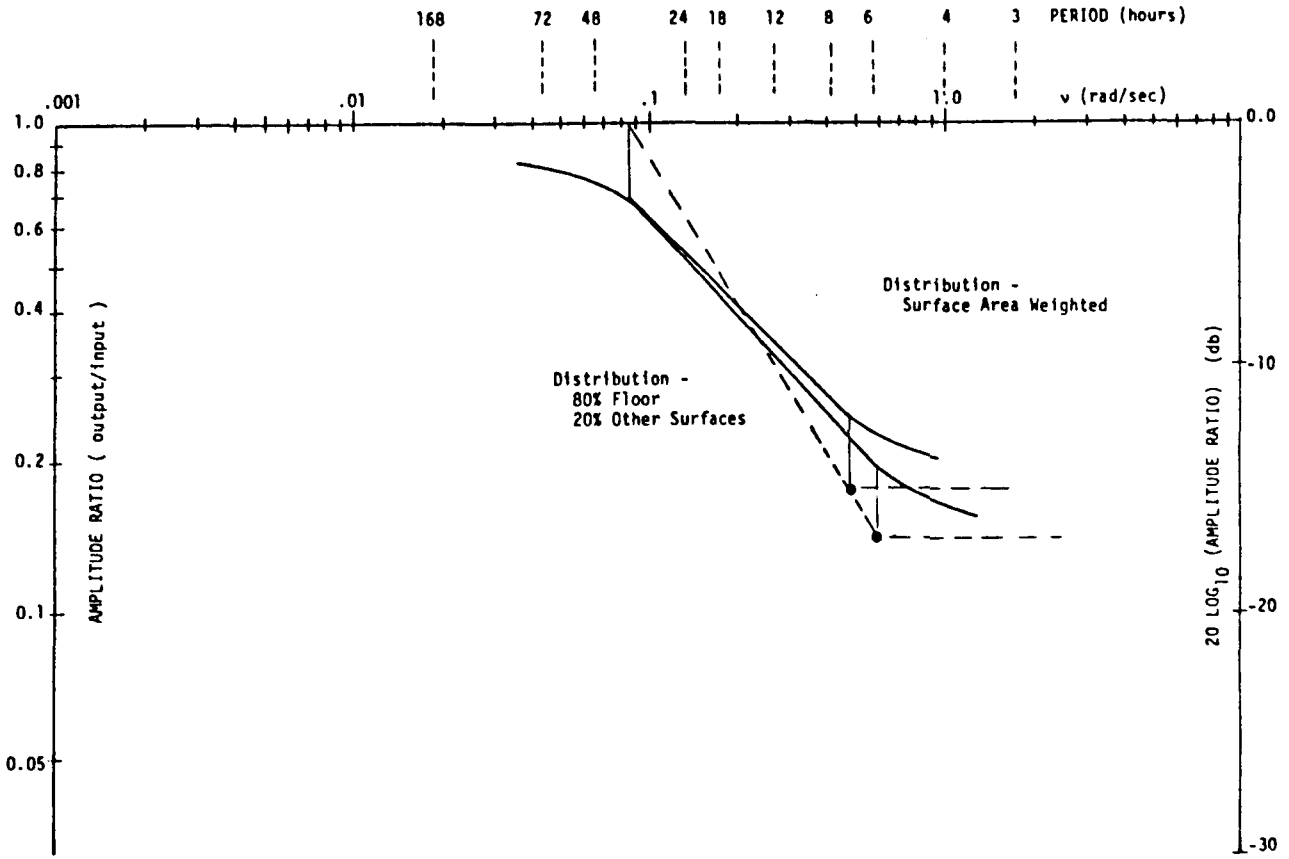

FIGURE D.27 - RESPONSE PHASE ANGLE vs FREQUENCY FOR A UNIT RADIATION INPUT FOR VARYING RADIATION DISTRIBUTION

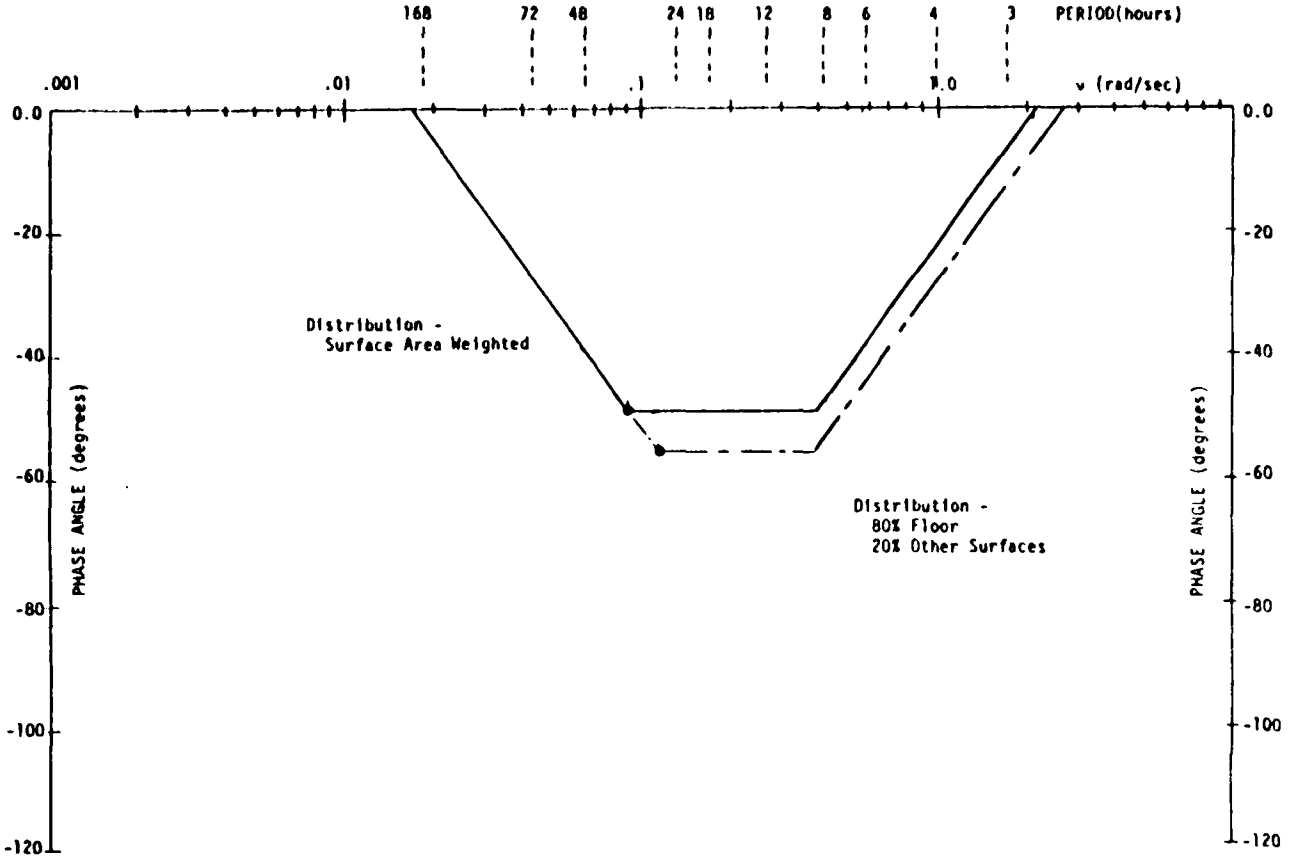

FIGURE D.28 - INITIAL RESPONSE AND COMMON RATIO VARIATION WITH FLOOR/CEILING CONVECTION COEFFICIENTS AND RADIATION DISTRIBUTION FOR A UNIT RADIATION PULSE

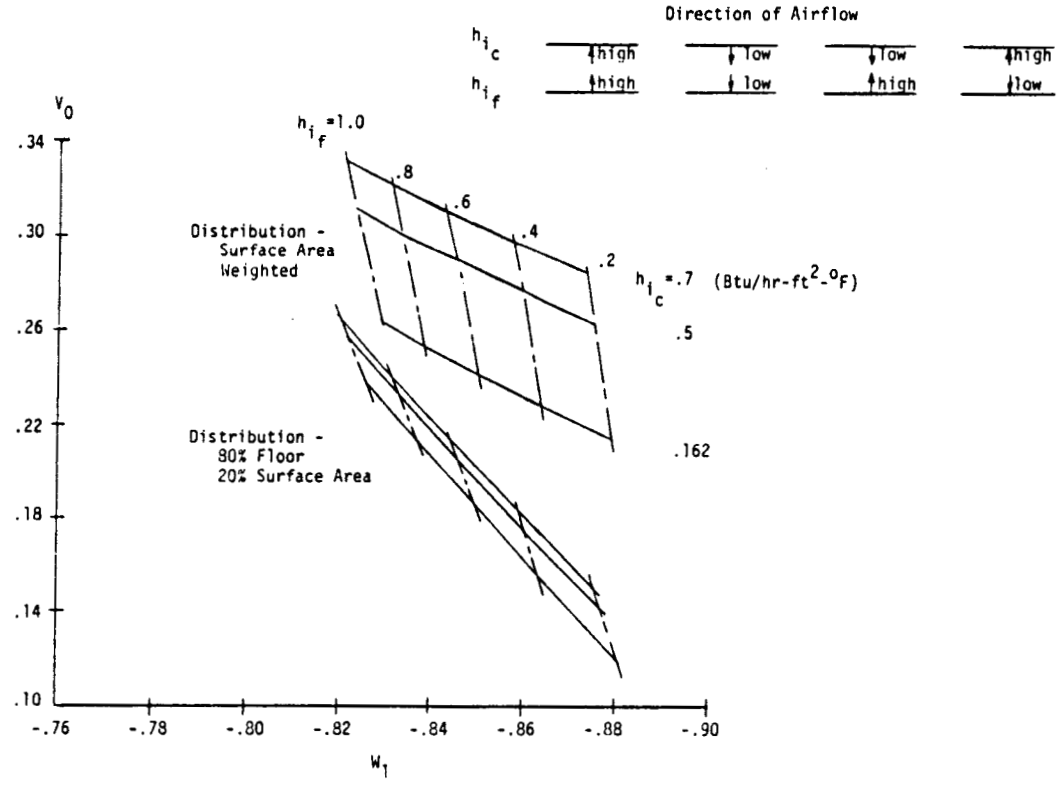

FIGURE D.29 - RESPONSE TO A UNIT SPACE AIR TEMPERATURE PULSE FOR VARYING FLOOR THICKNESS

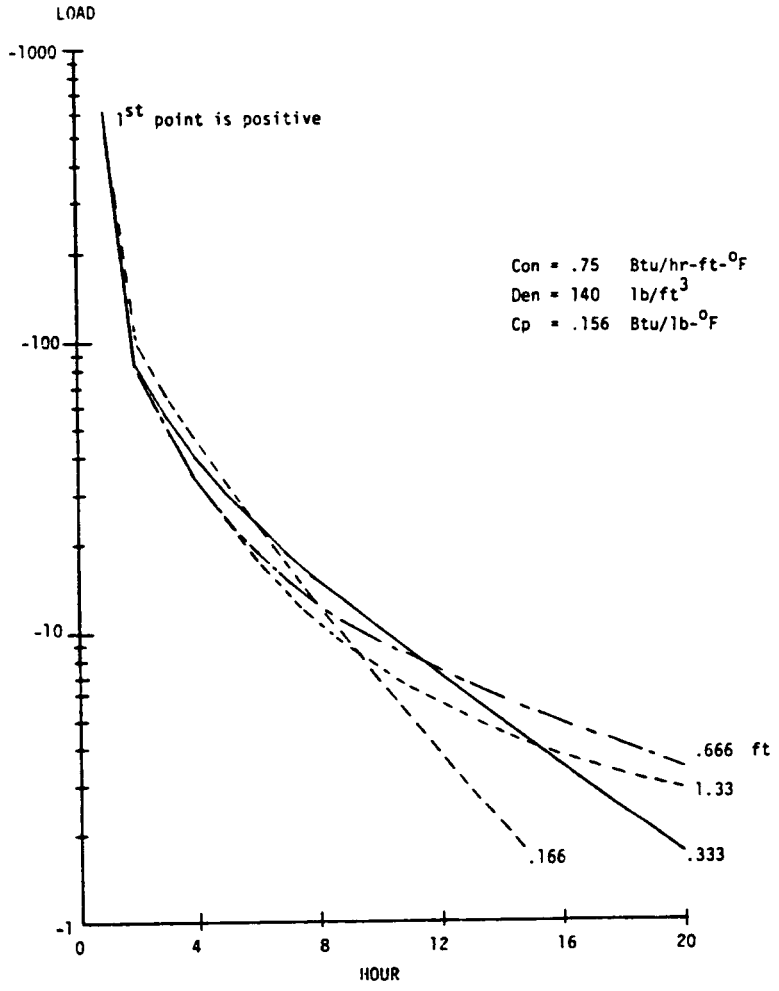

FIGURE D.30 - RESPONSE TO A UNIT SPACE AIR TEMPERATURE PULSE FOR VARYING FLOOR CONDUCTIVITY

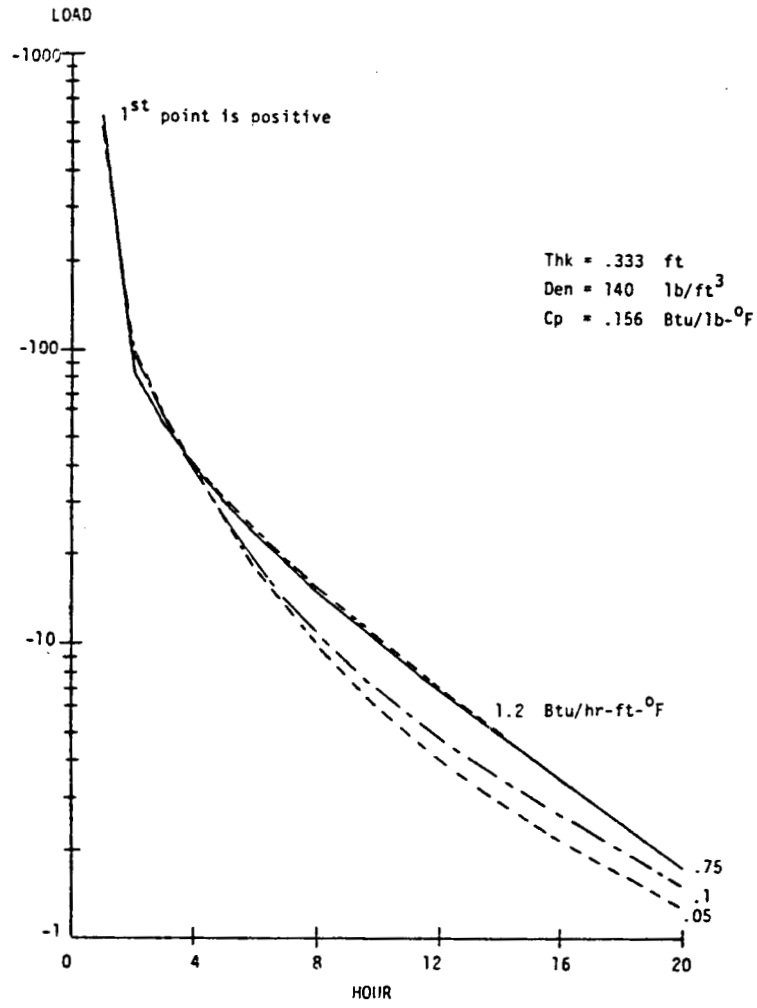

FIGURE D.31 - RESPONSE TO A UNIT SPACE AIR TEMPERATURE PULSE FOR VARYING FLOOR DENSITY

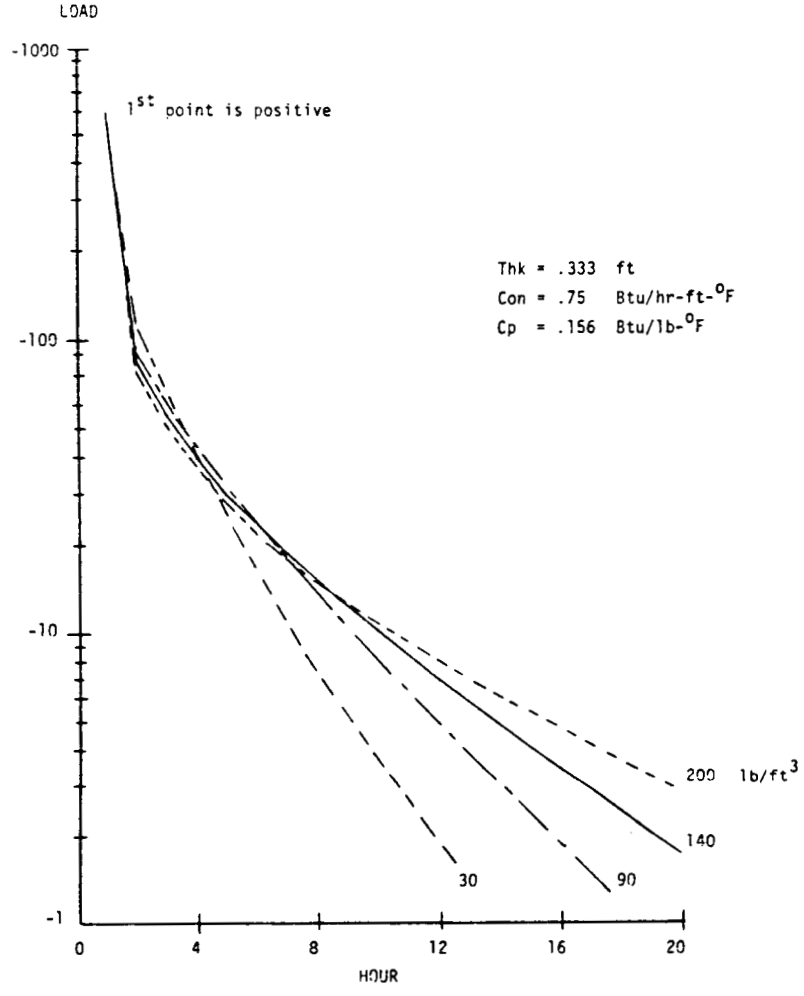

FIGURE D.32 - RESPONSE AMPLITUDE RATIO vs FREQUENCY FOR A UNIT SPACE AIR TEMPERATURE INPUT FOR VARYING FLOOR THICKNESS

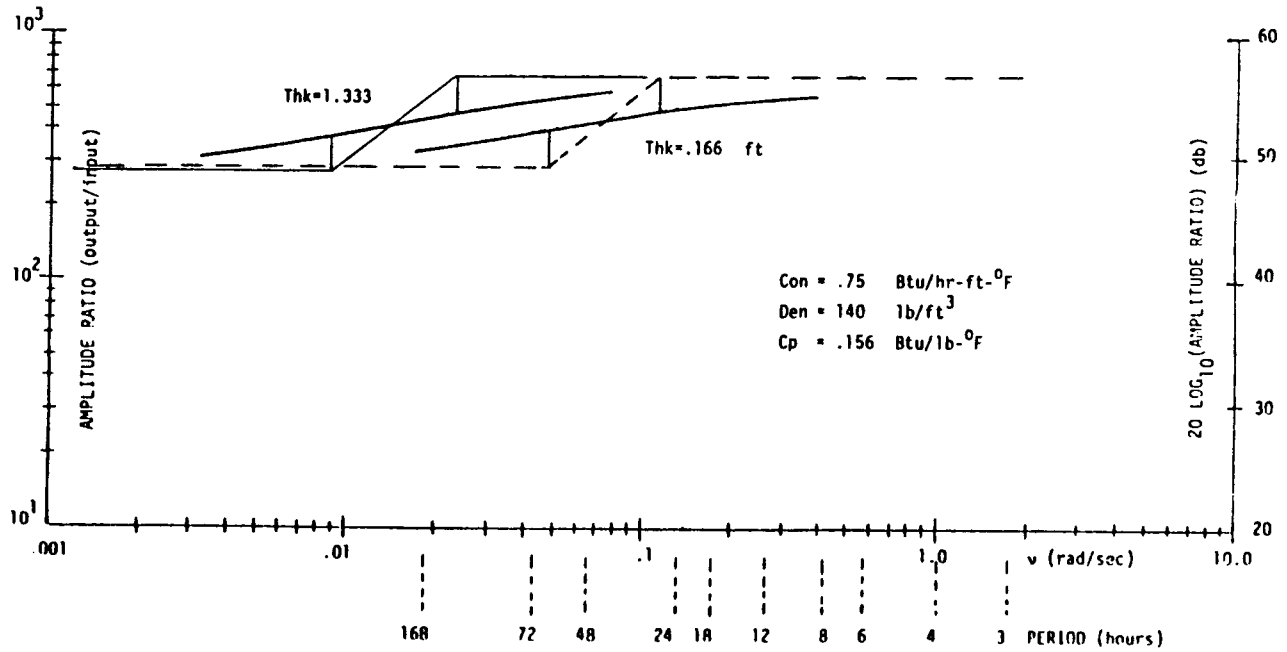

FIGURE D.33 - RESPONSE PHASE ANGLE vs FREQUENCY FOR A UNIT SPACE AIR TEMPERATURE INPUT FOR VARYING FLOOR THICKNESS

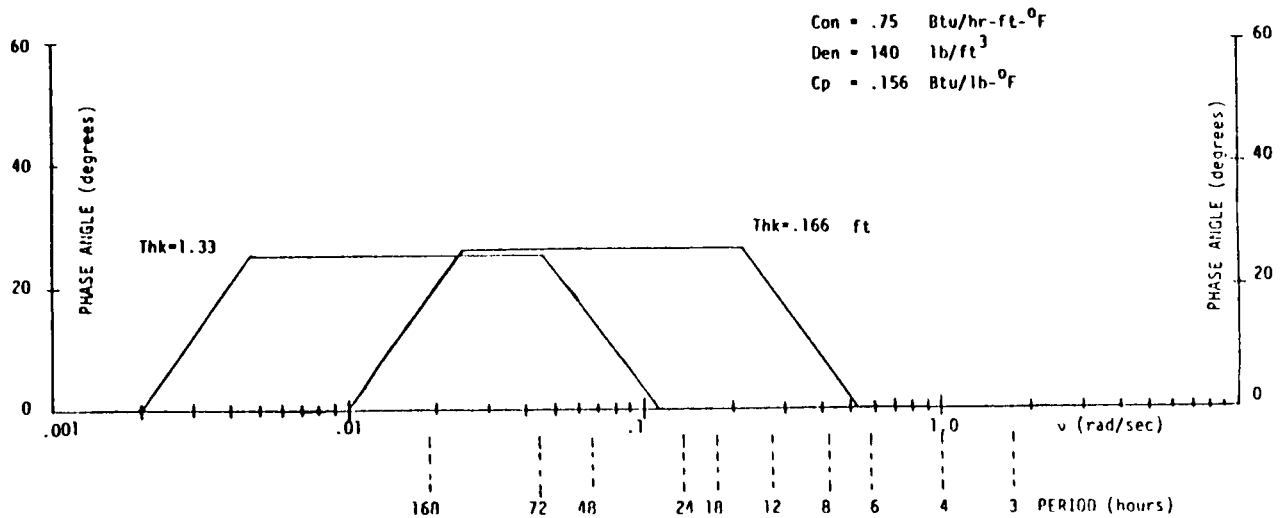

FIGURE D.34 - RESPONSE AMPLITUDE RATIO vs FREQUENCY FOR A UNIT SPACE AIR TEMPERATURE INPUT FOR VARYING FLOOR CONDUCTIVITY

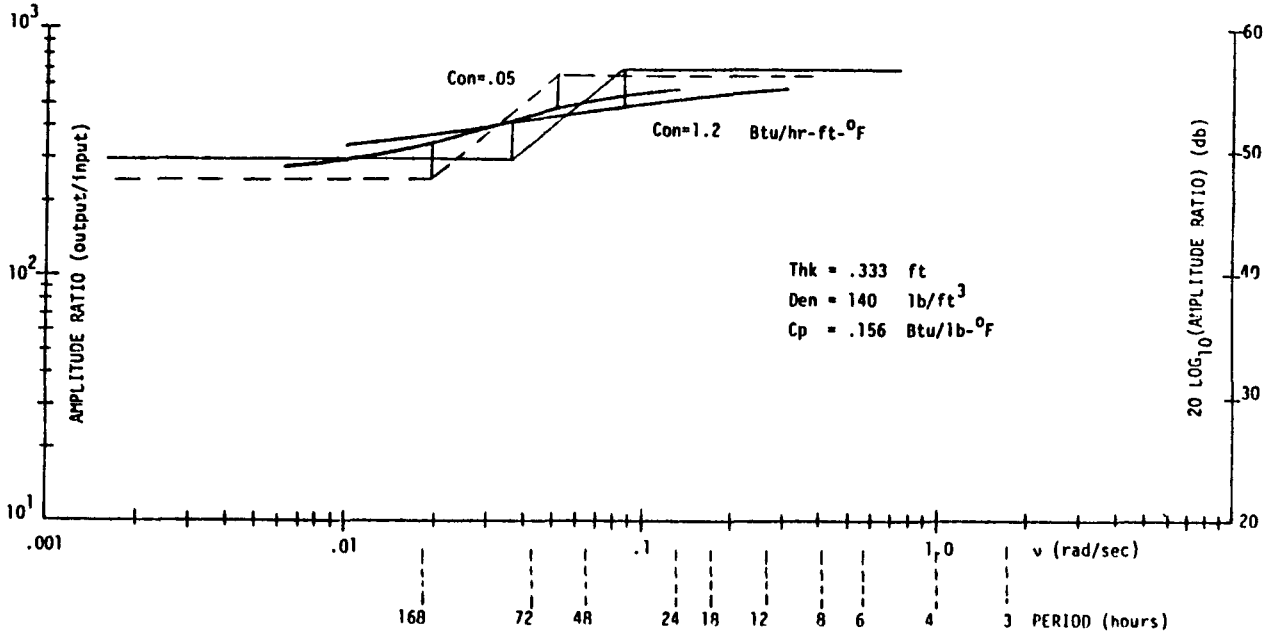

FIGURE D.35 - RESPONSE PHASE ANGLE vs FREQUENCY FOR A UNIT SPACE AIR TEMPERATURE INPUT FOR VARYING FLOOR CONDUCTIVITY

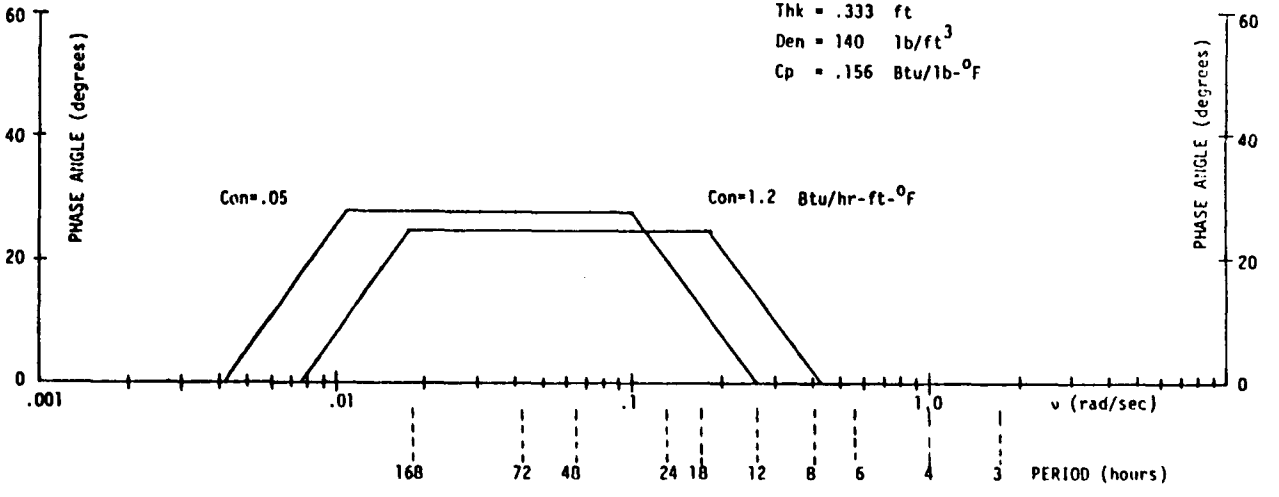

FIGURE D.36 - RESPONSE AMPLITUDE RATIO vs FREQUENCY FOR A UNIT SPACE AIR TEMPERATURE INPUT FOR VARYING FLOOR DENSITY

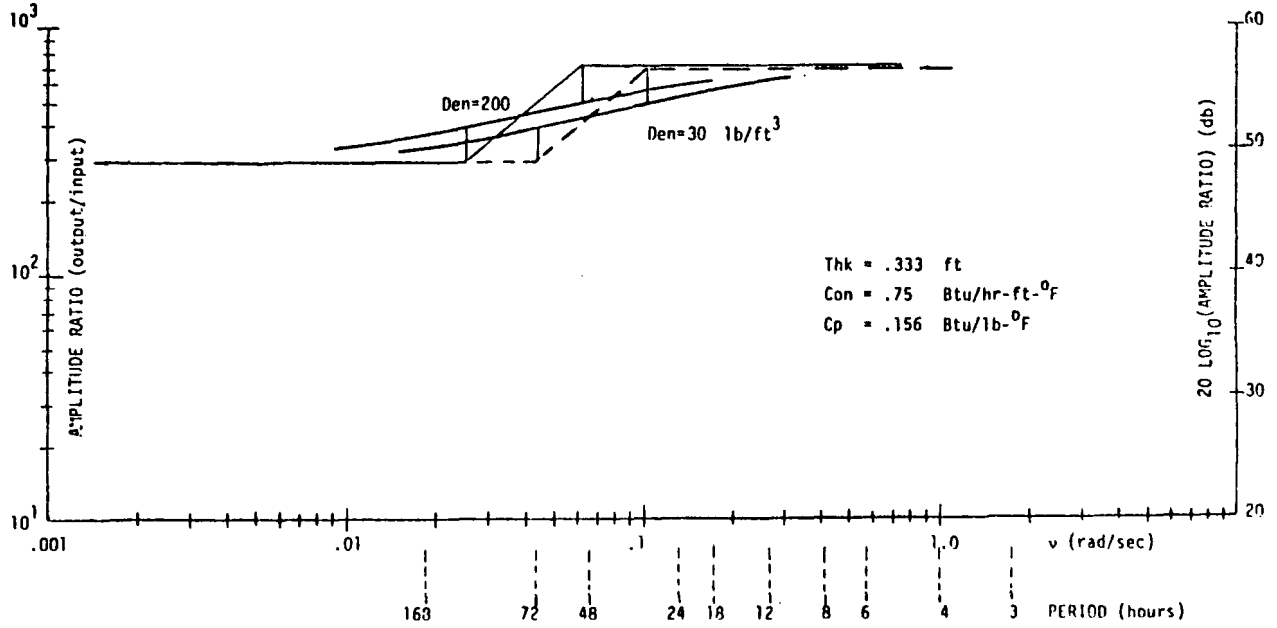

FIGURE D.37 - RESPONSE PHASE ANGLE vs FREQUENCY FOR A UNIT SPACE AIR TEMPERATURE INPUT FOR VARYING FLOOR DENSITY

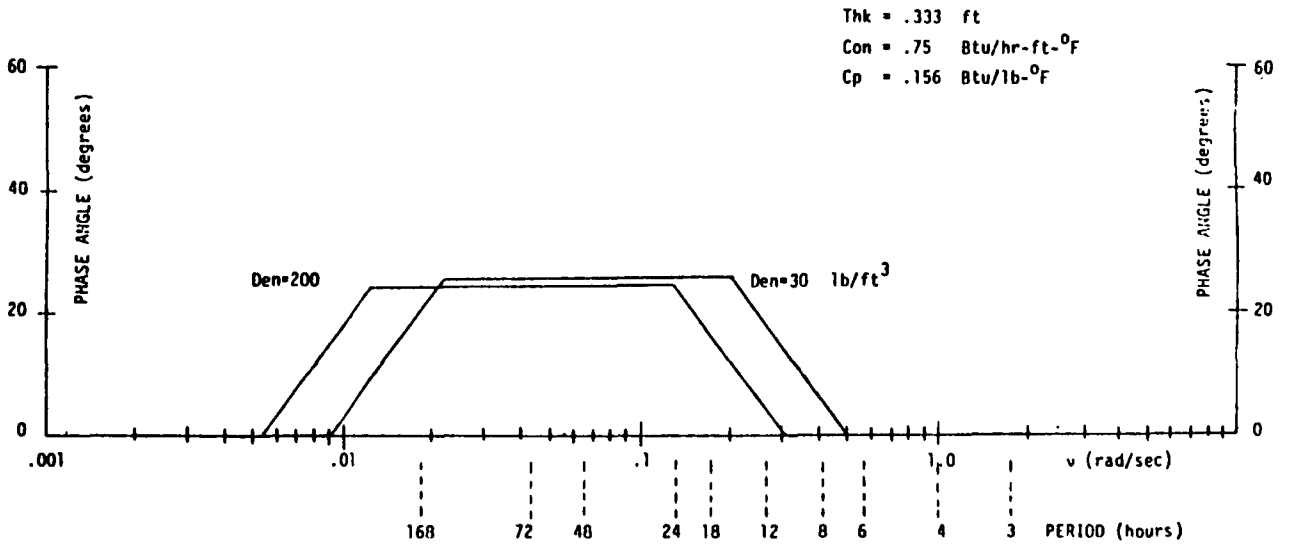

FIGURE D.38 - RESPONSE AMPLITUDE RATIO LIMITS FOR A UNIT SPACE AIR TEMPERATURE INPUT FOR VARYING FLOOR/ CEILING CONVECTION COEFFICIENTS

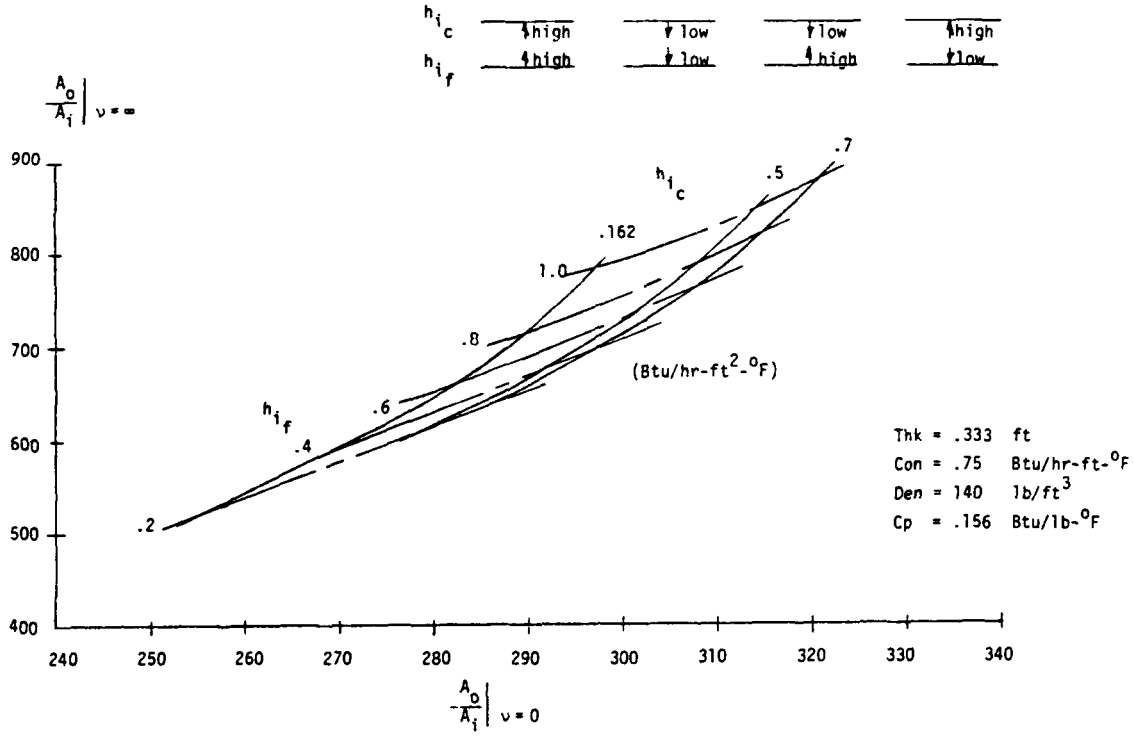

FIGURE D.39 - RESPONSE AMPLITUDE RATIO vs FREQUENCY FOR A UNIT SPACE AIR TEMPERATURE INPUT FOR VARYING FLOOR/CEILING CONVECTION COEFFICIENTS

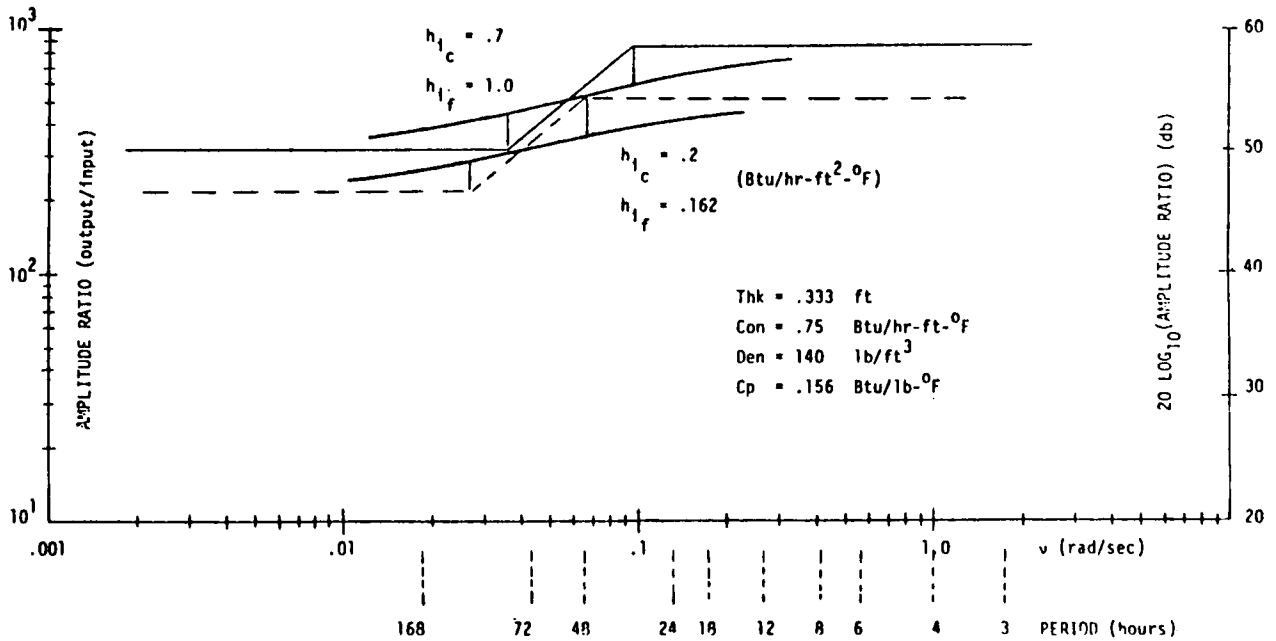

FIGURE D.40 - RESPONSE PHASE ANGLE vs FREQUENCY FOR A UNIT SPACE AIR TEMPERATURE INPUT FOR VARYING FLOOR/CEILING CONVECTION COEFFICIENTS

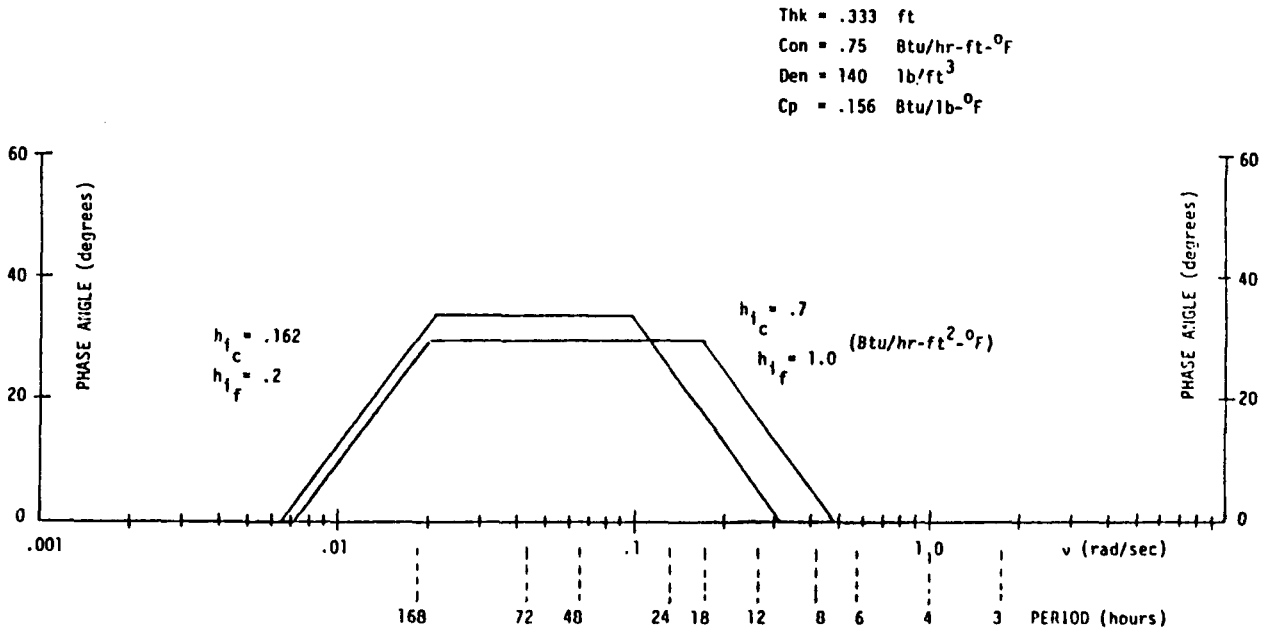

FIGURE D.41 - RESPONSE AMPLITUDE RATIO LIMITS FOR A UNIT SPACE AIR TEMPERATURE INPUT FOR VARYING SPACE SIZES

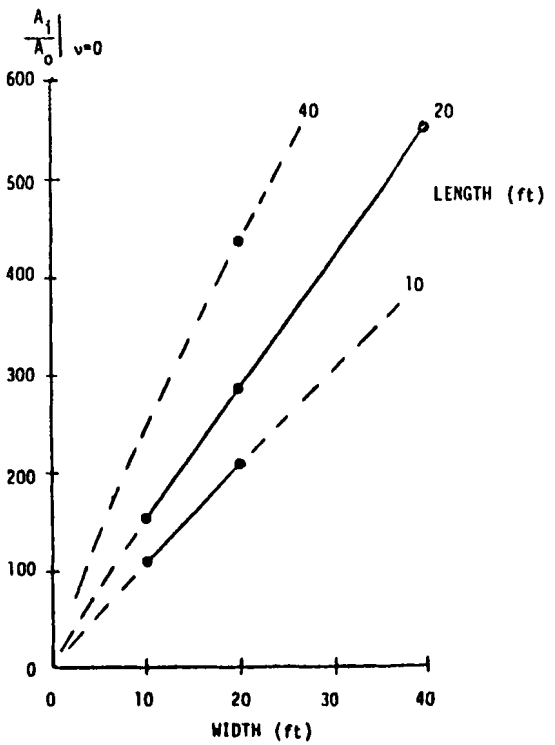

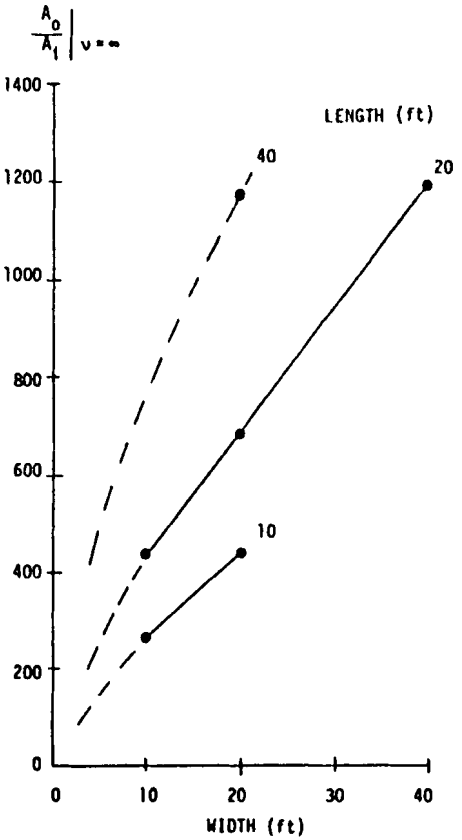

E. WEIGHTING FACTORS/THERMAL BALANCE DISCUSSION

The Interim Report, Reference 1, detailed the algorithms used in the weighting factor and thermal balance techniques to calculate the thermal loads and air temperature variations within a space. The analytical treatment was presented without regard to the current simulation programs which apply the techniques. However, at the time the Interim Report was written, actual comparisons between the results calculated by the methods could only be made by employing the published simulation routines. Although the loads and temperatures obtained by the two schemes were in general agreement, it was felt a more pure comparison could be made if the program peculiar aspects of the input quantity calculations were eliminated. Thus, CCB, in the course of this contract, compared the results from general purpose weighting factor and thermal balance techniques capable of accepting the same input excitations. In addition, the thermal balance scheme was used to define the weighting factors for use in the weighting factor method. Figure E.1 presents a diagram depicting the nature of the calculation procedure used for the comparison. The thermal balance technique performs a heat balance at both inside and outside surfaces of a space defined primarily by its structural properties. Since the algorithm accepts any arbitrary input excitation form in flux or temperature, coordinate orientation is unnecessary and the only geometrical considerations result from the view factors which are calculated in an approximate manner through the area ratio relationship discussed in Reference 1. A matrix solution is used to obtain inside surface temperatures from which the space load or air temperature is obtained. Initially, the space properties are defined after which a unit pulse in radiation and air temperature is applied to determine the weighting factors through the use of the recursion relationship described in Section B of this report. The next step entails the application of a sinusoidal radiation or other arbitrary radiation input at fixed space temperature. A direct comparison of the space load calculation is then made. In the thermal balance procedure, this same excitation is again input and the space temperature allowed to fluctuate. The weighting factor procedure, however, uses the constant

temperature load profile in conjunction with the previously defined space air weighting factors to calculate the temperature variation.

Figure E.2 and E.3 show the response to a unit pulse in radiation and space air temperature for the baseline configuration of the space defined in Section D of this report. The values of the weighting factors generated are somewhat different because the inside/outside surface heat balance recursion relationship was used for this analysis; whereas, in the parametric study, the recursion form presented in Reference 1 was used.

For the radiation pulse case, sets of 2, 3 and 4 weighting factors were generated by visual determination of succeeding common ratios. The load response to a 10,000 BTU amplitude sinusoidal radiation input for both the thermal balance and weighting factor methods is shown on Figure E.4. Readily apparent is the convergence of the two schemes with increased number of factors. A more exact procedure for determing the common ratios would no doubt improve the comparative results. Figure E.5 shows the space air temperature variation for the two methods. The maximum difference is roughly 1/2°F over a total excursion of 15°F. Presented on Figure E.6 is another temperature variation. In this case, the excitation arises from a 10° F sinusoidal variation in outside air temperature and a 10K Btu radiation input. The constant space temperature load generated by the thermal balance was used as input to the variable temperature weighting factor calculations.

These results indicate that there are no substantial differences between loads and temperatures calculated by either the weighting factor or thermal balance methods of approach. As stated in the Interim Report, whatever differences exist are due to the program specific aspects of the routines defining the input quantities necessary for solution.

FIGURE E.1 - WEIGHTING FACTOR / THERMAL BALANCE COMPARISON FLOW DIAGRAM

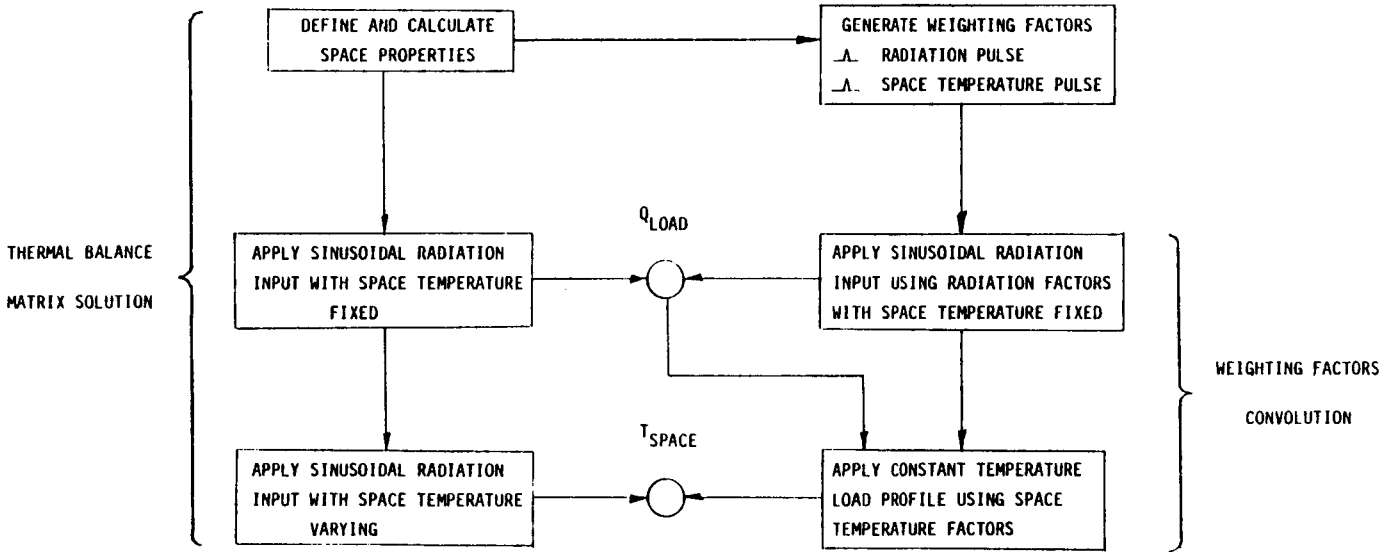

FIGURE E.2 - LOAD RESPONSE TO UNIT RADIATION PULSE
GENERATION OF WEIGHTING FACTORS

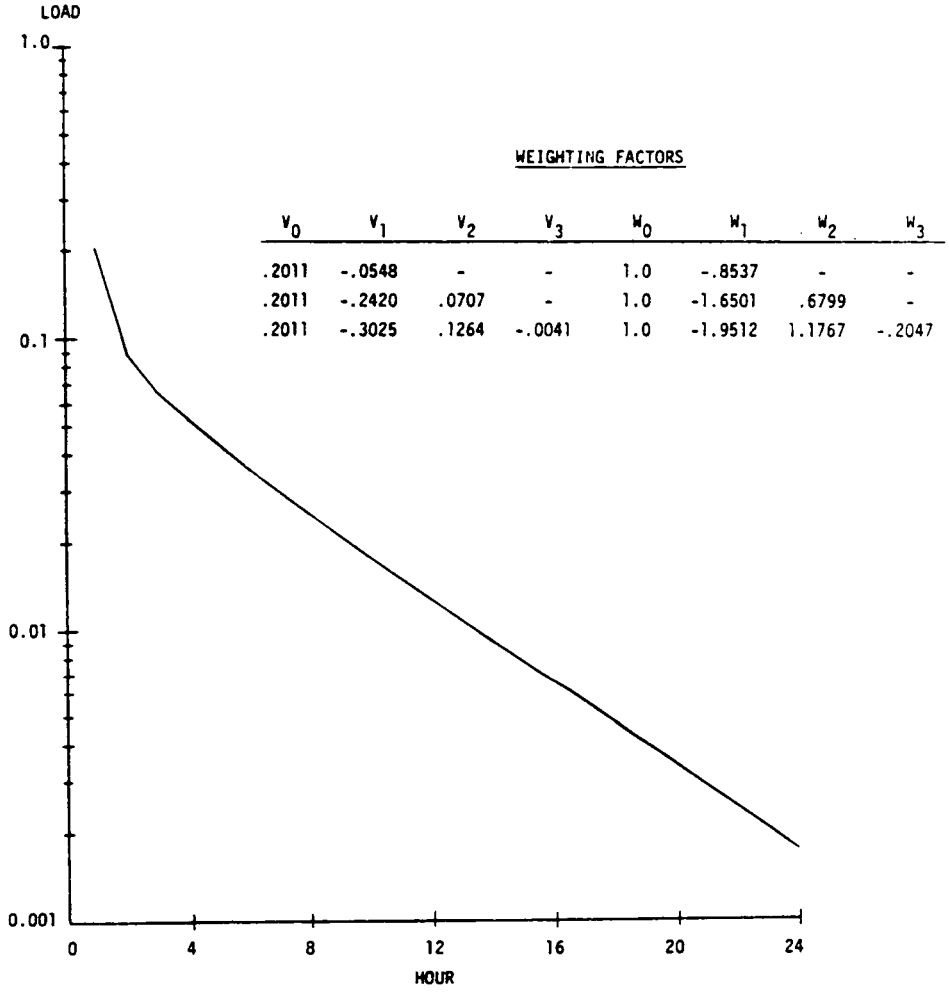

WEIGHTING FACTORS

V_0	V_1	V_2	V_3	W_0	W_1	W_2	W_3
.2011	-.0548	-	-	1.0	-.8537	-	-
.2011	-.2420	.0707	-	1.0	-1.6501	.6799	-
.2011	-.3025	.1264	-.0041	1.0	-1.9512	1.1767	-.2047

FIGURE E.3 - LOAD RESPONSE TO A UNIT SPACE AIR TEMPERATURE PULSE
GENERATION OF WEIGHTING FACTORS

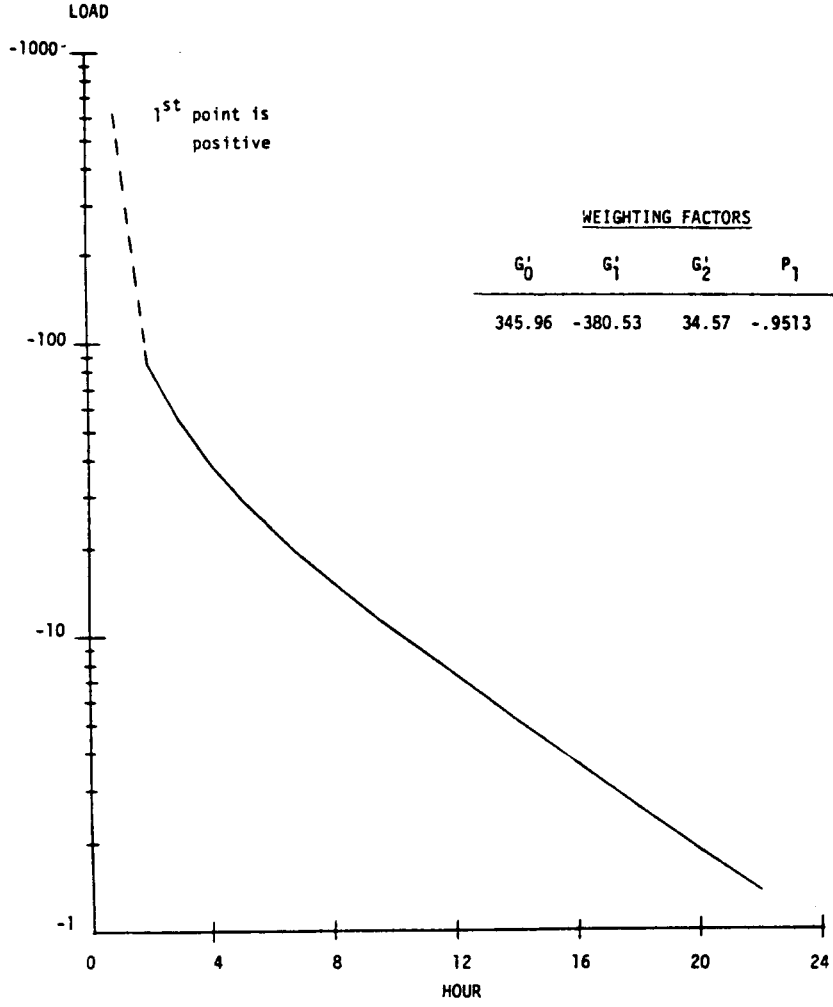

WEIGHTING FACTORS

G_0'	G_1'	G_2'	P_1	K_t
345.96	-380.53	34.57	-.9513	280.77

FIGURE E.4 - WEIGHTING FACTOR/THERMAL BALANCE LOAD RESPONSE COMPARISON FOR A 10k BTU SINUSOIDAL RADIATION INPUT

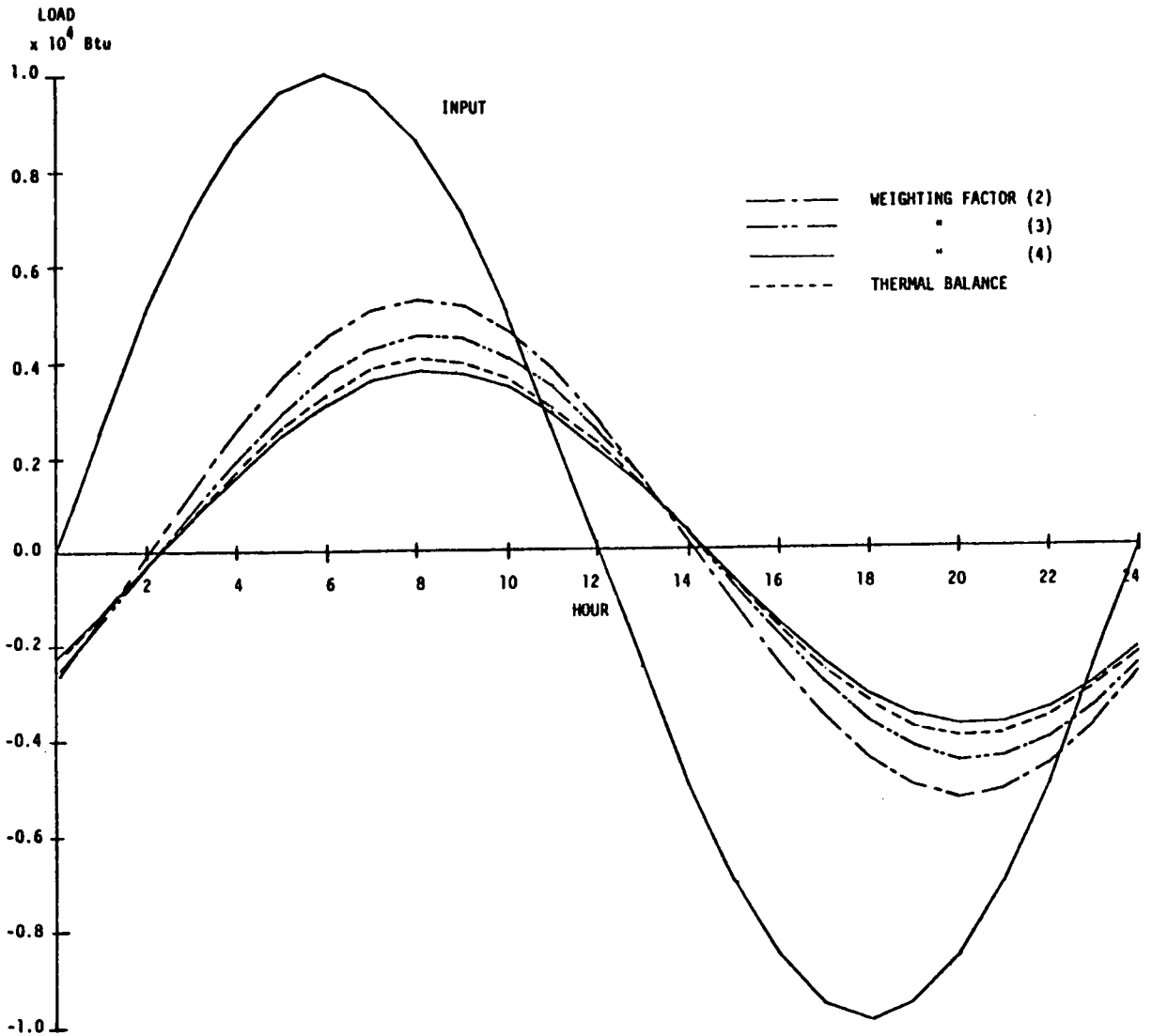

FIGURE E.5 - WEIGHTING FACTOR/THERMAL BALANCE SPACE AIR TEMPERATURE RESPONSE COMPARISON FOR A 10k BTU SINUSOIDAL RADIATION INPUT

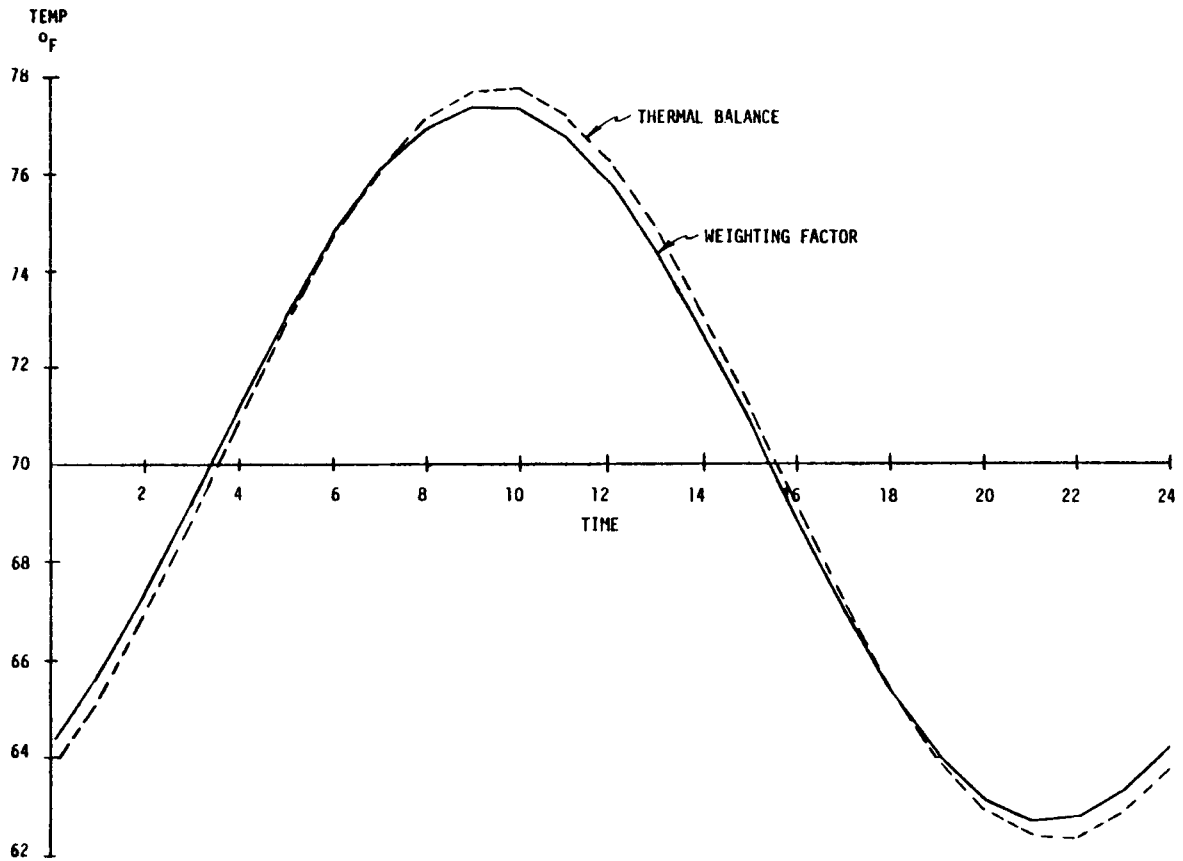

FIGURE E.6 - WEIGHTING FACTOR/THERMAL BALANCE SPACE AIR TEMPERATURE RESPONSE COMPARISON FOR A 10k BTU SINUSOIDAL RADIATION INPUT AND A $10^{o}F$ SINUSOIDAL OUTSIDE AIR TEMPERATURE INPUT

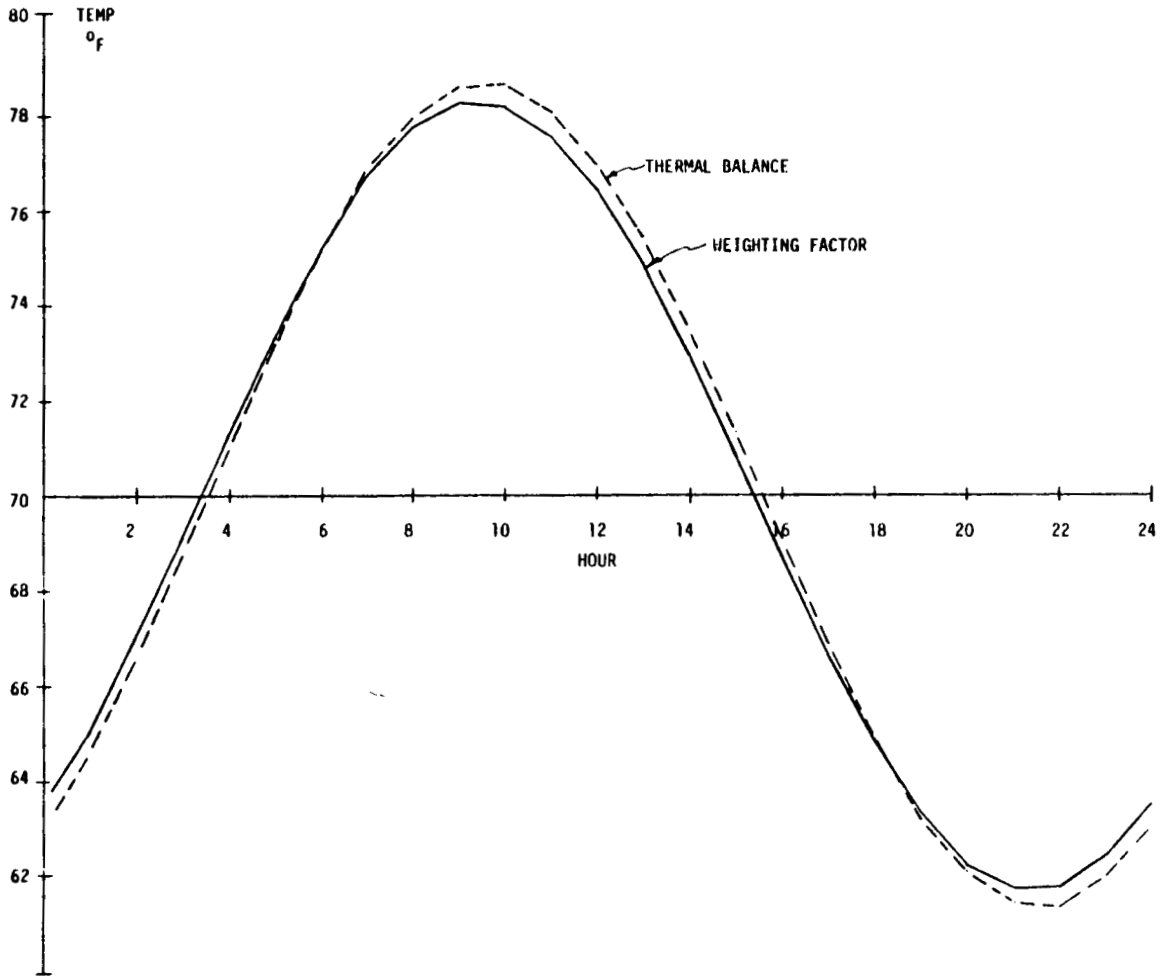

F. SUMMARY

This report has documented a portion of the work accomplished under DOE Contract number EM-78-C-01-5221, Passive Solar Calculation Methods. It is the final report and presents, along with the interim report (Reference 1), a consolidation of thermal load calculation methods for possible use in analyzing passive solar structures.

The recursion technique used for generating space specific weighting factors discussed in Reference 1 was expanded to include heat balances on the outside surfaces. The derivation shown in Section B makes feasible a technique for analyzing zone to zone heat transfer.

A first step in utilizing frequency response methods was presented in Section C. The radiative and space temperature discrete Z-transform representation of the weighting factors was related to a continuous S-transform. Amplitude ratio and phase angle parameters were defined across a frequency range such that output quantities were defined for a unit sinusoidal excitation input.

To assist in better understanding the influence of specific construction parameters, a comprehensive parametric study was conducted, with results published in Section D. Thickness, conductivity and density of the floor surface of a typical structure were varied Also the inside convective heat transfer coefficient of the floor and ceiling surfaces was varied in addition to the distribution of the input radiative heat gain. The frequency response methods discussed previously were used to analyze the results of the analysis.

Section E presented a comparison of thermal loads and temperatures using both weighting factor and thermal balance procedures. Input parameter differences were eliminated thus enabling a more satisfactory comparison than the one presented in the interim report. The results indicated that both methods are equivalent.

G. REFERENCES

1. CCB/Cumali Associates, Interim Report - Passive Solar Calculation Methods, DOE Contract Number EM 78 - C - 01 - 5221, April 15, 1979.

2. G. P. Mitalas and D. G. Stephenson, Cooling Load Calculations by Thermal Response Factor Method, ASHRAE Transactions, Vol. 73, Part 1, 1967.

3. G. P. Mitalas and D. G. Stephenson, Room Thermal Response Factors, ASHRAE Transactions, Vol. 33, Part 1, 1967.

4. Ken-Ichi Kimura, Scientific Basis of Air Conditioning, Applied Science Publishers Ltd., 1977.

5. D. C. Hittle, The Building Loads Analysis and System Thermodymanics Program (BLAST), Vols. I & II, U.S. Army Construction Engineering Research Laboratory, CERL-TR-E-119, 1977.

6. Procedure for Determing Heating and Cooling Loads for Computerizing Energy Calculations, Algorithms for Building Heat Transfer Subroutines, ASHRAE, 1975.

7. ASHRAE Handbooks of Fundamentals, ASHRAE, 1977.

8. R. M. Graven and P. R. Hirsch, CAL-ERDA Users Manual, Argonne National Laboratory, ANL/ENG-77-03,1977.

9. B. D. Hunn, CAL-ERDA Program Manual Draft, Los Alamos Scientific Laboratory, 1978.

10. Consultants Computation Bureau, DOE-1 Testing Methodology, Vol. I - Loads Program, 1978.

11. PASOLE: A General Simulation Program for Passive Solar Energy, Los Alamos Scientific Laboratory, LA-7433-MS, 1978.

12. S. M. Skinner, Control System Design, John Wiley & Sons, 1964.

13. F.W. Hutchinson, Heating and Humidifying Load Analysis, Ronald Press Company, 1962.

14. M. Jakob, Heat Transfer, John Wiley and Sons, 1957.

15. S. C. Gupta and L. Hasdorff, Fundamentals of Automatic Control, John Wiley and Sons, 1970.

16. T. Kusada, Fundamentals of Building Heat Transfer, Presented at the International Heat and Mass Transfer Center, Belgrade, Yugoslavia, 1978.

APPENDIX H.1 - SENSITIVITY STUDY TABULATED DATA

TABLE H.1.1 - RADIATION WEIGHTING FACTORS - TABULATED DATA

SPACE SIZE: L=20', W=20', H=10'

FLOOR PROPERTIES			WEIGHTING FACTORS					
			*DISTRIBUTION A			*DISTRIBUTION B		
THICKNESS (ft)	CONDUCTIVITY (Btu/hr-ft-°F)	DENSITY (lbs/ft^3)	V_0	V_1	W_1	V_0	V_1	W_1
.1666	.75	140	.2152	-.0077	-.7925	.2534	-.0587	-.8053
.3333	"	"	.2010	-.0435	-.8425	.2473	-.0911	-.8438
.5	"	"	.2006	-.0917	-.8911	.2472	-.1370	-.8898
.6666	"	"	.2006	-.1195	-.9198	.2472	-.1640	-.9168
1.0	"	"	.2006	-.1480	-.9474	.2472	-.1914	-.9442
1.3333	"	"	.2006	-.1587	-.9581	.2472	-.2006	-.9534
.3333	.05	140	.3512	-.2570	-.9057	.3114	-.2093	-.8979
"	.10	"	.3074	-.1910	-.8836	.2927	-.1724	-.8797
"	.40	"	.2291	-.0793	-.8501	.2594	-.1098	-.8505
"	.75	"	.2010	-.0435	-.8425	.2473	-.0911	-.8438
"	.90	"	.1940	-.0350	-.8410	.2444	-.0868	-.8424
"	1.20	"	.1842	-.0232	-.8390	.2402	-.0809	-.8407
.3333	.75	30	.3029	-.1187	-.8158	.2908	-.1086	-.8177
"	"	60	.2469	-.0447	-.7978	.2908	-.0755	-.8086
"	"	90	.2223	-.0195	-.7972	.2564	-.0637	-.8073
"	"	120	.2079	-.0322	-.8244	.2503	-.0781	-.8278
"	"	140	.2010	-.0435	-.8425	.2473	-.0911	-.8438
"	"	170	.1930	-.0578	-.8649	.2439	-.1087	-.8848
"	"	200	.1867	-.0691	-.8823	.2413	-.1228	-.8816

*DISTRIBUTION

A - 80% Floor, 20% Surface Area

B - 100% Surface Area Weighted

TABLE H.1.2 - RADIATION WEIGHTING FACTORS - TABULATED DATA

SPACE SIZE: L=10', W=10', H=10'

FLOOR PROPERTIES			WEIGHTING FACTORS					
			*DISTRIBUTION A			*DISTRIBUTION B		
THICKNESS (ft)	CONDUCTIVITY (Btu/hr-ft-°F)	DENSITY (lbs/ft^3)	V_0	V_1	W_1	V_0	V_1	W_1
.1666	.75	140	.2197	-.0009	-.7811	.2685	-.0635	-.7950
.3333	"	"	.2059	-.0393	-.8334	.2645	-.0979	-.8334
.5	"	"	.2055	-.0908	-.8853	.2644	-.1464	-.8820
.6666	"	"	.2055	-.1203	-.9148	.2644	-.1751	-.9107
1.0	"	"	.2055	-.1505	-.9450	.2644	-.2036	-.9392
1.3333	"	"	.2055	-.1618	-.9564	.2644	-.2127	-.9483
.3333	.05	140	.3501	-.2534	-.9032	.3062	-.1954	-.8892
"	.10	"	.3087	-.1884	-.8797	.2942	-.1659	-.8716
"	.40	"	.2334	-.0756	-.8423	.2725	-.1133	-.8408
"	.75	"	.2059	-.0393	-.8334	.2645	-.0979	-.8334
"	.90	"	.1190	-.0306	-.8316	.2625	-.0945	-.8319
"	1.20	"	.1893	-.0187	-.8293	.2598	-.0898	-.8300
.3333	.75	30	.3044	-.1049	-.8005	.2930	-.0959	-.8029
"	"	60	.2506	-.0363	-.7856	.2775	-.0745	-.7971
"	"	90	.2267	-.0127	-.7861	.2705	-.0679	-.7973
"	"	120	.2126	-.0269	-.8143	.2665	-.0837	-.8172
"	"	140	.2059	-.0393	-.8334	.2645	-.0979	-.8334
"	"	170	.1980	-.0551	-.8571	.2662	-.1176	-.8553
"	"	200	.1918	-.0674	-.8756	.2605	-.1335	-.8730

*DISTRIBUTION

A - 80% Floor, 20% Surface Area

B - 100% Surface Area Weighted

TABLE H.1.3 - RADIATION WEIGHTING FACTORS - TABULATED DATA
SPACE SIZE: L=20', W=10', H=10'

FLOOR PROPERTIES			WEIGHTING FACTORS					
			*DISTRIBUTION A			*DISTRIBUTION B		
THICKNESS (ft)	CONDUCTIVITY (Btu/hr-ft-°F)	DENSITY (lbs/ft^3)	V_0	V_1	W_1	V_0	V_1	W_1
.1666	.75	140	.2189	-.0054	-.7865	.2648	-.0657	-.8009
.3333	"	"	.2048	-.0432	-.8384	.2599	-.0994	-.8395
.5	"	"	.2045	-.0929	-.8884	.2598	-.1465	-.8867
.6666	"	"	.2045	-.1215	-.9171	.2598	-.1742	-.9144
1.0	"	"	.2045	-.1508	-.9463	.2598	-.2021	-.9424
1.3333	"	"	.2045	-.1618	-.9573	.2598	-.2113	-.9515
.3333	.05	140	.3521	-.2570	-.9049	.3113	-.2066	-.8953
"	.10	"	.3095	-.1916	-.8820	.2964	-.1734	-.8770
"	.40	"	.2327	-.0793	-.8466	.2696	-.1162	-.8466
"	.75	"	.2048	-.0432	-.8384	.2599	-.0994	-.8395
"	.90	"	.1979	-.0346	-.8367	.2575	-.0955	-.8381
"	1.20	"	.1881	-.0228	-.8346	.2541	-.0903	-.8363
.3333	.75	30	.3052	-.1166	-.8114	.2949	-.1088	-.8138
"	"	60	.2502	-.0421	-.7919	.2757	-.0800	-.8042
"	"	90	.2259	-.0176	-.7917	.2672	-.0701	-.8028
"	"	120	.2117	-.0314	-.8197	.2643	-.0856	-.8233
"	"	140	.2048	-.0432	-.8384	.2599	-.0994	-.8395
"	"	170	.1969	-.0582	-.8614	.2571	-.1180	-.8609
"	"	200	.1907	-.0700	-.8793	.2549	-.1330	-.8781

*DISTRIBUTION

A - 80% Floor, 20% Surface Area

B - 100% Surface Area Weighted

TABLE H.1.4 - RADIATION WEIGHTING FACTORS - TABULATED DATA
SPACE SIZE: L=40', W=20', H=10'

FLOOR PROPERTIES			WEIGHTING FACTORS					
			*DISTRIBUTION A			*DISTRIBUTION B		
THICKNESS (ft)	CONDUCTIVITY (Btu/hr-ft-°F)	DENSITY (lbs/ft^3)	V_0	V_1	W_1	V_0	V_1	W_1
.1666	.75	140	.2137	-.0112	-.7979	.2482	-.0583	-.8101
.3333	"	"	.1993	-.0465	-.8471	.2412	-.0899	-.8487
.5	"	"	.1990	-.0931	-.8941	.2410	-.1345	-.8935
.6666	"	"	.1990	-.1199	-.9209	.2410	-.1607	-.9197
1.0	"	"	.1990	-.1476	-.9487	.2410	-.1873	-.9463
1.3333	"	"	.1990	-.1580	-.9590	.2410	-.1965	-.9555
.3333	.05	140	.3531	-.2603	-.9072	.3'62	-.2177	-.9015
"	.10	"	.3079	-.1937	-.8858	.2942	-.1774	-.8832
"	.40	"	.2279	-.0821	-.8542	.2551	-.1101	-.8550
"	.75	"	.1993	-.0465	-.8471	.2412	-.0899	-.8487
"	.90	"	.1923	-.0380	-.8457	.2377	-.0851	-.8474
"	1.20	"	.1824	-.0263	-.8439	.2329	-.0787	-.8458
.3333	.75	30	.3033	-.1281	-.8248	.2919	-.1183	-.8264
"	"	60	.2460	-.0495	-.8035	.2640	-.0782	-.8143
"	"	90	.2209	-.0234	-.8024	.2517	-.0636	-.8119
"	"	120	.2063	-.0357	-.8294	.2446	-.0774	-.8329
"	"	140	.1993	-.0465	-.8471	.2412	-.0899	-.8487
"	"	170	.1912	-.0600	-.8688	.2372	-.1065	-.8693
"	"	200	.1849	-.0708	-.8858	.2341	-.1198	-.8856

*DISTRIBUTION

A - 80% Floor, 20% Surface Area

B - 100% Surface Area Weighted

TABLE H.1.5 - RADIATION WEIGHTING FACTORS - TABULATED DATA

SPACE SIZE: L=10', W=20'. H=10'

FLOOR PROPERTIES			WEIGHTING FACTORS					
			*DISTRIBUTION A			*DISTRIBUTION B		
THICKNESS (ft)	CONDUCTIVITY (Btu/hr-ft-°F)	DENSITY (lbs/ft^3)	V_0	V_1	W_1	V_0	V_1	W_1
.1666	.75	140	.2172	-.0028	-.7856	.2605	-.0587	-.7983
.3333	"	"	.2032	-.0394	-.8361	.2557	-.0922	-.8365
.5	"	"	.2029	-.0898	-.8869	.2556	-.1399	-.8843
.6666	"	"	.2029	-.1188	-.9160	.2556	-.1680	-.9125
1.0	"	"	.2029	-.1485	-.9456	.2556	-.1962	-.9407
1.3333	"	"	.2029	-.1597	-.9568	.2556	-.2055	-.9499
.3333	.05	140	.3491	-.2528	-.9037	.3053	-.1969	-.8915
"	.10	"	.3070	-.1877	-.8807	.2910	-.1648	-.8738
"	.40	"	.2309	-.0754	-.8446	.2651	-.1087	-.8436
"	.75	"	.2032	-.0394	-.8361	.2557	-.0922	-.8365
"	.90	"	.1963	-.0308	-.8344	.2534	-.0884	-.8350
"	1.20	"	.1867	-.0189	-.8323	.2501	-.0833	-.8332
.3333	.75	30	.3026	-.1065	-.8038	.2895	-.0955	-.8060
"	"	60	.2482	-.0383	-.7900	.2710	-.0714	-.8004
"	"	90	.2241	-.0142	-.7901	.2628	-.0634	-.8006
"	"	120	.2100	-.0274	-.8174	.2580	-.0784	-.8204
"	"	140	.2032	-.0394	-.8361	.2557	-.0922	-.8365
"	"	170	.1953	-.0547	-.8594	.2530	-.1111	-.8581
"	"	200	.1892	-.0667	-.8776	.2509	-.1265	-.8755

*DISTRIBUTION

A - 80% Floor, 20% Surface Area

B - 100% Surface Area Weighted

TABLE H.1.6 - RADIATION WEIGHTING FACTORS - TABULATED DATA
SPACE SIZE: L=20', W=40', H=10'

FLOOR PROPERTIES			WEIGHTING FACTORS					
			*DISTRIBUTION A			*DISTRIBUTION B		
THICKNESS (ft)	CONDUCTIVITY (Btu/hr-ft-°F)	DENSITY (lbs/ft^3)	V_0	V_1	W_1	V_0	V_1	W_1
.1666	.75	140	.2125	-.0084	-.7959	.2453	-.0530	-.8077
.3333	"	"	.1982	-.0433	-.8450	.2355	-.0848	-.8463
.5	"	"	.1979	-.0905	-.8927	.2383	-.1300	-.8917
.6666	"	"	.1979	-.1179	-.9200	.2383	-.1566	-.9183
1.0	"	"	.1979	-.1459	-.9481	.2383	-.1836	-.9453
1.3333	"	"	.1979	-.1565	-.9586	.2383	-.1928	-.9545
.3333	.05	140	.3506	-.2569	-.9063	.3115	-.2109	-.8994
"	.10	"	.3059	-.1905	-.8846	.2901	-.1713	-.8812
"	.40	"	.2266	-.0789	-.8523	.2520	-.1048	-.8528
"	.75	"	.1982	-.0433	-.8450	.2385	-.0848	-.8463
"	.90	"	.1912	-.0348	-.8436	.2351	-.0801	-.8451
"	1.20	"	.1814	-.0231	-.8417	.2304	-.0738	-.8434
.3333	.75	30	.3013	-.1194	-.8180	.2879	-.1076	-.8197
"	"	60	.2445	-.0456	-.8011	.2606	-.0716	-.8109
"	"	90	.2196	-.0202	-.8005	.2487	-.0586	-.8098
"	"	120	.2052	-.0323	-.8272	.2418	-.0723	-.8305
"	"	140	.1982	-.0433	-.8450	.2385	-.0845	-.8463
"	"	170	.1902	-.0572	-.8670	.2346	-.1017	-.8671
"	"	200	.1839	-.0681	-.8842	.2316	-.1153	-.8837

*DISTRIBUTION

A - 80% Floor, 20% Surface Area

B - 100% Surface Area Weighted

TABLE H.1.7 - RADIATION WEIGHTING FACTORS - TABULATED DATA

SPACE SIZE: L=20', W=20', H=10'

FLOOR/CEILING CONVECTION COEFFICIENTS		WEIGHTING FACTORS *DISTRIBUTION A			*DISTRIBUTION B		
h_{i_c} (Btu/hr-ft^2-^{o}F)	h_{i_f}	V_0	V_1	W_1	V_0	V_1	W_1
.162	.2	.1202	-.0005	-.8802	.2129	-.0922	-.8794
"	.4	.1540	-.0179	-.8639	.2273	-.0912	-.8639
"	.6	.1849	-.0347	-.8498	.2405	-.0909	-.8505
"	.712	.2010	-.0435	-.8425	.2473	-.0911	-.8438
"	.8	.2132	-.0503	-.8371	.2525	-.0914	-.8389
"	1.0	.2393	-.0652	-.8259	.2637	-.0928	-.8291
.5	.2	.1406	-.0176	-.8770	.2619	-.1376	-.8756
"	.4	.1738	-.0345	-.8607	.2756	-.1356	-.8600
"	.6	.2041	-.0502	-.8460	.2882	-.1344	-.8462
"	.8	.2320	-.0654	-.8334	.2997	-.1339	-.8342
"	1.0	.2577	-.0796	-.8219	.3104	-.1342	-.8239
.7	.2	.1492	-.025	-.8758	.2826	-.1569	-.8743
"	.4	.1821	-.0416	-.8594	.2961	-.1545	-.8585
"	.6	.2123	-.057	-.8447	.3084	-.1529	-.8445
"	.8	.2399	-.0717	-.8317	.3197	-.1520	-.8324
"	1.0	.2654	-.0858	-.8204	.3301	-.1519	-.8219

*DISTRIBUTION

A - 80% Floor, 20% Surface Area

B - 100% Surface Area Weighted

TABLE H.1.8 - SPACE AIR TEMPERATURE WEIGHTING FACTORS - TABULATED DATA

SPACE SIZE: L=20', W=20', H=10'

FLOOR PROPERTIES			WEIGHTING FACTORS			CONDUCTANCE		WEIGHTING FACTORS			
THICKNESS (ft)	CONDUCTIVITY (Btu/hr-ft-°F)	DENSITY (lbs/ft³)	G_0'	G_1'	G_2'	P_1	K_t	G_0	G_1	G_2	$\frac{A_o}{A_i}\Big\|_{v=\infty}$
			ZERO CONDUCTANCE					CONDUCTANCE CORRECTION			
.1666	.75	140	336.49	-361.61	25.12	-.7979	290.60	620.88	-593.48	25.12	692.86
.3333	"	"	340.25	-371.39	31.14	-.8427	286.66	626.91	-612.96	31.14	689.79
.5	"	"	343.88	-388.47	44.59	-.8903	283.20	627.08	-640.60	44.59	694.21
.6666	"	"	346.79	-400.41	53.62	-.9176	280.29	627.08	-657.60	53.62	697.91
1.0	"	"	350.54	-413.61	63.07	-.9455	276.54	627.08	-675.08	63.07	701.74
1.3333	"	"	345.23	-414.81	69.58	-.9553	278.85	627.08	-681.20	69.58	703.14
.3333	.05	140	317.32	-388.68	71.36	-.9008	245.52	562.84	-609.84	71.36	652.13
"	.1	"	322.06	-352.94	30.88	-.8810	258.46	581.52	-611.40	30.88	633.73
"	.4	"	334.18	-372.24	38.06	-.8499	280.74	614.92	-610.84	38.06	654.96
"	.75	"	340.25	-371.39	31.14	-.8427	286.66	626.91	-612.96	31.14	689.79
"	.9	"	341.96	-371.73	29.77	-.8413	287.92	629.88	-613.96	29.77	691.69
"	1.2	"	344.52	-377.67	28.15	-.8395	289.56	634.08	-615.76	28.15	694.75
.3333	.75	30	296.78	-352.42	55.64	-.8119	286.66	583.44	-585.16	55.64	675.67
"	"	60	320.64	-357.40	36.76	-.8009	286.68	607.32	-587.00	36.76	683.59
"	"	90	331.16	-357.83	26.67	-.8015	286.68	617.84	-587.60	26.67	683.94
"	"	120	337.29	-365.57	28.28	-.8256	286.67	623.96	-602.24	28.28	687.16
"	"	140	340.25	-371.39	31.14	-.8427	286.66	626.91	-612.96	31.14	689.79
"	"	170	343.66	-379.03	35.37	-.8646	286.66	630.32	-676.88	35.37	693.21
"	"	200	346.34	-385.30	38.96	-.8818	286.66	633.00	-638.08	38.96	696.16

TABLE H.1.9 - SPACE AIR TEMPERATURE WEIGHTING FACTORS - TABULATED DATA

SPACE SIZE: L=10', W=10', H=10'

FLOOR PROPERTIES			WEIGHTING FACTORS			CONDUCTANCE		WEIGHTING FACTORS			
THICKNESS (ft)	CONDUCTIVITY (Btu/hr-ft-^{o}F)	DENSITY (lbs/ft^{3})	G_0'	G_1'	G_2'	P_1	K_t	G_0	G_1	G_2	$\frac{A_o}{A_i}\Big\|_{v=\infty}$
			ZERO CONDUCTANCE					CONDUCTANCE CORRECTION			
.1666	.75	140	128.41	-141.85	13.44	-.7878	111.24	239.65	-228.70	13.44	269.93
.3333	"	"	130.98	-145.37	14.39	-.8326	110.23	241.21	-237.15	14.39	268.88
.5	"	"	131.88	-152.15	20.27	-.8828	109.37	241.25	-248.70	20.27	270.99
.6666	"	"	132.56	-156.56	24.00	-.9118	108.69	241.25	-255.66	24.00	272.47
1.0	"	"	133.25	-161.12	28.26	-.9404	108.00	241.25	-262.68	28.26	274.07
1.3333	"	"	132.36	-161.51	29.15	-.9506	108.89	241.25	-265.02	29.15	274.49
.3333	.05	140	125.04	-152.74	27.70	-.8926	99.95	224.99	-241.96	27.70	261.36
"	.1	"	126.57	-150.71	24.14	-.8733	103.08	229.65	-240.73	24.14	263.98
"	.4	"	129.40	-146.07	16.67	-.8405	108.72	238.12	-237.45	16.67	267.45
"	.75	"	130.98	-145.37	14.39	-.8326	110.23	241.21	-237.15	14.39	268.88
"	.9	"	131.43	-145.37	13.94	-.8310	110.55	241.98	-237.24	13.94	269.34
"	1.2	"	132.09	-145.48	13.39	-.8290	110.97	243.06	-237.47	13.39	270.05
.3333	.75	30	119.79	-138.65	18.86	-.7963	110.34	230.13	-226.51	18.86	264.71
"	"	60	125.95	-127.55	1.60	-.7899	110.23	236.18	-227.04	1.60	252.75
"	"	90	128.64	-140.24	11.60	-.7920	110.23	238.87	-227.54	11.60	266.75
"	"	120	130.23	-143.13	12.90	-.8151	110.22	240.45	-232.97	12.90	267.93
"	"	140	130.98	-145.37	14.39	-.8326	110.23	241.21	-237.15	14.39	268.88
"	"	170	131.86	-148.41	16.55	-.8554	110.23	242.09	-242.70	16.55	270.21
"	"	200	132.53	-150.86	18.33	-.8735	110.25	242.78	-247.16	18.33	271.30

TABLE H.1.10 - SPACE AIR TEMPERATURE WEIGHTING FACTORS - TABULATED DATA

SPACE SIZE: L=20', W=10', H=10'

FLOOR PROPERTIES			WEIGHTING FACTORS			CONDUCTANCE		WEIGHTING FACTORS			
THICKNESS (ft)	CONDUCTIVITY (Btu/hr-ft-^{o}F)	DENSITY (lbs/ft^{3})	G_0'	G_1'	G_2'	P_1	K_t	G_0	G_1	G_2	$\frac{A_o}{A_i}\Big\|_{v=\infty}$
			ZERO CONDUCTANCE					CONDUCTANCE CORRECTION			
.1666	.75	140	231.65	-254.94	23.29	-.7933	153.89	385.54	-377.02	23.29	438.21
.3333	"	"	236.86	-262.63	25.77	-.8386	151.76	388.62	-389.90	25.77	437.44
.5	"	"	238.81	-274.72	35.91	-.8872	149.89	388.70	-407.70	35.91	441.03
.6666	"	"	240.34	-282.75	42.41	-.9153	148.36	388.70	-418.54	42.41	443.61
1.0	"	"	242.19	-291.32	49.13	-.9438	146.51	388.70	-429.60	49.13	446.25
1.3333	"	"	240.65	-292.21	51.56	-.9535	148.05	388.70	-433.38	51.56	447.22
.3333	.05	140	226.41	-277.72	51.31	-.8982	129.79	356.20	-394.30	51.31	422.40
"	.1	"	228.65	-273.35	44.70	-.8784	136.55	365.58	-393.30	44.70	427.60
"	.4	"	233.93	-264.03	30.10	-.8461	148.55	382.48	-389.72	30.10	434.59
"	.75	"	236.86	-262.63	25.77	-.8386	151.76	388.62	-389.90	25.77	437.44
"	.9	"	237.72	-262.63	24.91	-.8370	152.44	390.16	-390.22	24.91	438.37
"	1.2	"	238.97	-262.81	23.84	-.8351	153.33	392.30	-390.86	23.84	439.76
.3333	.75	30	214.78	-251.89	37.11	-.8079	151.76	366.54	-374.50	37.11	430.41
"	"	60	226.85	-253.26	26.41	-.7967	151.77	378.62	-374.18	26.41	433.69
"	"	90	232.21	-253.29	21.08	-.7973	151.77	383.98	-374.30	21.08	433.59
"	"	120	235.36	-258.61	23.25	-.8212	151.76	387.12	-383.24	23.25	435.76
"	"	140	236.86	-262.63	25.77	-.8386	151.76	388.62	-389.90	25.77	437.44
"	"	170	238.62	-267.96	29.34	-.8608	151.76	390.38	-398.60	29.34	439.77
"	"	200	239.97	-272.27	32.30	-.8784	151.77	391.74	-405.58	32.30	441.67

TABLE H.1.11 - SPACE AIR TEMPERATURE WEIGHTING FACTORS - TABULATED DATA

SPACE SIZE: L=40', W=20', H=10'

FLOOR PROPERTIES			WEIGHTING FACTORS			CONDUCTANCE		WEIGHTING FACTORS			
THICKNESS (ft)	CONDUCTIVITY (Btu/hr-ft-^{o}F)	DENSITY (lbs/ft^{3})	G_0'	G_1'	G_2'	P_1	K_t	G_0	G_1	G_2	$\frac{A_o}{A_i}\Big\|_{v=\infty}$
			ZERO CONDUCTANCE					CONDUCTANCE CORRECTION			
.1666	.75	140	607.93	-666.75	58.82	-.8021	445.59	1053.52	-1024.16	58.82	1185.56
.3333	"	"	628.10	-684.04	55.94	-.8476	437.42	1065.52	-1054.80	55.94	1177.88
.5	"	"	635.67	-715.27	79.60	-.8938	430.17	1065.84	-1099.76	79.60	1185.55
.6666	"	"	641.88	-737.51	95.63	-.9203	423.96	1065.84	-1127.68	95.63	1192.08
1.0	"	"	650.49	-763.10	112.70	-.9475	415.35	1065.84	-1156.64	112.70	1199.02
1.3333	"	"	646.58	-765.64	119.08	-.9572	419.26	1065.84	-1166.96	119.08	1201.64
.3333	.05	140	585.61	-719.37	133.76	-.9041	351.99	937.60	-1037.60	133.76	1107.59
"	.1	"	596.59	-709.28	112.69	-.8843	378.61	975.20	-1044.08	112.69	1131.44
"	.4	"	616.64	-685.94	69.30	-.8543	425.12	1041.76	-1049.12	69.30	1164.96
"	.75	"	628.10	-683.36	55.26	-.8476	437.42	1065.52	-1054.12	55.26	1177.15
"	.9	"	631.33	-684.69	53.36	-.8462	440.03	1071.36	-1057.04	53.36	1181.76
"	1.2	"	636.17	-686.40	50.23	-.8445	443.43	1079.60	-1060.88	50.23	1187.70
.3333	.75	30	541.19	-651.77	110.58	-.8221	437.41	978.60	-1011.36	110.58	1152.82
"	"	60	588.76	-659.26	70.50	-.8067	437.46	1026.22	-1012.16	70.50	1167.25
"	"	90	610.04	-659.03	48.99	-.8061	437.48	1047.52	-1011.68	48.99	1167.26
"	"	120	622.24	-673.46	51.22	-.8306	437.44	1059.68	-1036.80	51.22	1173.22
"	"	140	628.10	-684.04	55.94	-.8476	437.42	1065.52	-1054.80	55.94	1177.88
"	"	170	624.83	-697.89	73.06	-.8690	437.41	1072.24	-1078.00	73.06	1184.22
"	"	200	640.10	-709.14	69.04	-.8857	437.42	1077.52	-1096.56	69.04	1189.54

TABLE H.1.12 - SPACE AIR TEMPERATURE WEIGHTING FACTORS - TABULATED DATA

SPACE SIZE: L=10', W=20', H=10'

FLOOR PROPERTIES			WEIGHTING FACTORS			CONDUCTANCE		WEIGHTING FACTORS			
THICKNESS (ft)	CONDUCTIVITY (Btu/hr-ft-°F)	DENSITY (lbs/ft³)	G_0'	G_1'	G_2'	P_1	K_t	G_0	G_1	G_2	$\frac{A_o}{A_i}\Big\|_{v=\infty}$
			ZERO CONDUCTANCE					CONDUCTANCE CORRECTION			
.1666	.75	140	191.87	-209.60	17.73	-.7908	212.21	404.08	-377.42	17.73	446.30
.3333	"	"	196.84	-215.38	18.54	-.8356	210.32	407.16	-391.12	18.54	444.99
.5	"	"	198.53	-225.41	26.88	-.8850	208.71	407.24	-410.12	26.88	447.87
.6666	"	"	199.83	-232.21	32.38	-.9135	207.41	407.24	-421.68	37.38	450.12
1.0	"	"	201.27	-239.31	38.04	-.9423	205.97	407.24	-433.40	38.04	452.39
1.3333	"	"	199.81	-239.91	40.10	-.9521	207.43	407.24	-437.40	40.10	453.23
.3333	.05	140	183.97	-224.03	40.06	-.8949	191.07	375.04	-395.02	40.06	427.53
"	.1	"	187.35	-221.77	34.42	-.8755	196.97	384.32	-394.22	34.42	433.46
"	.4	"	193.57	-215.87	22.30	-.8432	207.51	401.08	-390.84	27.30	441.74
"	.75	"	196.84	-215.38	18.54	-.8356	210.32	407.16	-391.12	18.54	444.99
"	.9	"	197.75	-215.56	17.81	-.8340	210.93	408.68	-391.48	17.81	446.00
"	1.2	"	199.03	-215.97	16.94	-.8321	211.77	410.80	-392.18	16.94	447.53
.3333	.75	30	174.95	-203.77	28.82	-.7991	210.33	385.28	-371.84	28.82	436.85
"	"	60	186.91	-207.03	20.12	-.7929	210.33	397.24	-373.80	20.12	441.27
"	"	90	192.23	-207.57	15.34	-.7951	210.33	402.56	-374.80	15.34	441.59
"	"	120	195.33	-211.97	16.64	-.8182	210.33	405.66	-384.06	16.64	443.49
"	"	140	196.84	-215.38	18.54	-.8356	210.32	407.16	-391.12	18.54	444.99
"	"	170	198.57	-219.94	21.37	-.8581	210.33	408.90	-400.42	21.37	447.07
"	"	200	199.90	-223.64	23.74	-.8760	210.36	410.26	-407.92	23.74	448.78

TABLE H.1.13 - SPACE AIR TEMPERATURE WEIGHTING FACTORS - TABULATED DATA

SPACE SIZE: L=20', W=40', H=10'

FLOOR PROPERTIES			WEIGHTING FACTORS			CONDUCTANCE		WEIGHTING FACTORS			
THICKNESS (ft)	CONDUCTIVITY (Btu/hr-ft-^{o}F)	DENSITY (lbs/ft^3)	G_0'	G_1'	G_2'	P_1	K_t	G_0	G_1	G_2	$\frac{A_o}{A_i}\Big\|_{v=\infty}$
			ZERO CONDUCTANCE					CONDUCTANCE CORRECTION			
.1666	.75	140	531.80	-578.86	47.06	-.7996	559.40	1091.20	-1026.16	47.06	1202.72
.3333	"	"	551.09	-592.69	41.60	-.8452	551.95	1103.04	-1059.20	41.60	1194.36
.5	"	"	557.98	-620.19	62.21	-.8921	545.38	1103.36	-1106.72	62.21	1200.94
.6666	"	"	563.54	-640.01	76.47	-.9191	539.82	1103.36	-1136.16	76.47	1216.33
1.0	"	"	571.00	-662.55	91.55	-.9466	532.36	1103.36	-1166.48	91.55	1213.09
1.3333	"	"	567.24	-664.53	97.29	-.9564	536.12	1103.36	-1177.28	97.29	1215.46
.3333	.05	140	501.74	-587.68	85.94	-.9023	474.34	976.08	-1040.40	85.94	1092.20
"	.1	"	514.91	-593.03	78.12	-.8825	498.45	1013.36	-1047.44	78.12	1128.50
"	.4	"	538.70	-592.44	53.74	-.8521	540.74	1079.44	-1053.20	53.74	1180.49
"	.75	"	551.49	-592.69	41.20	-.8452	551.95	1103.04	-1059.20	41.20	1194.36
"	.9	"	554.63	-593.80	39.17	-.8439	554.33	1108.96	-1061.60	39.17	1198.40
"	1.2	"	559.69	-596.19	36.50	-.8421	557.43	1117.12	-1065.60	36.50	1204.72
.3333	.75	30	465.18	-556.51	91.33	-.8138	551.94	1017.12	-1005.68	91.33	1165.58
"	"	60	512.50	-569.00	56.50	-.8030	551.98	1064.48	-1012.24	56.50	1183.15
"	"	90	533.49	-570.34	36.85	-.8039	551.99	1085.20	-1014.08	36.85	1184.33
"	"	120	545.31	-550.06	4.75	-.8882	551.97	1097.28	-1040.32	4.75	1134.60
"	"	140	551.09	-592.69	41.60	-.8452	551.95	1103.04	-1059.20	41.60	1194.36
"	"	170	557.08	-605.27	47.46	-.8669	551.95	1109.76	-1083.76	47.46	1200.37
"	"	200	563.06	-627.14	64.08	-.8839	551.98	1115.04	-1103.44	64.08	1217.77

TABLE H.1.14 - SPACE AIR TEMPERATURE WEIGHTING FACTORS - TABULATED DATA

SPACE SIZE: L=20', W=20', H=10'

FLOOR/CEILING CONVECTION COEFFICIENTS		WEIGHTING FACTORS			CONDUCTANCE		WEIGHTING FACTORS			
h_{i_c} (Btu/hr-ft^2-^{o}F)	h_{i_f}	G_0'	G_1'	G_2'	P_1	K_t	G_0	G_1	G_2	$\frac{A_o}{A_i}\Big\|_{v=\infty}$
		ZERO CONDUCTANCE					CONDUCTANCE CORRECTION			
.162	.2	219.93	-249.36	29.43	-.8788	254.35	474.28	-472.88	29.43	519.80
"	.4	267.90	-301.04	33.14	-.8636	270.18	538.08	-532.40	33.14	593.25
"	.6	314.79	-346.08	31.29	-.8498	281.57	596.36	-585.36	31.29	655.75
"	.8	359.76	-390.87	31.11	-.8375	290.16	649.92	-633.88	31.11	715.60
"	1.0	402.37	-433.89	31.52	-.8266	296.87	699.24	-679.28	31.52	771.95
.5	.2	262.48	-305.36	42.88	-.8749	277.24	539.72	-547.92	42.88	602.97
"	.4	311.25	-352.47	41.22	-.8598	290.87	602.12	-602.56	41.22	669.91
"	.6	358.44	-398.61	40.17	-.8461	300.76	659.20	-653.08	40.17	732.60
"	.8	403.36	-443.12	39.76	-.8339	308.24	711.60	-700.16	39.76	791.49
"	1.0	445.77	-485.70	39.33	-.8231	314.11	759.88	-744.24	39.33	846.94
1.0	.2	281.47	-329.50	48.03	-.8734	285.85	567.32	-579.16	48.03	637.62
"	.4	330.41	-376.70	46.29	-.8583	298.71	629.12	-633.08	46.29	704.13
"	.6	377.64	-422.72	45.08	-.8447	308.04	685.68	-682.92	45.08	766.35
"	.8	422.48	-467.02	44.54	-.8325	315.12	737.60	-729.36	44.54	824.83
"	1.0	464.79	-509.33	44.54	-.8217	320.69	785.48	-772.84	44.54	879.87

APPENDIX H.2 - STATEMENT OF WORK

APPENDIX H.2 - STATEMENT OF WORK

The statement of work for DOE contract number EM-78-C-01-5221 consisted of the tasks listed below. Following each task description is a brief summary of the work accomplished and conclusions which were ascertained.

1. Evaluation of Existing Analysis Techniques

    a. Identify the specific algorithms and techniques used for thermal load calculations in DOE-1.

DOE-1 is a thermal load calculation computer program which employs weighting factors to determine space loads and temperature variations. The program is well documented and as a result a minimum effort was required to define the calculation schemes employed. Certain revisions to the program have been recommended based on the techniques developed during the course of the contract. A brief discussion of DOE-1 was presented in Reference 1.

    b. Identify the specific algorithms and techniques used for thermal load calculations in BLAST.

BLAST is a thermal load calculation computer program which employs the thermal balance method to determine space loads and temperature variations. A significant amount of time was utilized, primarily at the start of the contract, in becoming familiar with the program flow and algorithmic characteristics of the BLAST program. Initially, it was envisioned to use BLAST to generate space specific weighting factors and although this aspect was accomplished, the development of a simple recursion relationship negated the subsequent use of BLAST for this purpose. The interim report, Reference 1, presented a cursory discussion of specific BLAST concepts.

    c. Establish approximate degree of divergence of the weighting factor technique from the thermal balance technique. DOE-1 uses pretabulated weighting factors published by ASHRAE.

The comparison of BLAST and DOE-1 results for a selected set of rooms with different constructions and parameters will be used to identify the degree of divergence. Thermally light rooms (negligible delay in heat transfer), medium, heavy and very heavy constructions will be used and some changes in surface and heat transfer parameters will be made.

Because of the successful derivation of generating space specific weighting factors through the use of a recursion technique (see paragraph 3d below), the degree of divergence between the thermal balance and weighting factor techniques essentially does not exist. The divergence arises because of the use of pretabulated weighting factors which were generated for spaces somewhat general in nature. Whatever differences exist between the two techniques is due to the algorithms which calculate the various input quantities necessary for solution, such as solar radiation quantities, infiltration, etc. Within Section E of this report are contained results comparing the weighting factor and thermal balance methods from which all input algorithmic differences have been eliminated. However, to provide insight into specific parameter influence on weighting factor values, a comprehensive parametric study was undertaken, the results of which are reported in Section D of this report. A space definition similar to the BR202 structure was defined and perturbations applied to floor thickness, conductivity and density values, floor/ceiling inside convection coefficients, space size and type of radiation distribution. Both radiative and air temperature weights were generated and the expected load response determined using frequency resonse methods outlined in Section C and reported in Paragraph 4d below.

d. Identify the methods used for coupling thermally massive elements in the load calculation and system simulation parts of DOE-1 and BLAST programs.

See Paragraph 4 below.

2. BLAST/DOE Program Interfaces and Comparison With BR-202

The purpose of this task is to implement an interface between DOE-1 program and the BLAST program and compare the pulse generated results of BLAST with that of the NRC program BR-202 which is the basis of the weighting factors used in ASHRAE and DOE-1 load calculations.

a. Implement a method for generating pulses on room surfaces and room air in BLAST due to radiative, conductive and convective loads. This will include direct and diffuse solar radiation, loads due to equipment, lights, external and internal surfaces and occupancy. Document changes made to BLAST.

b. Establish methods for converting the pulse generated results from BLAST to the pretabulated weighting factor form for entry into DOE-1.

A method was implemented in BLAST for generating radiative and room air temperature pulses. The radiative results agree with the recursion technique described in Paragraph 3d below. However, the room air pulse results from BLAST were unrealistic. To generate the room air response in BLAST, the thermal balance solution matrix had to be revised and it is thought at this time that perhaps the applied revision was not valid. The purpose of these tasks was to be able to generate space specific weighting factors; however continued work with BLAST in this regard was not necessary because of the recursion method derived.

c. Implement a method for entering weighting factors into DOE-1 and modify the Loads & Systems Programs so that new weighting factors are used in the calculations when provided.

With minor modifications to DOE-1, the recursion method for generating space specific weighting factors can be implemented in the program structure. Most of the data required for solution are already present in the standard file structure; however, additional commands might be necessary for adequate definition of space properties.

d. Compare pulse generated results of BR-202 with that of BLAST. The intent here is to establish a base of reference to previously published work done at NRC, ASHRAE and NBS and identify and, if feasible, reconcile differences in results produced by BLAST program. If the difference in results cannot be explained at this time, recommendations will be made either to investigate this problem further or to bypass it with the development of parallel thermal balance routines in DOE-1/2.

Results from the BR-202 program were compared with the BLAST generated responses to unit pulse inputs. To accomplish this task, a large quantity of time was spent becoming familiar with the BR-202 structure. Results of the comparison are presented in Reference 1 as well as a brief discussion of the BR-202 program. A shift of emphasis from continued comparisons with BR-202 was made because of the rather specific nature of the space structure intrinsic to the routines.

e. Utilize specific weighting factors developed for the test rooms in DOE-1 and compare with results of the pretabulated weighting factors in the previously divergent cases.

See Paragraph 1c above.

3. Development of Analytic Relationships Between the Thermal Balance and Weighting Factor Techniques

a. Develop analytical expressions from a very simple model for the weighting factors to establish their functional dependence on room parameters and surface thermal properties.

b. Compare the analytical forms to results obtained from an equivalent RC circuit in both continuous and sampled forms.

c. Investigate the use of perturbation techniques in more complex cases to relate the radiation coupled matrices to

vector forms, i.e. thermal balance requires the solution of a radiation coupled matrix which is used to provide a solution to a unit pulse input, this result is then used as the coupling mechanism in the weighting factor technique. Use matrix perturbation methods to provide at least to first order the functional dependence of weighting factors to room parameters.

The recursion relationship described in Paragraph 3d below was developed from initial work done on a simple two-surface model of the thermal balance scheme developed for completion of this task. A definite pattern was established during this analysis which related certain space parameters to the resultant weighting factors.

Both TASK 3b and 3c in the Statement of Work were thought necessary to assist in understanding the functional dependence of space specific weighting factors on room parameters, assuming an empirical or matrix perturbation analytical technique would have to be used to define the weighting factors. The recursion method negated further analysis in these areas.

d. Investigate the possibility of establishing weighting factors from room parameters either directly or with the use of a pretabulated set with appropriate correction elements.

A recursion relationship was developed such that space specific weighting factors can be generated for any arbitrarily defined space. Both radiation and air temperature weighting can be obtained. Investigations are continuing into conductive type factors - a situation which developed as a result of the analysis of the BR-202 program in which conductive weighting factors were not explicitly defined. The simple equations developed imply minor modifications to DOE-1 such that the use of pretabulated weighting factors are not needed. Two approaches were developed. Initially, a heat balance of the inside surface yielded a recursion equation from which the

aforementioned responses could be generated. Results were presented in the Interim Report, Reference 1. Within Section B of this report is contained an extension to the technique which employs a heat balance at both inside and outside surfaces. This enables the generation of weighting factors which could be used in multizone analysis.

4. Develop and Evaluate Alternative Analysis Techniques

   a. Review methods for coupling passive solar elements with the thermal balance and weighting factor methods and identify the assumptions required for such coupling.

   b. Develop and compare linearly coupled forms against detailed simultaneous or iterative solutions.

   c. If the results of subtask (b) are not acceptable, investigate other coupling techniques that may be more appropriate. The goals here are to develop techniques that approach the accuracy of detailed thermal balance method and the computational efficiency of the weighting factor method.

At the present time, neither the weighting factor nor thermal balance schemes have the capability for analyzing passive solar elements and their influence on load quantities. While some thought has gone into this portion of the Statement of Work nothing conclusive has been ascertained due to the unavailability of testing algorithms at the time of contract completion.

d. If time permits the feasibility of spectral methods will also be investigated as this method is the most efficient in contrast to the previously considered approaches.

Section D of this report presents a disucssion in which a set of weighting factors and thus Z-transform expressions are related to a Laplace or S-transform thus enabling the use of frequency domain analytical tools. An immediate observation can thus be made of the damping and phase shift characteristics of any arbitrarily defined space and structure. The parametric study mentioned in Task 1C above relied heavily on the procedures defined here. An initial investigation into pure spectral techniques indicates a significant scope of application particularly for passive solar structures because of the relative importance of excitation frequency on design optimization.

5. Multiple Thermal Zone Analysis

a. Review multizone coupling techniques in state-of-the-art building energy analysis programs.

b. Review interzone convection algorithms which couple zones through open doors, windows and stack effect.

c. Select a method for implementation which is compatible with the results of Task 4 and document.

A cursory discussion of the multizone coupling situation is presented in Section B of this report. However, prior to final recommendations being made, substantial coding change to DOE-2 would be necessary and appropriate testing conducted. In addition, the incomplete nature of Task 4 justified a reduction in scope for this Task.

U.S. GOVERNMENT PRINTING OFFICE: 1980—640-258/1879